12-2017

Exogenous Ubiquitin: Role in Myocardial Inflammation and Remodeling Post- Ischemia/ Reperfusion Injury

Stephanie Scofield
East Tennessee State University

Exogenous Ubiquitin: Role in Myocardial Inflammation and Remodeling Post-Ischemia/Reperfusion Injury

---

A dissertation

presented to

the faculty of the Department of Biomedical Science

East Tennessee State University

In partial fulfillment

of the requirements for the degree

Doctor of Philosophy in Biomedical Science

---

by

Stephanie L.C. Scofield

December 2017

Krishna Singh, Ph.D., Chair

Antonio Rusiñol, Ph.D.

Mahipal Singh, Ph.D.

Thomas Ecay, Ph.D.

Chuanfu Li, M.D.

Yue Zoe, Ph.D.

Keywords: Ubiquitin, Heart, CXCR-4, Ischemia/Reperfusion, Inflammation, Remodeling

ABSTRACT

Exogenous Ubiquitin: Role in Myocardial Inflammation and Remodeling Post-Ischemia/Reperfusion Injury

by

Stephanie L.C. Scofield

Sympathetic stimulation occurs in the heart after injuries such as ischemia/reperfusion (I/R) and myocardial infarction and affects myocardial remodeling. Prolonged sympathetic stimulation can result in myocardial dysfunction through its effects on cardiac myocyte apoptosis and myocardial fibrosis. Ubiquitin (UB) is well known for its role of tagging old or damaged proteins for degradation via the UB-proteosome pathway. The role of exogenous UB however, is not fully understood. Previously, our lab showed that β-adrenergic receptor (β-AR) stimulation increased levels of extracellular UB in the conditioned media of adult rat ventricular myocytes and that UB inhibits β-AR-stimulated apoptosis. This study investigates the role of extracellular UB after myocardial I/R injury in terms of infarct size, function, inflammation and proteomic changes *in vivo* as well as the effects of extracellular UB on cardiac fibroblast function *in vitro*. First, we validated a method of consistently measuring real-time myocardial ischemia and reperfusion *in vivo.* Second, cardiac function was studied 3 days post I/R injury in the presence or absence of UB infusion. Echocardiographic analysis determined UB infusion increased cardiac function after I/R injury in terms of ejection fraction and fractional shortening. UB decreased infarct size and infiltration of inflammatory cells including neutrophils and macrophages as well as reduced activity of neutrophils. UB increased protein levels of matrix metalloproteinase (MMP)-2 and transforming growth factor-β1 and increased activity of MMP-9. Third, in adult rat primary

cardiac fibroblasts, we demonstrate that extracellular UB interacts with CXCR-4. UB treatment decreased serum-mediated increases in fibroblast proliferation and enhanced the contraction of fibroblast-populated collagen gels. Thus, extracellular UB likely interacts with CXCR-4 to influence fibroblast function and proliferation. Additionally, UB influences cardiac remodeling in terms of heart function, infarct size, inflammatory response and proteomic profile.

DEDICATION

To my family Mom, Dad, Victoria and Travis: You have been the foundation that has allowed me to make it this far. Mom and Dad, your persistence in the pursuit of higher education while I was growing up taught me to set goals and to keep moving forward. Victoria and Travis, thank you for the best siblingship I could ever ask for. You two bring immeasurable joy to my life. Thank you all for supporting me in every way.

To Mark: I will never be able to fully express my thanks in words. Thank you for lending me your strength, your energy and your ear when I needed it most. I hope to spend the rest of my life trying to return the favor.

ACKNOWLEDGMENTS

To Dr. Krishna Singh: Thank you for all that you have done for me throughout my graduate student career. You found me as a young undergraduate volunteer and you helped me grow into a scientist. Thank you for opening your lab up to me; it has been a privilege and an amazing opportunity to work with you. Thank you for your patience, your guidance and for always keeping your door open.

To my committee members: Dr. Tom Ecay, Dr. Mahipal Singh, Dr. Chuanfu Li, Dr. Antonio Rusinol and Dr. Yue Zou. Thank you for supporting me, for always offering valuable feedback and for your continued interest in my success.

To my lab mates past and present: Dr. Cerrone Foster, thank you for introducing me to research and for always being available to talk about career development. Dr. Suman Dalal, thank you for extending your home to me during the snowstorm on my first day in lab. Thank you for all of your help with new techniques, for your friendship and for sharing this lab life with me. I will always remember my good friend, Dr. Barefoot. Dr. Christopher Daniels, thank you for introducing me to the ubiquitin project and for your friendship and support while I was a new graduate student. Dr. Laura Daniel: Thank you for your excitement when I started in the lab. Thank you also for your friendship, I will always remember our trip to Charleston. Ms. Patsy Thrasher: Thank you for your friendship. I can always count on you to give me honest and unbiased feedback. Your input has truly been invaluable. Ms. Kristina Lim: I don't think that I can thank you enough in this section. You have been my right-hand man since the start. I am so glad I had the pleasure of watching you grow as a scientist and as a young woman. Ms. Bobbie Connelly: Thank you for all of your help in lab, your words of wisdom, and for always keeping me entertained with your stories.

TABLE OF CONTENTS

Page

LIST OF FIGURES

CHAPTER 1

INTRODUCTION

Cardiovascular pathophysiologies consistently rank as the number one cause of mortality in the world[1]. Cardiovascular disease also causes disability and accounted for $316.6 billion of United States healthcare and lost productivity costs in 2011[2]. Approximately 735,000 Americans suffer heart attacks and 610,000 people die from heart disease every year, accounting for 25% of nationwide deaths. The most common type of heart disease is coronary heart disease, which was responsible for about 366,000 deaths in 2015. Geographically, the southeastern United States has the highest heart disease death rate with between 452-846 deaths annually per 100,000 population from 2008-2010. (Statistics provided by the Centers for Disease Control heart disease factsheet.)

Although heart disease can come in many different forms, the aforementioned coronary heart/artery disease is credited with being the most common type of heart disease. It is estimated to affect 16.8 million Americans. The diagnosis of coronary artery disease typically comes after patients report angina pectoris, more commonly known as chest pain, which is usually found to result from plaque occluding part of a coronary artery[3]. The gathering of plaque within the coronary artery walls is referred to as atherosclerosis[4].

Human progression to myocardial infarction, commonly called heart attack, typically begins years before any symptoms present. Atherosclerosis is a multifactorial disease that forms within the walls of the coronary arteries by deposition of lipoproteins, chronic inflammation, necrosis, fibrosis and calcification of plaque. These atherosclerotic plaques are contained by a fibrous cap, which when thinned, can rupture either spontaneously or upon physical exertion. Plaque rupture exposes highly thrombogenic material to the blood stream. The accentuated

thrombotic response associated with plaque rupture can be attributed to increased coagulation and reactivity of platelets at the site of the plaque rupture[5].

Once the thrombus is in place, it blocks the flow of oxygenated blood to the myocardium below the thrombus. The flow of oxygenated blood to the myocardium can also be occluded by the atherosclerosis alone, in which case it would push inward on the arterial walls and narrow the lumen. Regardless of if the occlusion occurs because of atherosclerotic luminal narrowing or due to plaque rupture, the result is restricted flow of oxygenated blood to the myocardium. Cardiac myocytes are highly aerobic cells and therefore need a constant supply of oxygen to maintain function and cellular homeostasis. Within minutes, the oxygen-depleted myocardium begins to die. Ischemia in cardiac myocytes can cause irregularities in function as quickly as 5 minutes after onset and can cause irreversible myocyte injury within 20 minutes[6]. In an attempt to reduce the extent of irreversible ischemic injury, the guidelines for treatment of acute myocardial infarction recommend that patients experiencing an ischemic myocardial event be treated within 90 minutes of arriving at the hospital[7].

The heart is made up of multiple cell types but cardiac myocytes dominate the heart in terms of mass[8]. Cardiac myocytes are terminally differentiated meaning that once the heart reaches adulthood, the cardiac myocytes will not mitotically divide, and thus will not give rise to new myocytes. Therefore, the population of cardiac myocytes that are present in the heart before injury will be the same cardiac myocytes present after the injury minus any myocytes lost during ischemia or subsequent reperfusion injury. Cardiac regenerative therapies have met limited success[9; 10].

Ischemia/Reperfusion Injury

Ischemia refers to an inadequate or absent supply of oxygen to an organ. Since oxygen is carried via red blood cells, arterial occlusions make it impossible for oxygenated blood to perfuse the myocardium beneath the point of the ligature. Therefore, the myocardium below the ligature that is unable to access oxygenated blood flow is said to be "ischemic," and quickly begins to die. In human patients, the arterial occlusion is due to build-up of atherosclerotic plaque and/or arterial rupture and subsequent clotting, forming a thrombus in the affected coronary artery.

Reperfusion refers to the state of the myocardium after the occlusion is cleared and the oxygenated blood is allowed to perfuse the previously ischemic tissue. In human patients experiencing myocardial infarction, clearance of the occlusion is achieved pharmaceutically by using thrombolytic drugs or invasively through coronary angioplasty and stent placement. In patients, reperfusion is critical to survival and recovery.

Many models have been developed to investigate heart disease. The myocardial infarction model (MI) is a surgical model which, involves ligating the left anterior descending coronary artery with a suturing silk. The ischemia/reperfusion model (I/R) is similar to the MI model but instead of ligating the artery closed permanently, a temporary snare around the coronary artery is created for the duration of ischemia and released for the period of reperfusion.

Of the discussed heart disease animal models, the I/R model most closely parallels the progression of human myocardial infarction injuries. This is due to the reperfusion period which, corresponds with medical interventions and treatments to clear the thrombus in affected patients. MI animal models do not ever release the ligature occluding the artery and thus, such models fail to investigate any of the consequences that would be brought about during the

reperfusion phase. Reperfusion is considered medically necessary as it reestablishes oxygen and nutrient supply to support cellular metabolism and also allows for the clearance of metabolic waste but is well known for its association with serious complications[11]. If the myocardium is not reperfused, the ischemic area below the thrombus or occlusion will succumb to necrosis[12]. Reperfusion injury has been described as a paradox "in which the reoxygenation of ischemic myocardium generates a degree of myocardial injury that greatly exceeds the injury induced by ischemia alone[13]."

One of the major consequences of reperfusion following ischemia is a large-scale myocardial inflammatory response. Toll-like receptors (TLR) are activated via NF-κB signaling mechanisms during ischemic injury which in turn increases expression of cytokines and chemokines within the injured heart[14]. Chemokines from TLR activation and endogenous danger signals released by necrotic cells then recruit inflammatory cell types into the injured area of the myocardium[15]. Neutrophils infiltrate the infarcted region of the myocardium rapidly after injury and peak at 1 day[13]. A number of animal studies have demonstrated that anti-neutrophil or anti-inflammatory therapies reduced infarct sizes by up to 50%[16-19].

Cardiac Remodeling

Cardiac remodeling refers to changes in the structure of the heart. A healthy heart has a mixture of different cell types that work synergistically to create the rhythmic beating of the heart. Cardiac myocytes are the heart's muscle cells that are responsible for the contraction of the heart. Cardiac fibroblasts are non-polar cells which typically lie senescent, between myocytes, quietly contributing to the makeup and turnover of extracellular matrix[6]. The extracellular matrix refers to the proteins that exist within the myocardium but outside of the

cells. This extracellular matrix creates the perfect microenvironment for the transduction of electrical signals, arrangement of cardiac myocytes and the alleviation of tension for cellular sensors of mechanical stress.

Cardiac remodeling occurs when the heart cannot meet the hemodynamic demands of the body and begins to change its structure in an attempt to compensate. A change in hemodynamic demand could result from either chronic stress due to conditions like uncontrolled hypertension, or a sudden large injury such as myocardial infarction. Remodeled hearts can normally be identified by a few characteristic features including loss of myocytes, increased fibrosis and an increase in the size of the myocytes, called hypertrophy[20]. Hypertrophy is the heart's attempt at compensating for the loss of myocytes by making the existing myocytes larger. However, hypertrophic myocytes are more prone to cellular death and hypertrophic hearts are predisposed to sudden death[21].

Despite the attempt to compensate for chronic stress or acute injury by remodeling, the remodeled heart will never regain the complete functionality that it had prior to the stressor or injury. After myocardial infarction injury, fibrotic scar material gathers in both the infarcted and non-infarcted myocardium. This deposition of fibrous material increases the rigidity of the tissue, changes the composition of the tissue, distorts the shape of the heart and its chambers and ultimately accounts for cardiac dysfunction. Initially the changes brought about by cardiac remodeling are considered to be cardiac-preserving but chronically, these changes contribute to a progressive deterioration of left ventricular function ultimately resulting in heart failure[22].

Inflammation After Cardiac Injury

Inflammation of the ischemic and reperfused myocardium occurs through innate immune pathways to orchestrate a way of clearing the injured area of necrotic cell debris as well as damaged portions of the extracellular matrix. The substantial injury to the myocardium creates endogenous signals sometimes referred to as danger signals or damage associated molecular patterns (DAMPs), which, alongside heat shock proteins, function to initiate the innate inflammatory response[23]. These DAMPs and heat shock proteins bind TLRs and a pro-inflammatory signaling cascade begins.

The danger signaling pathways that are activated by necrotic cell debris promote the influx of inflammatory cell types, namely inflammatory leukocytes. These inflammatory leukocytes are recruited due to chemotactic properties of the pro-inflammatory chemokines which are present in the injured area[23]. The C-C and CXC-motif families constitute some of the chemokines that are upregulated in the infarct area. These groups of chemokines function to recruit neutrophils and phagocytic monocytes that then clear debris from the wounded myocardium[23].

Although infiltration of neutrophils helps clear the wound from debris and apoptotic cells, excessive inflammation after reperfusion has cytotoxic effects resulting in increased proapoptotic signaling and negative outcomes[15]. Activation of neutrophils in the reperfused myocardium is associated with increased expression of cytokines, oxidative stress and the secretion of proteases, leading to exacerbation of the tissue damage[14]. This creates a predicament in trying to develop treatments that allow the inflammatory infiltration to clear the wound while also limiting the extent of the inflammatory response to avoid exacerbating injury.

Inflammatory response post-I/R associates with both positive and negative outcomes. This is suspected to be due to the nature of macrophages. Macrophages are characterized as heterogeneous in that they display a wide variety of activities and functions, differentially encompassing both pro- and anti-inflammatory roles. It is reported that reduction of infiltrating macrophages decreases inflammation, fibrosis, the extent of ventricular remodeling and furthermore dysfunction[24]. However, macrophages also play a role in wound healing processes such as angiogenesis and extracellular matrix reconstruction in the myocardium post ischemia/reperfusion injury[15].

After the first day when neutrophils dominate the injured myocardium, monocytes and monocyte-derived macrophages move into the wounded area. Macrophages can have many roles in wound healing including the removal of apoptotic cells and both the promotion and resolution of inflammation, depending on macrophage phenotype[25]. Other cell types such as dendritic cells and T-lymphocytes also migrate into the wounded area[15]. Infiltration of monocytes occurs in a highly regulated sequence. The first monocytes to infiltrate the wound after neutrophil peak are pro-inflammatory monocytes that participate in phagocytosis and proteolysis. The next wave of monocytes is largely anti-inflammatory monocytes that promote wound healing via processes such as revascularizing angiogenesis, accumulation of myofibroblasts and deposition of collagen[15]. The switch from pro-inflammatory to anti-inflammatory monocytes is referred to as resolution of inflammation.

Fibrosis After Cardiac Injury

Chronic mechanical stress or DAMPs released during acute cardiac injury can cause cardiac fibroblasts to begin to transdifferentiate into tensile, contractile, proliferative, super-

secretory myofibroblasts[26]. The transdifferentiation of fibroblasts to myofibroblasts can be triggered by mechanical stress due to changes in cardiac contractility or by cytokine signaling. One of the major cytokines attributed with the role of initiating fibroblast to myofibroblast transdifferentiation is transforming growth factor β (TGF-β)[27]. These myofibroblasts then deposit collagen either interstitially between the myocytes or specifically in a wounded area depending on the cause of cardiac stress.

While pro-inflammatory cytokines recruit cells to clear the debris, the pro-inflammatory cytokines function also to delay fibroblast transdifferentiation[6]. Once the pro-inflammatory signals subside, the cardiac fibroblasts gain unrestricted access to growth factor signaling which promotes fibroblast proliferation and transdifferentiation into the myofibroblast phenotype[6]. Myofibroblasts in the injured myocardium are suspected to arise from multiple different sources. One of the sources is the resident fibroblasts that lie senescent in the interstitium under normal conditions. They undergo activation and proliferate in response to paracrine growth signaling[6]. Fibroblasts are proposed to move in response to chemotactic stimulation via cytoskeletal reorganization and signaling through primary cilium[28].

Depending on the size of the infarct and the activity of the fibroblasts, fibroblasts can over-deposit fibrotic scar materials, namely collagen. This over-deposition of collagen accumulates in the wounded area and interrupts the electrical homeostasis of the beating heart, making it more susceptible to arrhythmias[29]. Collagens type I and III make up the complex lattice of myocardial fibrillar collagens in the extracellular matrix. The lattice of collagens ensures that the synchronized contractions of the individual myocytes are amplified into a contraction of the entire heart muscle since the myocytes are linked to this collagen network[30]. These fibrotic scar collagens do not have the contractile flexibility that cardiac myocytes do. The

collagen creates a degree of rigidity around and between the myocytes that affects the heart's ability to contract and/or relax fully.

Extracellular Matrix and Matrix-Metalloproteinases

Matrix metalloproteinases (MMPs) are enzymes that are responsible for degrading extracellular matrix proteins by proteolysis[30]. There are different types of MMPs and they each degrade different target substrates. The most commonly studied myocardial MMPs are MMP-2 and MMP-9. They are also called collagenases and gelatinases as they degrade collagen and gelatin[31]. MMPs play a very important role in normal tissue homeostasis by degrading old or damaged parts of the extracellular matrix to allow for new matrix to be formed. However, MMP expression is shown to increase under various pathological conditions including plaque rupture[31].

MMPs are secreted into the extracellular matrix in their latent proenzyme form where they await activation by serine protease before they can proteolytically degrade material[30]. The extracellular matrix accumulates latent MMPs at specific substrates depending on protein sequence and is therefore able to recruit and activate MMPs quickly if needed. Additionally, because the secreted MMPs bind to specific substrates based on sequence, the activation of MMPs can occur within specific regions or patterns within the affected myocardium[30].

Ubiquitin

Ubiquitin (UB) is a small protein of 76 amino acids and approximately 8.5 kDa. It is found in all eukaryotic cells. UB was first discovered in 1975 from bovine thymus. It was initially named "ubiquitous immunopoietic polypeptide" and was believed to be important due to its ubiquitous nature and its high degree of evolutionary conservation. The name was later

shortened as UB[32]. The UB protein contains seven lysine residues which all have the ability to be utilized for the *in vivo* chain formation associated with polyubiquitination[33]. UB is found to have 3.5 turns of α-helix, 5strands of mixed β-sheet, 7 reverse-turns and 1 shorter 3_{10} helix. Additionally, UB has a hydrophilic binding area, a hydrophobic interaction site and the protein's C-terminus ends with flexible di-glycine residues[34].

UB is well known for its intracellular role in tagging damaged, old or misfolded proteins for proteasomal degradation via a polyubiquitin tag[35]. Ubiquitination is a covalent posttranslational modification that occurs on specific residues within the target protein. Polyubiquitin chains are formed when ubiquitin proteins are covalently bound to other UB proteins, most commonly at Lys48 which is specific for proteasomal degradation, but also at the other six lysine residues for other processes[36]. A variety of UB posttranslational modifications including poly- and mono-ubiquitination on different target residues lead to diverse homeostatic processes such as recruitment of specialized polymerases, initiation of chromosomal segregation during anaphase, and tagging of proteins for degradation[37]. With all of UB's important roles it is no surprise that functional intracellular UB is critical for cellular and organismal viability with Lys-Arg mutants proving to have lethal phenotypes[38]. Since its discovery in the 1970s, UB's role within the cell has become a widely studied topic. Recently however, evidence has emerged regarding extracellular roles for UB.

Extracellular UB

UB is normally found at low levels in serum (<50 ng/mL[39]), urine and cerebrospinal fluid in humans and other mammals. Circulating UB levels increase dramatically under many pathologic conditions including parasitic infection, alcoholic liver cirrhosis and type 2 diabetes

among others[40-42]. UB levels were also found to increase in the cerebrospinal fluid of humans and pigs after traumatic brain injury[43; 44].

Extracellular UB is found to bind to cell surface chemokine receptor CXCR-4 in THP-1 human monocytic leukemia cells[45] as well as other cell types. CXCR-4 is a protein consisting of 352 amino acids. It has seven transmembrane helices organized into a central bundle which is similar to other G-protein coupled receptors[46]. It is able to form both homo- and hetero-dimers to receive inhibition or activation signals from ligands[47; 48]. Protein modeling software alongside site-directed mutagenesis showed that CXCR-4 interacts with UB via Phe20, Phe189 and Lys271, while competitive binding assays determined that UB requires Phe4 and Val70 to interact with CXCR-4. UB-CXCR-4 axis utilizes a two site binding mechanism. The first binding event functions to connect extracellular loops on CXCR-4 with critical binding sites, Phe4 and Val70 on UB. The second binding event functions to activate the receptor and is proposed to occur when the flexible diglycine C-terminus falls near the third of CXCR-4's extracellular loops, altering the conformation of CXCR-4 and triggering a "switch" in an intracellular loop, thus activating a G protein signaling cascade[49].

Extracellular UB is suggested to have many functions including immune regulation, antimicrobial activities and anti-inflammatory activities[33]. High levels of circulating UB are found to correlate with increased survival in patients with burn injury[50]. UB is also found to have a pro-survival and anti-inflammatory role in lethal endotoxemia animal models[51]. UB treatment of whole blood and peripheral blood mononuclear cell cultures exposed to lipopolysaccharide reduced the expression of tumor necrosis factor α (TNF-α), a major cytokine often responsible for the onset of an inflammatory response[52]. The discovery of UB levels increasing under pathological conditions paired with the discovery that UB has anti-inflammatory and perhaps

pro-survival effects is intriguing and warrants attention with regard to ischemia/reperfusion injury due to its highly inflammatory nature.

Extracellular UB induced lymphocyte differentiation of B-cells *in vitro* and T-cells *in vitro* and *in vivo*[32; 53]. Treatment with extracellular UB decreased expression of TNF-α post-injury in a trauma model as well as an endotoxic shock animal model[51; 54]. In a model of rat pulmonary ischemia/reperfusion, treatment with intravenous UB improved lung function and increased expression of anti-inflammatory cytokine, interleukin-10[55]. Extracellular UB treatment of hematopoetic cells is noted to result in growth arrest via apoptosis and potentially the proteosome pathway[56]. Treatment of rats with intravenous UB after suffering focal cortical contusion brain injuries resulted in significant decreases in contusion volume as well as significant improvements in brain morphology at 7 days post-injury[57].

Extracellular UB: Role in β-AR Stimulated Myocyte Apoptosis and Myocardial Remodeling

The β-adrenergic receptors (β-AR) are a family of transmembrane receptors that receive signals from catecholamines such as epinephrine and norepinephrine. In the heart, β-AR agonists are responsible for increases in chronotropy, inotropy, and dromotropy meaning heart rate, pump force and cardiac conduction velocity, respectively. Typically, β-AR stimulation is transient and is available to increase the workload on the heart for physically demanding tasks like running. However, amplified β-AR stimulation is often sustained in the heart after cardiac injury or during heart failure in an attempt to compensate for the decrease in pumping efficacy by increasing pump frequency and vigor. This chronic β-AR stimulation stresses the heart and causes the death of cardiac myocytes and adverse restructuring of the heart, cardiac remodeling. Isoproterenol (ISO) is a chemical β-AR agonist. ISO injections have been used as a model of cardiac injury

and have been noted to create infarct-like lesions in the myocardium of rats as well as increase myocyte death and myocardial fibrosis in mice[58].

Myocardial ischemia can trigger the release of catecholamines that cause fluctuations in cardiac function[59]. Sustained myocardial ischemia is associated with the accumulation of norepinephrine which is thought to be released by a local, non-exocytotic mechanism[60; 61]. The release of norepinephrine is found to generate oxidation products that increase the rate of myocardial injury[62; 63].

Prolonged stimulation of β-AR is also shown to be cytotoxic, causing apoptosis of adult rat ventricular myocytes via the c-Jun NH_2terminal kinase dependent mitochondrial death pathway[64; 65]. Our lab previously reported that in isolated adult rat ventricular myocytes (ARVMs), sympathetic stimulation via β-AR agonist, ISO, induces apoptosis via the mitochondrial death pathway[65]. Additionally, our lab reported ISO increases myocardial apoptosis in mouse hearts *in vivo*[66].

It was observed that in culture, only ~15-20% of ARVMs underwent apoptosis despite all of the ARVMs being exposed to the same ISO conditions. This led to the hypothesis that the apoptotic ARVMs were secreting survival factors. Analysis of conditioned media using 2D gel electrophoresis followed by sequencing of a protein, ARVMs exposed to ISO were found to secrete higher levels of UB vs control. Treatment of ARVMs with UB inhibited β-AR stimulated apoptosis[65]. Extracellular UB was found to inhibit signaling pathways activated by β-AR stimulation including GSK-3β and downstream, JNKs[65]. This finding prompted investigation into the potential for UB as a therapeutic agent in cardiac disease models.

Our lab also studied a mouse model of β-AR stimulation using chronic ISO infusion and found UB to modulate ISO-mediated increases in cardiac function, myocyte apoptosis and

myocardial fibrosis after 7 days of ISO stimulation. The ISO stimulated group had large interstitial lesions of fibrosis while the UB+ISO group had significantly less fibrosis. UB+ISO also had significantly fewer apoptotic myocytes vs ISO group. Animals that received UB+ISO experienced anti-apoptotic signaling similar to the *in vitro* study, including increased activation of Akt and decreased activation of GSK-3β and JNK. The decrease in fibrosis in UB+ISO group associated with increased expression of MMP-2, MMP-9 and the tissue inhibitor of metalloproteinases 2 (TIMP-2)[66].

Specific Aims

The overall goal of this investigation was to determine if UB has the potential to reduce damage of the heart after I/R injury (Fig. 1.1). Inflammation and ECM deposition are essential events of infarct healing post-I/R injury. These events are modulated mainly by inflammatory cells (neutrophils and macrophages) and fibroblasts.

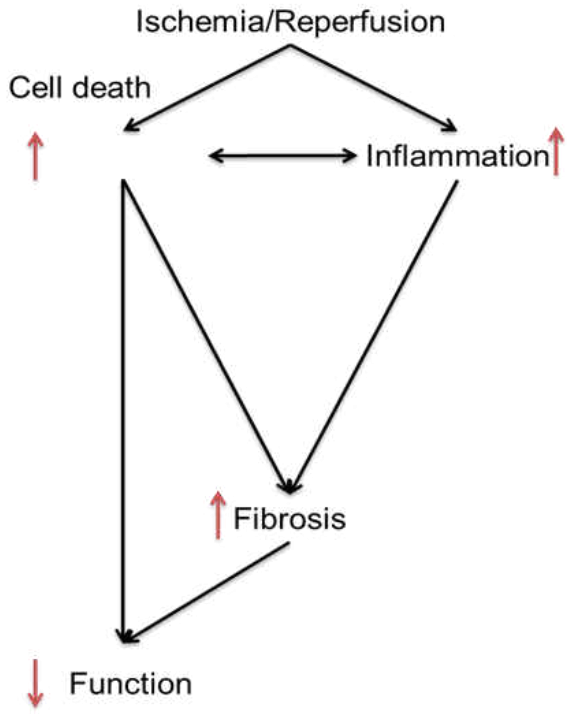

Figure 1.1 Schematic Diagram Illustrating Effects of I/R Injury

We hypothesized that UB treatment would result in decreased infarct size, reduced inflammation, decreased fibrosis, less myocyte death and therefore improvement in heart function following myocardial I/R injury (Fig. 1.2). The specific aims of this study were: 1) to validate a method of consistently measuring *in vivo* myocardial ischemia and reperfusion events in real time; 2) use *in vivo* assays to determine if UB treatment reduces damage and improves outcomes of myocardial I/R injury in adult male mice; and 3) use *in vitro* assays to determine if

UB interacts with fibroblasts via CXCR-4 receptor to exert phenotypic changes.

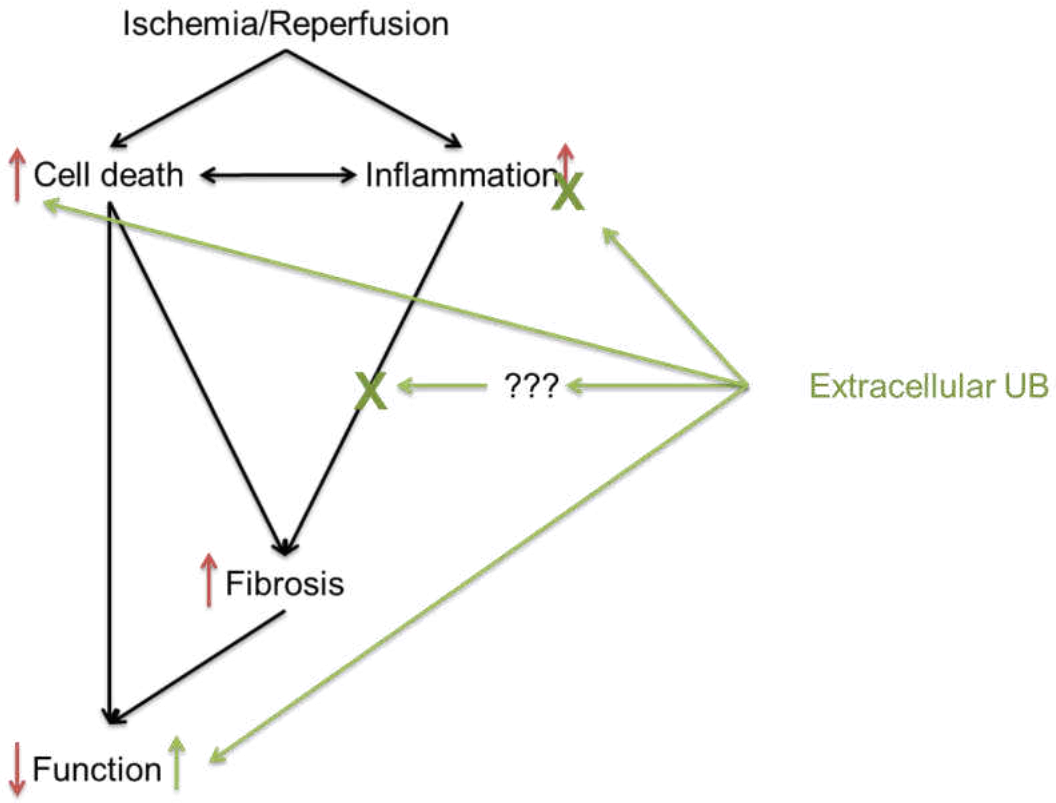

Figure 1.2. Hypothesis: Schematic Diagram Illustrating Hypothesized Effects of UB on I/R Injury

CHAPTER 2

CONFIRMATION OF MYOCARDIAL ISCHEMIA AND REPERFUSION INJURY IN MICE USING SURFACE PAD ELECTROCARDIOGRAPHY

Stephanie L.C. Scofield[1], Krishna Singh[1,2,3,#]

[1]Department of Physiology, James H Quillen College of Medicine

[2]James H Quillen Veterans Affairs Medical Center

[3]Center of Excellence for Inflammation, Infectious Disease and Immunity

East Tennessee State University

Johnson City, TN 37614

Running Title: Mouse ECG during myocardial ischemia/reperfusion injury

Key words: Heart; Electrocardiogram; Ischemia/Reperfusion; Ischemia/Reperfusion Injury; Myocardial Infarction

#Correspondence: Krishna Singh, Ph.D., FAHA
Dept of Biomedical Sciences
James H Quillen College of Medicine
East Tennessee State University
PO Box 70582, Johnson City, TN 37614
Ph: 423-439-2049,
Fax: 423-439-2052
E-mail: singhk@etsu.edu

SHORT ABSTRACT:

During murine myocardial ischemia/reperfusion surgery, correct placement of the occluding ligature is typically confirmed by visible observation of myocardial pallor. Herein, a method of electrocardiographically confirming ischemia and reperfusion, to supplement observed myocardial pallor, is demonstrated in male C57Bl/6 mice.

LONG ABSTRACT:

Many animal models have been established for the study of myocardial remodeling and heart failure due to its status as the number one cause of mortality worldwide. In humans, a pathologic occlusion forms in a coronary artery and reperfusion of that occluded artery is considered essential to maintain viability of the myocardium at risk. Although essential for myocardial recovery, reperfusion of the ischemic myocardium creates its own tissue injury. The physiologic response and healing of an ischemia/reperfusion injury is different from a chronic occlusion injury. Myocardial ischemia/reperfusion injury is gaining recognition as a clinically relevant model for myocardial infarction studies. For this reason, parallel animal models of ischemia/reperfusion are vital in advancing the knowledge base regarding myocardial injury. Typically, ischemia of the mouse heart after left anterior descending (LAD) coronary artery occlusion is confirmed by visible pallor of the myocardium below the occlusion (ligature). However, this offers only a subjective way of confirming correct or consistent ligature placement, as there are multiple major arteries that could cause pallor in different myocardial regions. A method of recording electrocardiographic changes to assess correct ligature placement and resultant ischemia as well as reperfusion, to supplement observed myocardial pallor, would help yield consistent infarct sizes in mouse models. In turn, this would help decrease the number

of mice used. Additionally, electrocardiographic changes can continue to be recorded non-invasively in a time-dependent fashion after the surgery. This article will demonstrate a method of electrocardiographically confirming myocardial ischemia and reperfusion in real time.

INTRODUCTION:

Heart disease remains the leading cause of death worldwide[1,2]. Not only is the left ventricle (LV) the most muscular chamber, responsible for pumping blood from the heart to the entire body[3], it is a common cardiac injury site post-myocardial infarction[4]. Left ventricular tissue death often results in systolic heart failure. Animal models of heart disease are imperative for the advancement of biomedical cardiovascular research. The C57Bl/6 strain of mice have been a popular choice for animal models due to their quick breeding time, low cost and ease in genetic alterations. Most murine surgical models for the study of heart disease involve occlusion of the LAD branch of the left coronary artery. The LAD is sometimes called the left obtuse marginal[5,6]. The LAD supplies blood to the left ventricular anterior and antero-lateral walls. LAD occlusion studies are aimed at inducing anterior infarctions, sometimes extending into the inferior and lateral wall regions[7].

Two models that are used frequently for myocardial infarction studies include chronic occlusion myocardial infarction and myocardial ischemia/reperfusion injury. The chronic occlusion is created by surgically suturing around and permanently blocking blood flow through the LAD. The ischemia/reperfusion injury is created much in the same way only with a transient, usually 30-60 min, ischemic period. To achieve transient ischemia, the occluding suture ties around the

LAD and a small PE-10 tube which is placed parallel to the LAD on the epicardial surface of the heart, followed by a reperfusion period where the tubing and occluding suture is removed and blood is allowed to once again flow through the artery and into the myocardium. The ischemia/reperfusion surgery has been deemed to be clinically relevant due to the nature of reperfusion injury paralleling the treatment of human infarctions which includes prompt coronary angioplasty and stenting of the artery, or coronary artery bypass. Typically, during these surgeries, ischemia of the LV in a mouse heart is confirmed by visible pallor of the myocardial wall. However, by simply performing the surgeries on an electrocardiogram (ECG) pad under constant monitoring conditions, visible changes can be observed in the ECG waveform, thereby confirming ischemia and reperfusion of the mouse myocardium.

Although the murine heart is similar to the human heart in many respects, including its four-chambered structure, the hearts also have differences. One obvious difference is the average resting heart rate of adult mice is 600-700 beats per min (bpm) whereas that of adult humans is ~60-100 bpm[8,9]. Additionally, in mice the repolarization waves, J and T, often merge with the depolarization QRS-complex making a clear ST-segment difficult to discern[10]. To complicate the process of electrocardiographically confirming myocardial ischemia, it is the elevation of the T-wave and the ST-segment which are used as markers for the diagnosis of ischemia and myocardial infarction injury in humans, clinically referred to as ST elevation myocardial infarction or STEMI. One of the key differences between human and murine waveforms is that S-wave is immediately followed be a J-wave that transfers directly into a negative T-wave. During acute myocardial ischemia in mice the amplitude of S-wave decreases and is directly followed by an abnormal J-wave and an inverted T-wave[11]. The T-wave does not seem to

represent a significant portion of the repolarization in mice[11]. Despite nomenclature and mouse vs. human differences, ECG confirmation of murine myocardial ischemia and reperfusion is still feasible and relatively simple. For the sake of simplifying waveform interpretation, the segment between the S-J-T is referred to as ST-segment herein.

STEMI guidelines published in 2013 recommend a patient door-to-balloon time of less than 90 min[12].This means that the time frame from the identification of the patient's coronary artery occlusion until the artery is reopened should be less than 90 min. The beating heart is constantly working and therefore, has a high oxidative metabolism and a high level of oxygen consumption[3]. To provide for this, a network of capillaries is available to each myocyte[3]. It only takes a heart a few beats to exhaust its oxygen and nutrient supply. In a 90 min window, an ischemic heart region in a human will have been blocked from receiving between 5,400 and 9,000 heart beats worth of oxygen-rich blood. In that same 90 min window, a mouse would have 54,000 to 63,000 heart beats. Experimental time points for murine ischemia/reperfusion injury are typically between 30 and 60 min.

The importance of developing a supplemental method of confirming myocardial ischemia and reperfusion in a murine model has profound implications on the consistency and reproducibility of data in myocardial ischemia/reperfusion studies. The current practice of visually observing the heart for a change in tissue color is not adequate as a stand-alone diagnostic. Additionally, reperfusion after removal of the tubing and suture is not guaranteed. Although the artery is no longer tied off, the artery may have sustained damage during the procedure and may become impossible to reperfuse. It would be beneficial to have a record of electrocardiographic changes

to confirm reperfusion rather than relying on observations of myocardial pallor and rubor (red color). Hearts that do not show the markers of ischemia/reperfusion injury can then quickly be flagged and a decision on how to proceed can be made by the investigators.

Lastly, establishing a record of ECG changes from baseline throughout the ischemic and reperfusion periods allows investigators to continue to monitor the heart after the initial surgery. Investigators currently lose sight of the heart as soon as the surgery is completed. ECG is a simple way to gain insight into changes occurring in the myocardium hours to days after the surgery. ECG recorded at time points after surgery could reveal late-developing Q-waves indicating continued or worsening tissue death. However, to effectively gage new or worsening electrocardiographic markers, a baseline ECG must be available for comparison.

This protocol will demonstrate how to prepare, obtain, and interpret the ECG to confirm ischemia and reperfusion of the mouse heart using 8-12 week old male C57Bl/6 mice.

PROTOCOL:

All surgical procedures performed on animals should be carried out in accordance with Guide for the Care and Use of *Laboratory Animals*[13] *or other appropriate ethical guidelines. Protocols should be approved by the animal welfare committee at the appropriate institution before proceeding.*

1. Preparing for the ECG

Before beginning, don personal protective equipment including gloves, eyewear and a clean laboratory coat or disposable gown.

1.1. Clean the ECG pad using a non-alcohol and non-bleach based decontamination solution. Gently use a delicate task wipe to blot off excess solution to ensure that the electrode pad does not become damaged.

1.2. If the ECG pad has a heating feature, use it. Anesthetized mice tend to lose body heat rapidly. Heat the pad to 42 °C to maintain normothermic body temperature of 37 °C throughout the surgery[14]. Monitor the mouse to make sure the mouse's skin is not burning, adjust pad temperature as necessary. Body temperature can be monitored using a rectal thermometer probe.

1.3. As most thoracotomies are performed with the mouse lying on its back (supine), ensure that the toggle is flipped to the "supine" setting. Many ECG pads have a function to toggle between prone and supine positions. Failure to select the right orientation can result in misrepresentation of electrocardiographic events.

1.4. Anesthetize mouse using 5% inhaled isoflurane and 1 L/min Oxygen. Once mouse is anesthetized, transfer mouse to ECG pad equipped with an anesthesia nose-cone and reduce isoflurane to 2% and 1 L/min Oxygen. Confirm proper anesthesia by ensuring mouse does not react when the mouse's foot is pinched with forceps.

1.5. Apply a thin coat of eye lubrication ointment over the mouse's eyes to prevent dryness and corneal damage while anesthetized.

1.6. Clean the mouse's paws with a wet wipe to remove all visible bedding that may be stuck to the paws or may interfere with the transmission of electrical impulses from the paws to the ECG pad. Dry paws with a wipe.

1.7. Apply a small amount (slightly smaller than a USD dime) of highly conductive electrolyte gel to each of the four metallic electrodes on the ECG pad.

Note: Be sure to only apply a small amount of gel as too much gel makes it difficult to restrain the paws to the pad using tape. Additionally, paws are likely to slip out of the restraint during surgery if they were wet before applying tape.

1.8. With the mouse in supine position, use clear medical tape to restrain each paw to its corresponding electrode (Figure 1). First press each paw to its piece of tape and then adhere the tape to the ECG pad. Ensure that each restrained paw is in contact with the electrolyte gel and the electrode.

2. Acquiring the ECG

2.1. Depending on the equipment used for ECG acquisition, there may be different ways to configure the machine so that the ECG waveform can be visualized in real time.

2.1.1. For ECG recordings using the physiologic monitoring settings on an echocardiography machine, a live B-mode image will have the ECG waveform running along the bottom of the screen.

Note: See individual machine user guides to determine how best to configure that equipment.

2.2. Enable real time visualization of ECG waveform by pressing the B-mode key on an echocardiography machine or the equivalent on other ECG recording devices.

2.2.1) Adjust the resolution to account for differences in amplitude. If the peak of the R-wave or the trough (valley) of the Q-wave are out of the visual frame, adjust the resolution until the entire height of the waveform can be observed.

Note: This can be done under the physiological settings tab on an echocardiography machine. Click the increase or decrease arrows until the entire waveform is visible.

2.3. Any time that an image is to be obtained, clear the ECG pad of tools. Touching the mouse during ECG recording with forceps or fingers will disturb the waveform. Ensure that the mouse is still and untouched on the ECG pad before recording any ECGs.

2.4. Use the machine's "record" or "store" feature before making any surgical incisions on the mouse. This image will be used as a baseline for comparison later on.

3. *Surgical Procedure and Recording ECG*

3.1. Inject anesthetized mouse with analgesic (Buprenorphine, 1.5 μg, intraperitoneal) before beginning. The details of the ischemia/reperfusion surgical procedure can also be found elsewhere[5].

3.2. Remove hair around the surgical site chemically or mechanically and disinfect the area with betadine solution. Use a scalpel to make a vertical incision parallel to the esophagus and trachea. Gently move the lymph nodes to each side of the incision until the thin tissue covering the trachea is exposed. Using forceps, gently separate the tissue until the white cartilage rings of the trachea are visible.

Note: Chemical hair removal has been used in our laboratory because high resolution echocardiography (which can detect hair follicles) is performed before surgery and before endpoint. If using chemical hair removal, rinse skin thoroughly with saline or water to ensure that the chemical hair removal agent has been washed off. Skin burns can occur if the chemical agent is left on the skin.

3.3. Quickly remove the mouse's nose from the nose-cone and insert ventilation tubing into the mouth of the mouse and towards the throat. When the tip of the ventilation tubing is visible

through the exposed neck area, align the tube with the start of the trachea. Gently wiggle the tube side to side while applying upward pressure until the tubing slides into the trachea which can be confirmed visually through the translucent trachea.

3.4. Ensure that the mouse remains anesthetized during the intubation procedure. Pause from intubation and return the mouse to the nose-cone if it begins to stir.

3.5. Using a loop of string, hook the mouse's two front teeth through the loop and tape the string ends to the ECG pad to steady the head of the mouse and to ensure the ventilation tubing does not move during surgery. Quickly attach ventilation tubing to rodent ventilator and adjust ventilation settings according to the weight of the mouse. Tape ventilation tubing in place.

3.6. Cover the mouse's exposed trachea with a gauze soaked in warm saline to keep tissue from drying.

3.7. Make a vertical incision using a scalpel along the left side of the sternum.

3.8. Using forceps, gently separate the fascia layer from the muscle layer. Carefully cut the underlying muscle layers without cutting visible blood vessels.

3.9. Using forceps, grab the third rib and pull upwards gently. Maintain grip on the rib with one hand and use surgical scissors to carefully cut the intercostal tissue between the third and fourth rib. Ensure that the lungs are not damaged.

Note: Lungs will retract deep into the chest cavity almost immediately after the chest cavity is punctured by the surgical incision due to the loss of the pressure gradient. Wait until the lungs have retracted before continuing.

3.10. Use forceps to grab and gently separate the thin layer of pericardium which surrounds the heart.

3.11. Insert retractors or manually use forceps as rib retractors to move the ribs into a position where the heart is visible between the ribs.

Note: It is common practice to move the mouse's lower left paw so that it is overlapping the lower right paw during the placement of the ligature. This helps to position the heart so that the left atrial appendage, or auricle, is easily visible during placement of the ligature. Be aware that valid ECG waveforms will not be obtained while the lower left paw is off of the electrode. For this reason it is advisable to return the paw to its electrode after the suturing ligature is passed through the myocardial tissue but before a knot is tightened.

3.12. Locate the LAD visually, beneath the left auricle. Swiftly insert a 7-0 silk tapered suturing needle into the myocardium deeply enough to pass under the LAD but not so deep as to penetrate the LV cavity. Pull the suturing ligature through until there is about 4 cm of suturing silk left on the free (non-needle) end of the suturing ligature.

3.13. Begin to tie a simple suture knot. Once the free end of the suturing silk has been pulled through the loops to form the knot, pause.

3.14. Holding both the free and needle ends of the suturing silk with forceps, insert a ~1 cm section of PE-10 tubing underneath the forming knot and atop the epicardial surface.

3.15. If the mouse's left paw is crossed, return the paw to its proper electrode. Tighten knot so that the PE-10 tubing is sutured to the heart. Release all physical contact with the mouse to allow ECG to be recorded.

3.16. Allow ECG waveform to cycle through for ~10 sec. Check ECG waveform visually and record waveform as "Time of Occlusion". If the T-wave does not increase in amplitude within 1 min, reassess placement of ligature and make a decision on how to proceed.

Note: If the T-wave amplitude does not increase, investigators should either discard the animal from the study or attempt to correct the ligature placement.

3.17. Visually check the color of the myocardium to confirm ischemic paling of the LV.

3.18. If ECG changes and myocardial color changes indicate ischemia, double knot the suture around the PE-10 tubing.

3.19. Cover the open chest cavity with warm saline gauze.

3.20. Record ECG every 5-10 min for the duration of the ischemic period.

4. Confirmation of Reperfusion Using ECG

4.1. Remove saline gauze covering the chest cavity and visualize the heart.

4.2. Use a blade to cut the suturing silk atop the PE-10 tubing. Once the ligature is cut, remove the section of PE-10 tubing and gently remove the suturing ligature from the myocardium.

4.3. Release all physical contact with the mouse and allow the ECG waveform ~10 sec to cycle. Record waveform as "Time of Reperfusion." Continue to record ECG waveforms every 5-10 min until the desired experimental time point is reached.

4.4. Adjust resolution for changes in amplitude as needed. If the T-wave does not change upon removal of the PE-10 tubing and ligature, reperfusion is not confirmed. Make a decision about how to proceed.

Note: If the T-wave does not change upon removal of tubing, investigators should discard the animal from the study or attempt to correct the ligature placement.

4.5. Visually inspect myocardium to additionally confirm reperfusion by return to red color.

4.6. Close chest cavity by suturing the intercostal space with a 5-0 silk suture while applying gentle pressure to the mouse's chest to expel excess air that has entered during surgery. Then suture the muscle layers and finally, skin.

Note: Applying pressure to the chest cavity may not be sufficient to evacuate the chest cavity of air in all mice. Therefore, the syringe and needle method of evacuation should be employed to ensure that all air has been expelled.

4.7. Record the last ECG before turning inhaled anesthesia off and removing the mouse's paws from the electrodes. Increase oxygen to 2 L/min and maintain ventilation until the mouse regains consciousness.

4.8. Allow mouse to recover in a constant temperature controlled environment, e.g. heating pad or warm incubator, to avoid infarct variability. Treat mouse with buprenorphine 24 hours after the surgery and then as needed as indicated by the mouse grimace scale.

Note: Procedure for reperfusion is also discussed in detail by Xu *et al.*[5]

REPRESENTATIVE RESULTS:

A normal murine ECG is displayed in figure 2 with alphabetic markers for electrical events P, Q, R, S, J and T. P is the initial atrial depolarization. QRS is the wave of depolarization over the ventricles. J is early repolarization and T represents heterogeneous repolarization also known as

recovery[11]. It should be noted that many labs do not use the J-wave nomenclature and instead refer to the SJT-segment as the ST-segment[10,15-17]. Here, results and analyses are representative and based off of laboratory observations of 40 mice. Most mice exhibited similar waveform progressions over the course of the surgery. Mice that did not exhibit similar waveforms were flagged for further analysis and were considered non-infarcted animals. Similar waveform results have also been reported by Jong *et al.*[15].

Murine hearts suffering from regional ischemia due to LAD occlusion typically show increased amplitude of the R-wave as well as hyperacute peaking of the JT-segment followed by eventual elevation of the ST-segment. Figure 3 shows the first sign of acute myocardial ischemia; hyperacute peaking of the T-wave. As can be seen in this figure, the T-wave has increased in amplitude from baseline conditions. However, this is not yet ST-segment elevation because the S-wave is still projecting deeply and negatively as it does on the baseline waveform.

Baseline ECG configuration displays a negatively projecting S-wave (Figure 2). As time progresses, ECG changes are noted. The ST-segment is defined as the segment between the end of the S-wave and the start of the T-wave. This ST-segment is clear in humans. Due to high heart rate, this segment is merged in mice and an additional, early repolarization "J-wave" separates the S- and T-waves. Therefore, the elevation of the S-wave to the isoelectric line or higher should be considered as the murine version of ST-segment elevation. In figure 4 the progression of ischemia to early infarction can be seen by ST-segment elevation. Here the S-wave is displaying at elevated amplitude, above the isoelectric line. The J-wave is also elevated,

especially when compared to the baseline waveform (Figure 2). Therefore, the ST-segment is elevated which is indicative of injury/infarction[10].

Figure 5 follows the progression of one mouse from baseline all the way through reperfusion. The first waveform displays a normal sinus rhythm which was the recorded baseline. The second waveform displays the ECG 1 min after the ligature was tied and the artery became occluded. The red circle on this line indicates hyperacute T-wave peaking. If compared with "Baseline," it is clear that the T-wave is elevated. The third waveform shows the complete ST-segment elevation at the 5 min time point. In the "1 min Ischemia" image, the S-wave was still projecting negatively, passing the isoelectric line. However, at 5 min the S portion of the complex does not reach as far negative as it should before progressing into the J- and T-waves. This is described as ST-segment elevation because the segment between the S- and T-waves is elevated from the isoelectric line. Another electrophysiological marker of regional ischemia is widening of the QT-interval[16] which extends from the beginning of the QRS complex and continues until the end of the T-wave. At 20 min of ischemia, the QT-interval has widened and the ST-segment is still elevated. After 45 min of ischemia, the QT-interval remains widened and the ST-segment remains elevated.

Reperfusion of myocardium that has been ischemic for 30 min or less should result in the ECG returning back to baseline conditions in a mouse. Preda and Burlacu established a correlation between murine electrocardiographic changes, ischemic time, and infarct severity[17]. It was observed that ischemic periods of 30 min did not cause permanent ECG changes whereas ischemic periods of 1 hr did cause permanent ECG changes. Additionally, reperfusion of the

occluded artery after 24 hr of ischemia had no salvage effect[17]. Normally, Q-waves can be identified as the slight downward projection just before the depolarization QRS-complex. Significant, or pathologic Q-waves can develop shortly after onset of myocardial ischemia as considerable muscle death begins to set in[10]. Significant Q-waves are defined as at least 1/3rd of the height of the corresponding R-wave or by their elongated time, resulting in a wide Q-wave. The significant Q-wave results from a region of dead myocardium deflecting electrical currents away from the electrode[7]. After 5 min of reperfusion, evidence of deep, significant Q-waves begin to appear (Figure 5). Additionally, the T-wave returns to the isoelectric line (Figure 5). After 30 min of reperfusion, the negative Q-waves remain and are likely showing permanent damage. At this time point, the Q-waves are wide and deep, and indicate that the dying heart tissue is deflecting electrical currents around the damaged area (Figure 5).

After continuous ischemia, the progression to injury and infarction leads to enhanced negative T-wave projection (Figure 5, 30 min reperfusion, second red circle). This enhanced T-wave projection due to a true infarction will usually be permanent[7]. The second red circle in the 30 min reperfusion waveform shows what appears to be an inverted T-wave (Figure 5). If the 5 and 30 min T-waves are compared it is clear that the T-wave is projecting more negatively. This, coupled with the significant Q-waves provides evidence for permanent tissue damage to this heart. It should be noted that inhaled isoflurane anesthesia reduces heart rate, and therefore increases QT-intervals. However, amplitude of recovery T-waves remains unaffected[18].

The aforementioned changes can be quantitatively analyzed in terms of voltage. Figure 6 shows that exporting physiological data as a .csv file will provide a very large amount of data. In

addition to offering ECG values (amplitudes) at fractions-of-millisecond rates there may be options to include other data from respirations, temperature probes, blood pressure cuffs etc. if so desired. These quantitative data can be graphed as shown in Figure 7. Graphing a series of waveforms from P-wave to P-wave helps visualize an ECG configuration trend. The time period of 500 ms is a good time frame to visualize since any less time may not result in enough waveforms and any additional time will make the graph appear cluttered and electrophysiological events may be missed or difficult to recognize when viewed on a standard computer monitor.

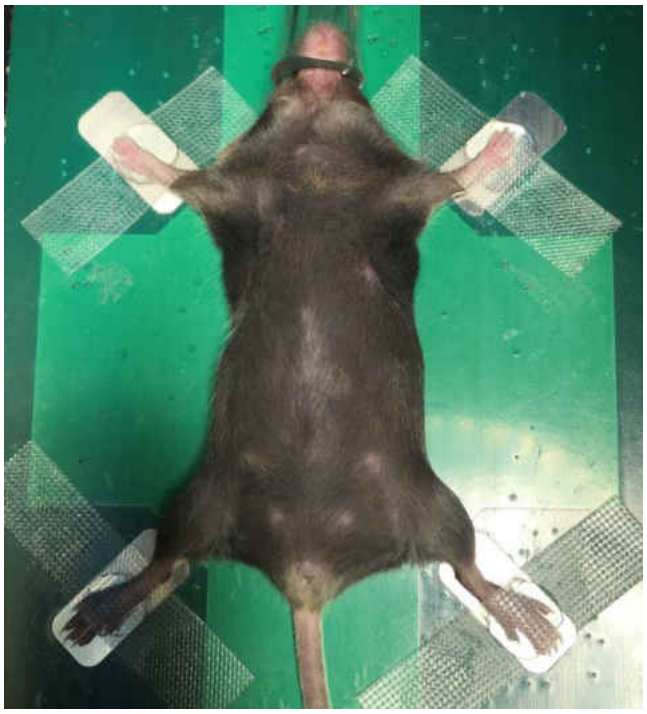

Figure 2.1. Correct placement of mouse on ECG pad. This mouse is positioned in supine position. Each one of the mouse's paws are taped to the corresponding electrodes on the ECG surface pad.

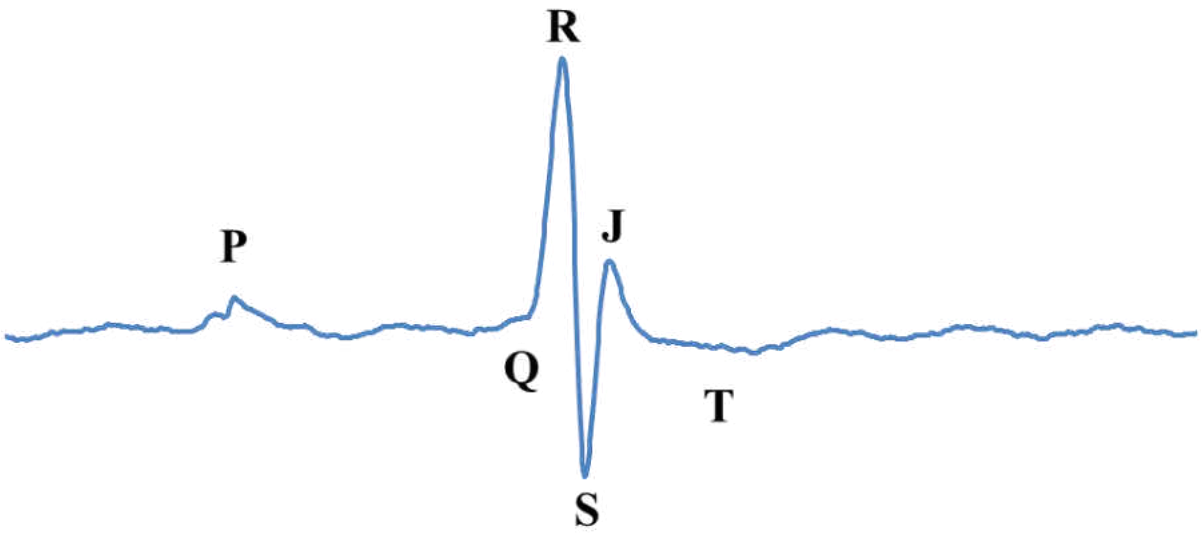

Figure 2.2. Normal murine baseline ECG waveform. The normal murine baseline ECG is labeled with the letters P, Q, R, S, J and T which are used to describe electrical events in the heart.

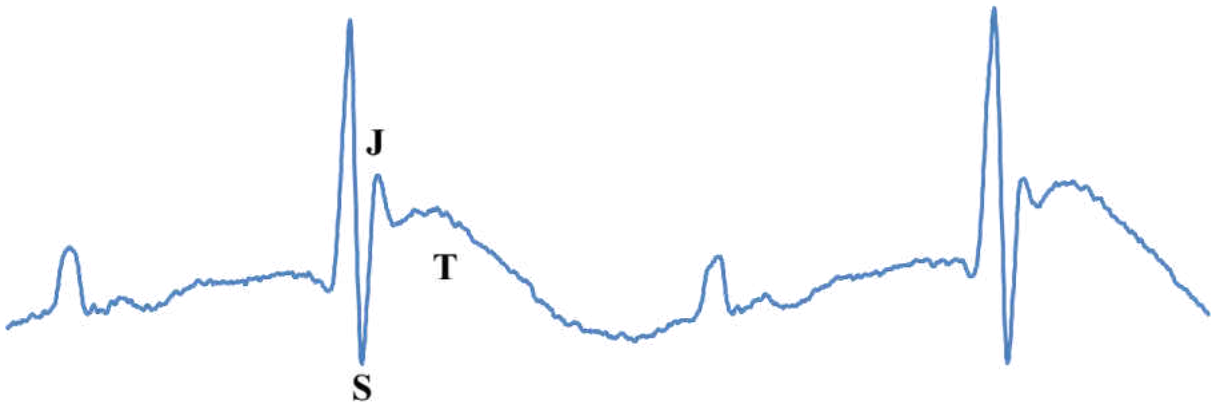

Figure 2.3. T-wave elevation. Also known as hyperacute T-wave or peaking. The T-wave is amplified and higher than the baseline T-wave (Figure 2).

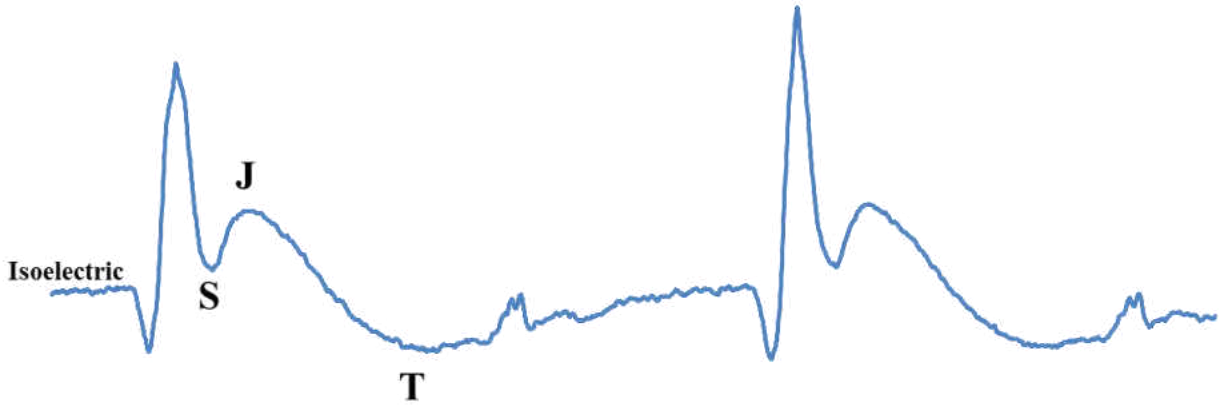

Figure 2.4. ST-segment elevation. This figure displays ST-segment elevation which can be observed as the ST-segment is higher than the isoelectric point.

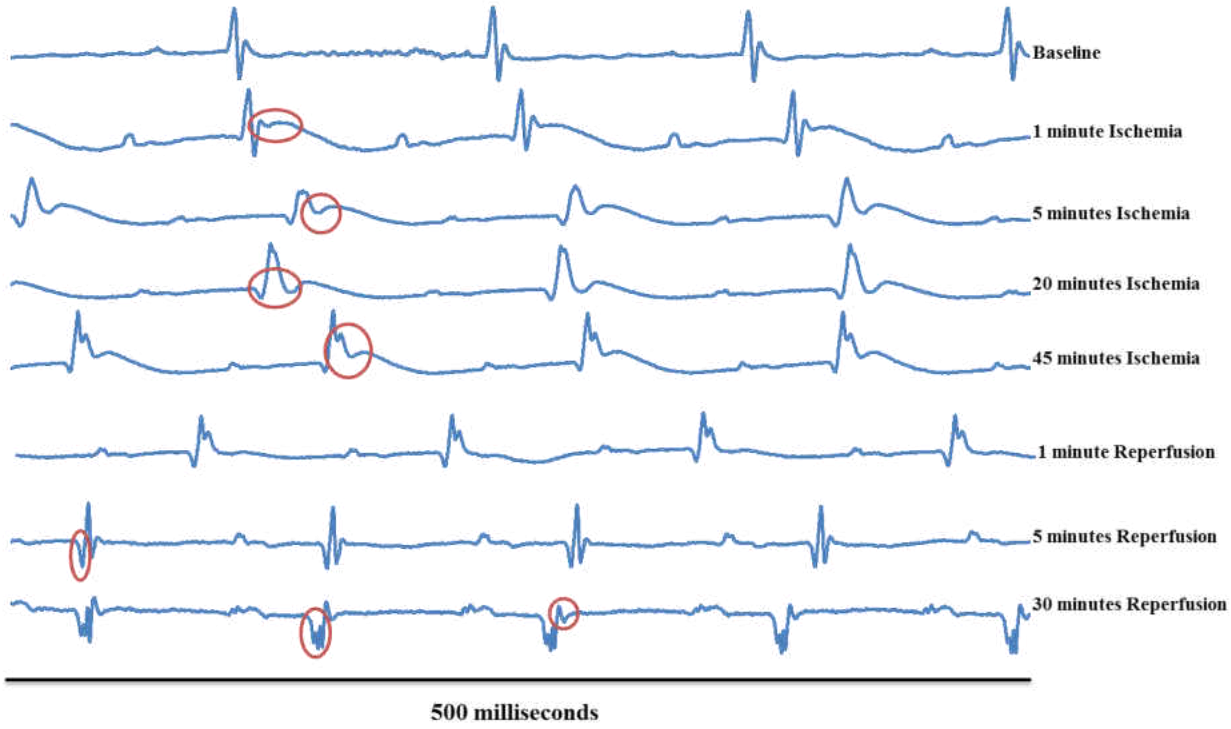

Figure 2.5. Typical ECG changes over the course of an ischemia/reperfusion surgery. This figure follows one mouse over the duration of myocardial Ischemia/Reperfusion surgery. The first waveform displays a normal sinus rhythm which was the recorded baseline (Baseline). The second waveform (1 minute Ischemia) displays the waveform 1 min after the ligature was tied and the artery became occluded. The red circle on this line shows hyperacute T-wave peaking. The red circle on the third waveform (5 minutes Ischemia) displays the complete ST-segment elevation. The red circle on the fourth waveform (20 minutes Ischemia) displays a widened QT-

interval and the S-wave is still elevated. The red circle on the fifth waveform (45 minutes Ischemia) displays widened QT-segment and elevated ST-segment. The sixth waveform (1 minute Reperfusion) displays no significant changes versus 45 minutes ischemia. The red circle on the seventh waveform (5 minutes Reperfusion) displays deep, significant Q-wave form. The first red circle in the eighth waveform (30 minutes Reperfusion) displays significant Q-waves, while the second red circle displays possible T-wave enhancement.

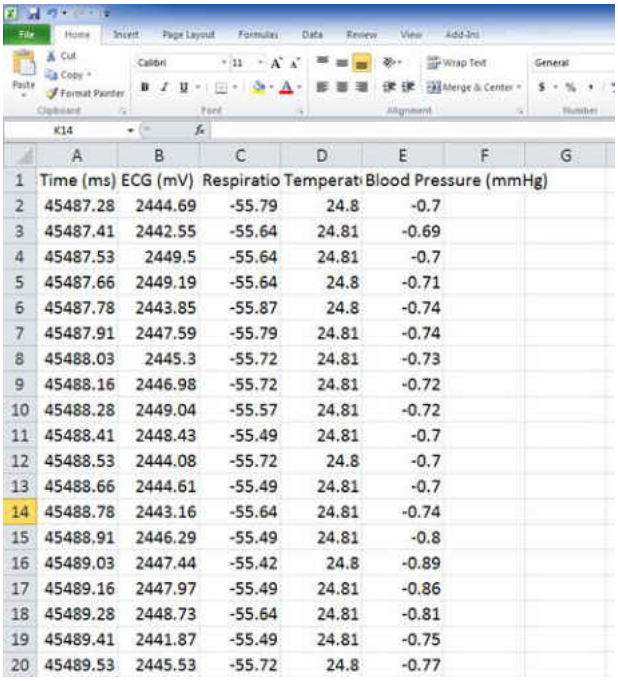

	A	B	C	D	E	F	G
1	Time (ms)	ECG (mV)	Respiratio	Temperati	Blood Pressure (mmHg)		
2	45487.28	2444.69	-55.79	24.8	-0.7		
3	45487.41	2442.55	-55.64	24.81	-0.69		
4	45487.53	2449.5	-55.64	24.81	-0.7		
5	45487.66	2449.19	-55.64	24.8	-0.71		
6	45487.78	2443.85	-55.87	24.8	-0.74		
7	45487.91	2447.59	-55.79	24.81	-0.74		
8	45488.03	2445.3	-55.72	24.81	-0.73		
9	45488.16	2446.98	-55.72	24.81	-0.72		
10	45488.28	2449.04	-55.57	24.81	-0.72		
11	45488.41	2448.43	-55.49	24.81	-0.7		
12	45488.53	2444.08	-55.72	24.8	-0.7		
13	45488.66	2444.61	-55.49	24.81	-0.7		
14	45488.78	2443.16	-55.64	24.81	-0.74		
15	45488.91	2446.29	-55.49	24.81	-0.8		
16	45489.03	2447.44	-55.42	24.8	-0.89		
17	45489.16	2447.97	-55.49	24.81	-0.86		
18	45489.28	2448.73	-55.64	24.81	-0.81		
19	45489.41	2441.87	-55.49	24.81	-0.75		
20	45489.53	2445.53	-55.72	24.8	-0.77		

Figure 2.6. Physiological data. This figure shows the physiological data as it is exported as .csv file to spreadsheet.

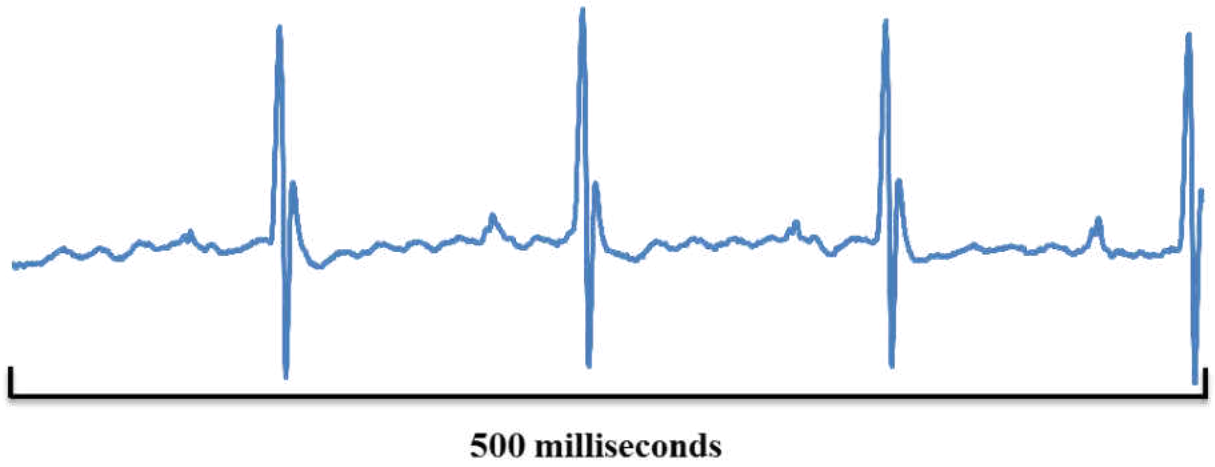

Figure 2.7. Graphed mV values. The graph displayed in this figure shows mV values from three consecutive and complete waveforms using the physiological data file (Figure 6). The graph is a simple line graph using points from the physiological data file.

DISCUSSION:

Using ECG changes as a supplemental method for confirming myocardial ischemia and reperfusion ensures the accurate placement of the occluding ligature. Accuracy of ligature placement is critical to reducing data variability among animals. The LAD in a mouse heart is a difficult artery to visualize. Therefore, supplementing visual pallor with electrocardiographic changes will help ensure the correct placement of the ligature and resulting tissue damage.

Since the ECG pad offers a non-invasive view of the heart, multiple ECGs can be obtained during the course of the study. This can help provide a better understanding of cardiac changes that occur during and after the surgery. It is critical to obtain a baseline ECG to use for comparison after the surgical procedure. Later stage tissue death and even ventricular aneurysm

can be observed by deflections of electrophysiological signals and ECG configuration changes. This may provide insight into the progression of heart failure.

The advantages of measuring ECG using echocardiographic machine include the simultaneous measurement of structural and functional parameters of the heart prior to or after the ischemia/reperfusion surgery. The limitations of the system to record ECG include the high cost to purchase an echocardiography machine. However if the experiments require constant ECG monitoring over multiple days, there are a variety of apparatuses available for ECG recording including remote telemetric ECG units with corresponding software that can be programed to record and analyze waveforms at various time intervals. However, many of the ECG telemetry units require an implantation procedure or specialized habitats. Additionally, many alterative electrode options exist including electrode clips and needles. Ischemia/Reperfusion surgery via thoracotomy is a highly invasive procedure. Advantages to using the ECG pad with an echocardiography machine include non-invasive procedure with no wires connected to the animal during surgery and no extra surgical procedure. However, investigators should determine the best equipment for their laboratory and experimental needs.

As mentioned previously, isoflurane anesthesia decreases heart rate. Additionally, isoflurane may be cardioprotective via activation of K^{ATP} channels and therefore reduce infarct size, as has been found in dogs[19]. General anesthesia in mice can be induced using injectable agents. Inhalation anesthesia does provide greater safety, particularly for prolonged procedures. However, inhalation anesthesia requires complex and expensive equipment such as precision vaporizers and flowmeters, specific breathing systems, and efficient scavenging systems to

prevent pollution. The disadvantages of injectable anesthetics include difficulty in choosing an initial dose, no chance of accurately modulating the depth of prolonged anesthesia, prolonged recovery, etc. The choice of anesthesia must be adapted according to the length of the procedure and aim of the study[20].

Using ECG as a supplemental method for confirming ischemia/reperfusion injury in mice will help improve consistency and reproducibility of infarctions but also opens the possibility for future applications of the technique through establishing quantitative trends. Investigators may notice similar ECG configurations within certain experimental groups. For instance, a genetically modified animal group may exhibit unusually wide QT-intervals after surgery when compared to the wild type. This informative data would have been missed if investigators use myocardial color changes as a sole confirmation of ischemia and reperfusion injury. For comparative studies between wild type and transgenic mice, considerations to the Lambeth Conventions guidelines may also be valuable, especially with respect to age, sex, blinding and randomization of animals[21].

In conclusion, supplemental confirmation of myocardial ischemia/reperfusion injury offers multiple benefits. Using ECG as a supplemental technique can help establish consistency in surgery. This may help decrease the number of animals used, while providing higher quality data. It also allows investigators to monitor cardiac injury, tissue death and/or remodeling non-invasively over time. Lastly, using ECG as a confirmation of myocardial ischemia/reperfusion offers the possibility of establishing quantitative electrophysiological trends.

ACKNOWLEDGEMENTS:

This work was supported by Merit Review awards (BX002332 and BX000640) from the Biomedical Laboratory Research and Development Service of the Veterans Affairs Office of Research and Development, National Institutes of Health (R15HL129140), and funds from Institutional Research and Improvement account. The project is supported in part by the National Institutes of Health grant C06RR0306551.

DISCLOSURES:

The authors have nothing to disclose.

REFERENCES:

1 Kochanek, K. D., Murphy, S. L. & Xu, J. Deaths: Final Data for 2011. *Natl Vital Stat Rep.* 63 (3), 1-120 (2015).

2 WHO. *The 10 leading causes of death in the world*, <http://www.who.int/mediacentre/factsheets/fs310/en/> (2012).

3 Klabunde, R. E. *Cardiovascular Physiology Concepts* 2edn, 243 (Wolters Kluwer Health Lippincott Williams & Wilkins 2012).

4 Bhardwaj, R., Kandoria, A. & Sharma, R. Myocardial infarction in young adults-risk factors and pattern of coronary artery involvement. *Niger Med J.* 55 (1), 44-47, doi:10.4103/0300-1652.128161, (2014).

5 Xu, Z., Alloush, J., Beck, E. & Weisleder, N. A murine model of myocardial ischemia-reperfusion injury through ligation of the left anterior descending artery. *J Vis Exp.* (86), doi:10.3791/51329, (2014).

6 Fernández, B. *et al.* The coronary arteries of the C57BL/6 mouse strains: implications for comparison with mutant models. *J Anat.* 212 (1), 12-18, doi:10.1111/j.1469-7580.2007.00838.x, (2008).

7 Thaler, M. S. *The Only EKG Book You'll Ever Need*. 4 edn, (Lippincott Williams & Wilkins, 2003).

8 Poirier, P. Exercise, heart rate variability, and longevity: the cocoon mystery? *Circulation.* 129 (21), 2085-2087, doi:10.1161/CIRCULATIONAHA.114.009778, (2014).

9 Boudoulas, K. D., Borer, J. S. & Boudoulas, H. Heart Rate, Life Expectancy and the Cardiovascular System: Therapeutic Considerations. *Cardiology.* 132 (4), 199-212, doi:10.1159/000435947, (2015).

10 Wehrens, X. H., Kirchhoff, S. & Doevendans, P. A. Mouse electrocardiography: an interval of thirty years. *Cardiovasc Res.* 45 (1), 231-237 (2000).

11 Boukens, B. J., Rivaud, M. R., Rentschler, S. & Coronel, R. Misinterpretation of the mouse ECG: 'musing the waves of Mus musculus'. *J Physiol.* 592 (21), 4613-4626, doi:10.1113/jphysiol.2014.279380, (2014).

12 O'Gara, P. T. *et al.* 2013 ACCF/AHA guideline for the management of ST-elevation myocardial infarction: executive summary: a report of the American College of Cardiology Foundation/American Heart Association Task Force on Practice Guidelines: developed in collaboration with the American College of Emergency Physicians and Society for Cardiovascular Angiography and Interventions. *Catheter Cardiovasc Interv.* 82 (1), E1-27, doi:10.1002/ccd.24776, (2013).

13 *Guide for the Care and Use of Laboratory Animals*. 8 edn, (National Academies Press, 2011).

14 Gao, S., Ho, D., Vatner, D. E. & Vatner, S. F. Echocardiography in Mice. *Curr Protoc Mouse Biol.* 1 71-83, doi:10.1002/9780470942390.mo100130, (2011).

15 Jong, W. M. *et al.* Reduced acute myocardial ischemia-reperfusion injury in IL-6-deficient mice employing a closed-chest model. *Inflamm Res.* 65 (6), 489-499, doi:10.1007/s00011-016-0931-4, (2016).

16 Nadtochiy, S. M. *et al.* In vivo cardioprotection by S-nitroso-2-mercaptopropionyl glycine. *J Mol Cell Cardiol.* 46 (6), 960-968, doi:10.1016/j.yjmcc.2009.01.012, (2009).

17 Preda, M. B. & Burlacu, A. Electrocardiography as a tool for validating myocardial ischemia-reperfusion procedures in mice. *Comp Med.* 60 (6), 443-447 (2010).
18 Speerschneider, T. & Thomsen, M. B. Physiology and analysis of the electrocardiographic T wave in mice. *Acta Physiol (Oxf).* 209 (4), 262-271, doi:10.1111/apha.12172, (2013).
19 Kersten, J. R., Schmeling, T. J., Pagel, P. S., Gross, G. J. & Warltier, D. C. Isoflurane mimics ischemic preconditioning via activation of K(ATP) channels: reduction of myocardial infarct size with an acute memory phase. *Anesthesiology.* 87 (2), 361-370 (1997).
20 Gargiulo, S. *et al.* Mice anesthesia, analgesia, and care, Part I: anesthetic considerations in preclinical research. *ILAR J.* 53 (1), E55-69, doi:10.1093/ilar.53.1.55, (2012).
21 Curtis, M. J. *et al.* The Lambeth Conventions (II): guidelines for the study of animal and human ventricular and supraventricular arrhythmias. *Pharmacol Ther.* 139 (2), 213-248, doi:10.1016/j.pharmthera.2013.04.008, (2013).

CHAPTER 3

EXOGENOUS UBIQUITIN REDUCES INFLAMMATORY RESPONSE AND PRESERVES MYOCARDIAL FUNCTION 3 DAYS POST ISCHEMIA/REPERFUSION INJURY

Stephanie L.C. Scofield[1], Kristina A. Lim[1], Patsy R. Thrasher[1], Suman Dalal[1], Christopher R. Daniels[1], Mahipal Singh[1], Krishna Singh[1,2,3,#]

[1]Department of Physiology, James H Quillen College of Medicine

[2]James H Quillen Veterans Affairs Medical Center

[3]Center of Excellence for Inflammation, Infectious Disease and Immunity

East Tennessee State University

Johnson City, TN 37614

Running Title: Ubiquitin in myocardial ischemia/reperfusion injury

Key words: Ubiquitin, Heart, Apoptosis, Myocytes, Fibrosis

#Correspondence: Krishna Singh, Ph.D., FAHA
Dept. of Biomedical Sciences
James H Quillen College of Medicine
East Tennessee State University
PO Box 70582, Johnson City, TN 37614
Ph: 423-439-2049,
Fax: 423-439-2052
E-mail: singhk@etsu.edu

Abstract

Aims: β-adrenergic receptor (β-AR) stimulation increases levels of extracellular ubiquitin (UB). Extracellular UB plays a protective role in β-AR stimulated myocyte apoptosis and myocardial remodeling. Here, we hypothesized that exogenous UB plays anti-inflammatory and anti-fibrotic roles in cardiac remodeling 3-days post ischemia/reperfusion (I/R) injury. *Methods and Results:* Mice (22-27 g) were infused with vehicle (saline) or UB (1μg/g/h) using micro-osmotic pumps, and subject to I/R injury. The structure and function of the left ventricle (LV) were investigated 3 days after the onset of reperfusion. UB alone had no effect on any of the structural and functional parameters of the heart. Infarct size was significantly lower in UB-I/R vs I/R group. M-mode echocardiography showed that I/R decreases heart function as indicated by decreased percent fractional shortening (%FS) and ejection fraction (%EF). UB infusion significantly improved I/R-mediated decrease in %FS and %EF. LV end systolic diameter was significantly lower in UB-I/R vs I/R group. UB-I/R group displayed significant decrease in inflammatory infiltrates, neutrophils, and macrophages vs I/R group. Additionally, UB-I/R group had significantly reduced neutrophil activity vs I/R group. Western blotting analyses showed significant increase in MMP-2 and TGF-β1 protein levels in UB-I/R group. MMP-9 activity as measured by in-gel zymography was higher in UB-I/R group. Conclusion: Extracellular UB plays a protective role in myocardial remodeling post-I/R injury with effects on cardiac function, infarct size, inflammatory response, expression and activity of MMPs and TGF-β1 expression.

Introduction

Ubiquitin (UB) is a highly conserved protein of ~8.5 kDa and is found in all eukaryotic cells. It is best known for its role in regulating protein turnover via the ubiquitin-proteasome pathway[1]. Within cardiac myocytes, the ubiquitin-proteosome pathway has been proposed to regulate internalization of cell-surface receptors, hypertrophic response, apoptosis and tolerance to ischemic and reperfusion insults[2]. UB is a normal constituent of plasma. Elevated levels of circulating extracellular UB have been found in patients experiencing various pathologies including parasitic and allergic diseases[3], alcoholic liver disease[4], type 2 diabetes[5], β2-Microglobulin amyloidosis[6] and in patients undergoing chronic hemodialysis[7]. Increase in extracellular UB levels have also been described in the cerebrospinal fluid of traumatic brain injury patients[8, 9]. Extracellular UB is suggested to have multiple functions including immune response regulation, anti-inflammatory properties and neuroprotective activities[1, 10-12], as well as a role in growth and apoptosis of hematopoetic cells[13]. Previously, our lab has provided evidence that stimulation of β-adrenergic receptors (β-AR) in adult rat ventricular myocytes (ARVMs) increases extracellular levels of UB, and UB plays an anti-apoptotic role in β-AR–stimulated myocardial remodeling with effects on left ventricular function, fibrosis and myocyte apoptosis[14, 15]. However, the role of exogenous UB following myocardial ischemia/reperfusion injury, a clinically relevant model, has not yet been investigated.

Myocardial remodeling after I/R injury typically involves a period of cell death via necrosis and apoptosis. Necrosis and reperfusion of the ischemic area trigger an inflammatory response in the heart with infiltration of cells such as neutrophils and macrophages (monocytes) in the area of injury to clear dead cells and cellular debris[16]. Next, fibroblasts proliferate and move into the infarcted area, depositing collagenous scar material to fill the void of irreplaceable myocytes.

Cytokines and growth factors play a role in differentiation of fibroblasts into myofibroblasts. TGF-β1 plays an important role in differentiation of fibroblasts into myofibroblasts[17]. Myofibroblasts are a major producer of extracellular matrix (ECM) proteins. They also produce matrix metalloproteinases (MMPs) and their inhibitors, tissue inhibitors of matrix metalloproteinases (TIMPs). A highly regulated balance between MMPs and TIMPs is imperative to maintaining ECM homeostasis[18].

Here, we investigated the *in vivo* role of exogenous UB in myocardial remodeling following 3 days I/R injury in mice. We report that UB plays a protective role in myocardial remodeling post-I/R injury with effects on cardiac function, infarct size, infiltration of immune cell types, expression and activity of MMP-2 and MMP-9, and expression of TGF-β1.

Methods and Material

Animal Care

The study conforms to the regulations provided in the Guide for the Care and Use of Laboratory Animals published by the US National Institutes of Health (NIH Publication No. 85-23, revised 1996). The animal protocols were approved by the University Committee on Animal Care. Animals were anesthetized using a mixture of isoflurane (2.5%) and oxygen (0.5 l/min) when undergoing termination by exsanguination. The heart was excised through an incision in the diaphragm. For this study, male C57Bl/6 mice (8-12 weeks; Jackson Laboratories) were used.

Ischemia/Reperfusion (I/R) Injury

I/R was performed as described[19]. Mice were anesthetized with a mixture of isoflurane (2.5%) and oxygen (0.5 l/min) inhalation and ventilated using a small rodent ventilator (Harvard

Apparatus). Body temperature was maintained for the duration of the surgery at ~37°C using a heating pad. The heart was exposed via left thoracotomy and the left anterior descending coronary artery was ligated for 45 minutes using a 7-0 braided silk suture that formed a snare around a piece of polypropylene tubing (1mm diameter). After 45 min, the snare was released and reperfusion was allowed to occur. I/R was confirmed by myocardial color changes and electrocardiogram changes as described[19]. Sham mice underwent left thoracotomy without coronary ligation. At the 3 day time point, hearts were isolated and used for either histology or protein analyses.

Mice treatment

Mice were grouped at random into 4 different treatment groups (sham, UB, I/R, and UB-I/R). 12 h prior to surgery, mice were implanted with micro-osmotic pumps (Alzet) that released either normal saline (sham) or UB (1μg/g/h) dissolved in normal saline over a 3 day period. The dose of ubiquitin was selected based on a previously published report[24].

Echocardiography

Transthoracic two-dimensional M-mode echocardiograms were obtained using a VEVO 1100 (VisualSonics, Fujifilm) equipped with a 22-55 MHz MS550D transducer[22;25]. Echocardiography was performed at baseline and 3 days after I/R surgery. During echocardiography, animals were anesthetized using a mixture of isoflurane (1.5%) and oxygen (0.5 l/min), and their body temperature maintained at ~37°C using a heating pad. M-mode tracings were used to measure left ventricle (LV) dimensions. Percent fractional shortening (%FS) and ejection fraction (EF %) were calculated by Fujifilm software on the VEVO 1100. All echocardiography measurements were performed by a single investigator and confirmed by a second investigator.

Morphometric Analyses

Animals were euthanized and the isolated hearts were perfused using KH buffer to clear the tissue of blood. The hearts were then arrested in diastole using KCl (30 mmol/L) followed by fixation with 10% buffered formalin and subsequent paraffin embedding. Cross sections of the heart (4µm thick) were stained with Masson's trichrome. Infarct size was calculated as a percentage of affected LV using NIS elements software (Nikon).

Hematoxylin and Eosin Staining

Tissue sections (4µm) were stained with basic histologic staining hematoxylin and eosin to analyze inflammatory infiltrates. Images were acquired using Nikon Eclipse TE-2000-S microscope (Nikon, New York, USA) equipped with an Andor Zyla sCMOS camera (Andor, Belfast, United Kingdom). Quantitative analysis of inflammatory infiltrate was carried out using NIS elements software (Nikon, New York, USA). Three random fields of infarcted LV were analyzed per animal.

Immunohistochemistry

Myocardial cross sections (4µm) were deparaffinized and rehydrated using xylene and ethanol washes. Epitope retrieval was performed using proteinase XXIV at 37° (0.1% in PBS). Tissue sections were then incubated in anti-neutrophil antibody (1:50; Santa Cruz) or anti-F4/80 (1:200; Santa Cruz) to quantify neutrophils and macrophages, respectively. The sections were then stained using ABC DAB kit (Vectastain) for colorimetric analysis. Images were acquired using a Nikon Eclipse TE-2000-S microscope (Nikon, New York, USA) equipped with an Andor Zyla sCMOS microscope camera (Andor, Belfast, United Kingdom) and analyzed using Nikon Elements software. The data is expressed as number of positively stained cells/0.1mm^2 of infarct area. Four randomly selected fields of infarcted LV were analyzed per animal.

Neutrophil Activity Assay

Myocardial cross sections were stained with Napthol AS-D Chloroacetate esterase kit (Sigma), also known as Leder stain, for the measurement of enzymatic activity of neutrophils using the manufacturer's instructions. The areas stained pink were considered to be positive for neutrophil activity. The data are presented as an average percentage of positive stained area to the total infarct area per image. Three randomly selected fields of infarcted LV were analyzed per animal.

Western Analysis

Left ventricles were snap frozen in liquid nitrogen and pulverized using a mortar and pestle. LV lysate powder was then suspended in RIPA buffer (1%Triton X-100, NaCl 150 mmol/l, Tris 10 mmol/l, pH 7.4, EDTA 1 mmol/l, EGTA 1mmol/l, phenylmethylsulfonyl fluoride 0.2 mmol/l, sodium orthovanadate 0.2 mmol/l and 0.5% Nonidet P-40). Equal amounts of total protein, (50 μg), were resolved on 10% SDS-polyacrylamide gels and transferred onto PVDF membranes. Membranes were then probed with primary antibodies directed against MMP-2 (Santa Cruz), MMP-9 (Santa Cruz), TGF-β (Santa Cruz), or GAPDH (Cell Signaling Technologies) followed by corresponding HRP-conjugated secondary antibodies. Band intensities were quantified using ImageQuant LAS 500 imaging system (GE, Massachusetts, USA).

In-gel zymography:

Gelatin in-gel zymography using LV (70 μg) lysates was performed as described[20]. Digested clear bands representing the activity of MMP-9 were quantified using imageJ software. Due to negligible presence of MMP-9 activity, sham groups were combined for statistical analysis.

Statistical analysis:

Data are expressed as mean ± SEM. Data were analyzed using two-way ANOVA followed by post-hoc (Student-Newman-Keuls unless otherwise specified) or Student's *t* test. Probability (p) values of <0.05 were considered significant.

Results

Survival and morphometric studies

Fourteen out of total 78 animals died during the course of the experiment. Seven out of 33 mice died in I/R group, while 6 out of 33 died in UB-I/R group. Mortality rate was not significantly different between the two I/R groups. All of the deaths can be attributed to known and recorded surgical errors. Four animals were excluded from the study due to lack of infarctions or lack of reperfusion. There were no significant changes in heart weights or body weights in any of the groups during the course of the study. There was a significant increase in lung wet:dry ratio in I/R versus sham group (Table 3.1).

Table 3.1 Morphometric Measurements

Parameters	Sham (n=5)	UB (n=4)	I/R (n=10)	UB-I/R (n=9)	P Value
BW, g	24.05±0.59	23.74±0.97	23.48±0.38	23.23±0.48	NS
HW, mg	109.22±5.83	106.83±6.29	114.72±3.63	108.01±3.09	NS
HW:BW, mg/g	4.54±0.17	4.49±0.11	4.89±0.16	4.66±0.13	NS
Lung Wet:Dry	1.02±0.18	1.28±0.02	2.77±0.55*	2.86±0.63	<0.05*

Values are means±SEM; BW, body weight; HW, heart weight; NS, not significant; *comparison vs sham.

Infarct Size

Analysis of infarct size using Masson's trichrome staining showed that UB infusion significantly decreases infarct size 3 days post-I/R surgery (%LV infarct, I/R, 28.93 ± 4.61; UB-I/R, 12.97 ± 2.74[#]; [#]P<0.05 vs I/R; n=3-5; Fig 3.1).

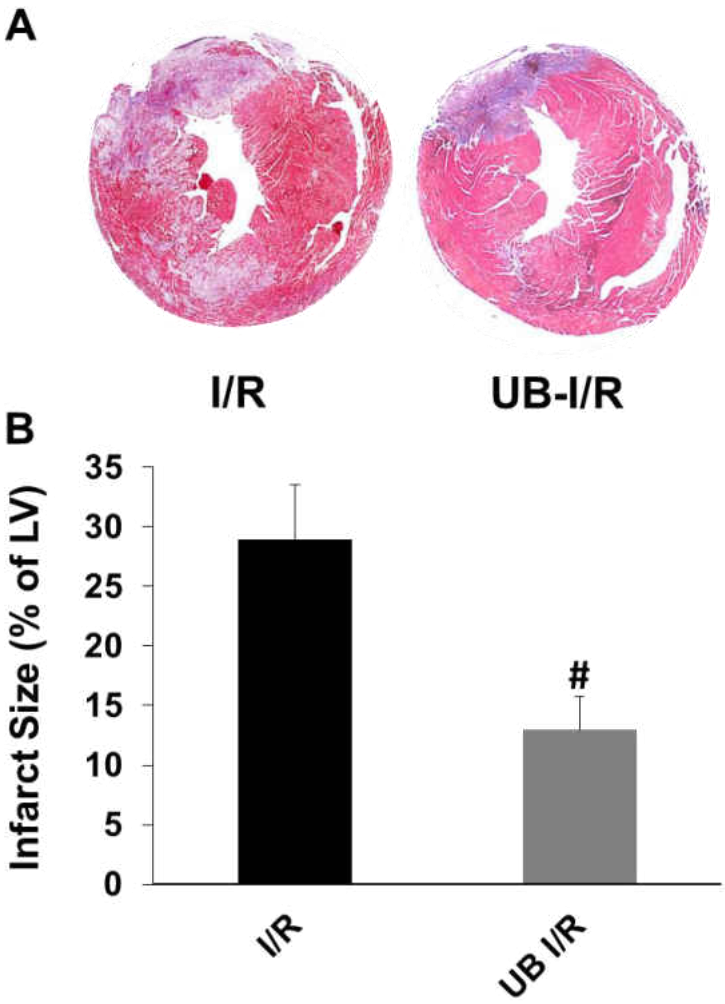

Figure 3.1. Infarct Size. A. Masson's trichrome stained images of the hearts. Pink staining indicates myocardium; purple-blue staining indicates fibrotic scar material. B. Graphical representation of infarct size; #P<0.05 vs I/R; n =5.

Echocardiographic measurements

M-mode echocardiographic parameters were not significantly different between sham and UB alone groups. I/R significantly reduced heart function as evidenced by decreased %FS and EF vs

sham group. UB infusion improved %FS (%FS, Sham, 37.85 ± 2.77, UB, 34.88 ± 1.32; I/R, 27.66 ± 1.05*; UB-I/R, 32.95 ± 1.83#; *P<0.05 vs respective sham; #P<0.05 vs I/R; n=4-6; Fig 3.1A) and %EF (%EF, Sham, 68.50 ± 3.56, UB, 64.85 ± 1.63; I/R, 54.62 ± 1.74*; UB-I/R, 62.35 ± 2.56#; *P<0.05 vs respective sham; #P<0.05 vs I/R; n=4-6; Fig 3.2B) post-I/R.

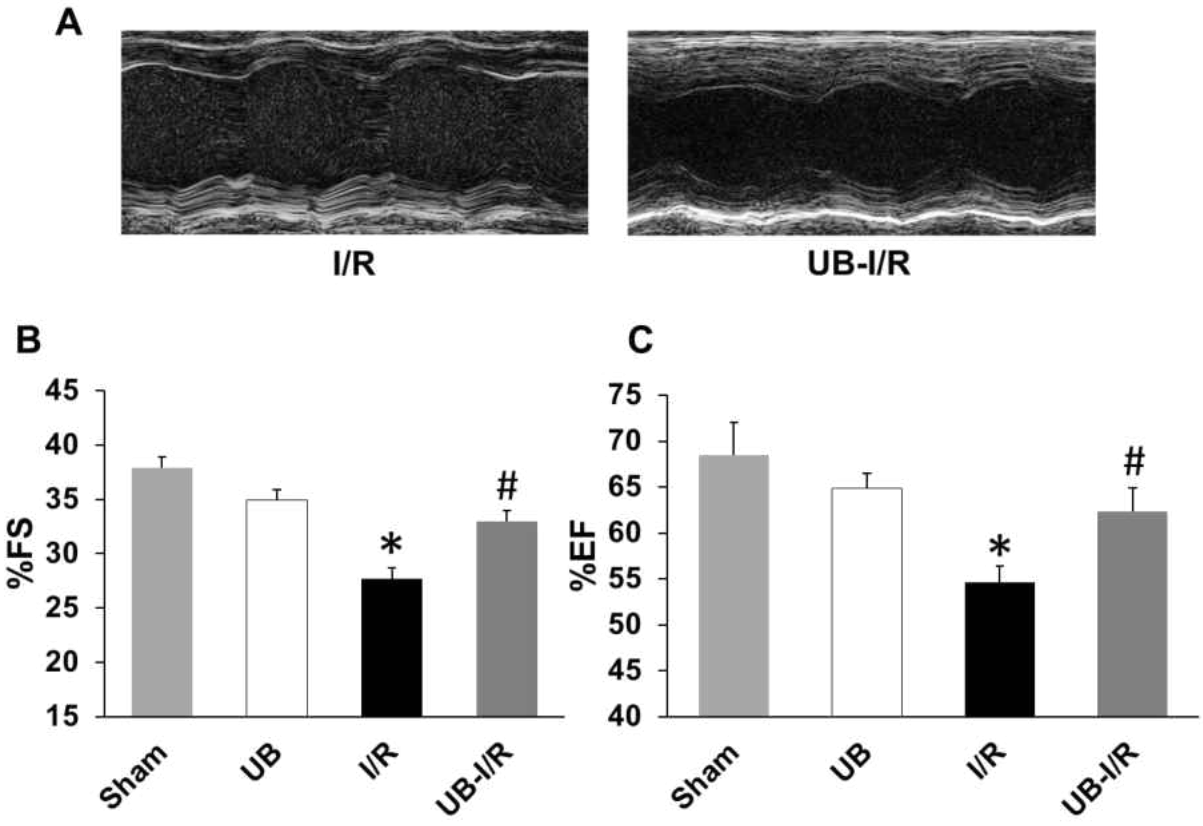

Figure 3.2. UB Infusion Improves Heart Function 3 Days post-I/R. Indices of heart function; percent fractional shortening (%FS), ejection fraction (%EF) were calculated using echocardiographic images 3 days post-I/R. A. M-mode images; B. %FS; C. %EF. *P<0.05 vs sham and UB; #P<0.05 vs I/R; n = 4-6.

Inflammatory Infiltration

Hematoxylin and Eosin staining of myocardial cross-sections showed a significant presence of inflammatory cells in the infarct LV regions of both I/R groups. Quantitative analysis revealed a

significant decrease in the number of infiltrates in the UB-I/R vs I/R group. (Infiltrates per $0.1mm^2$, I/R, 106.63 ± 15.95; UB-I/R, 46.52 ± 6.80$^{\#}$; $^{\#}P<0.05$ vs I/R; n=3; Fig 3.3).

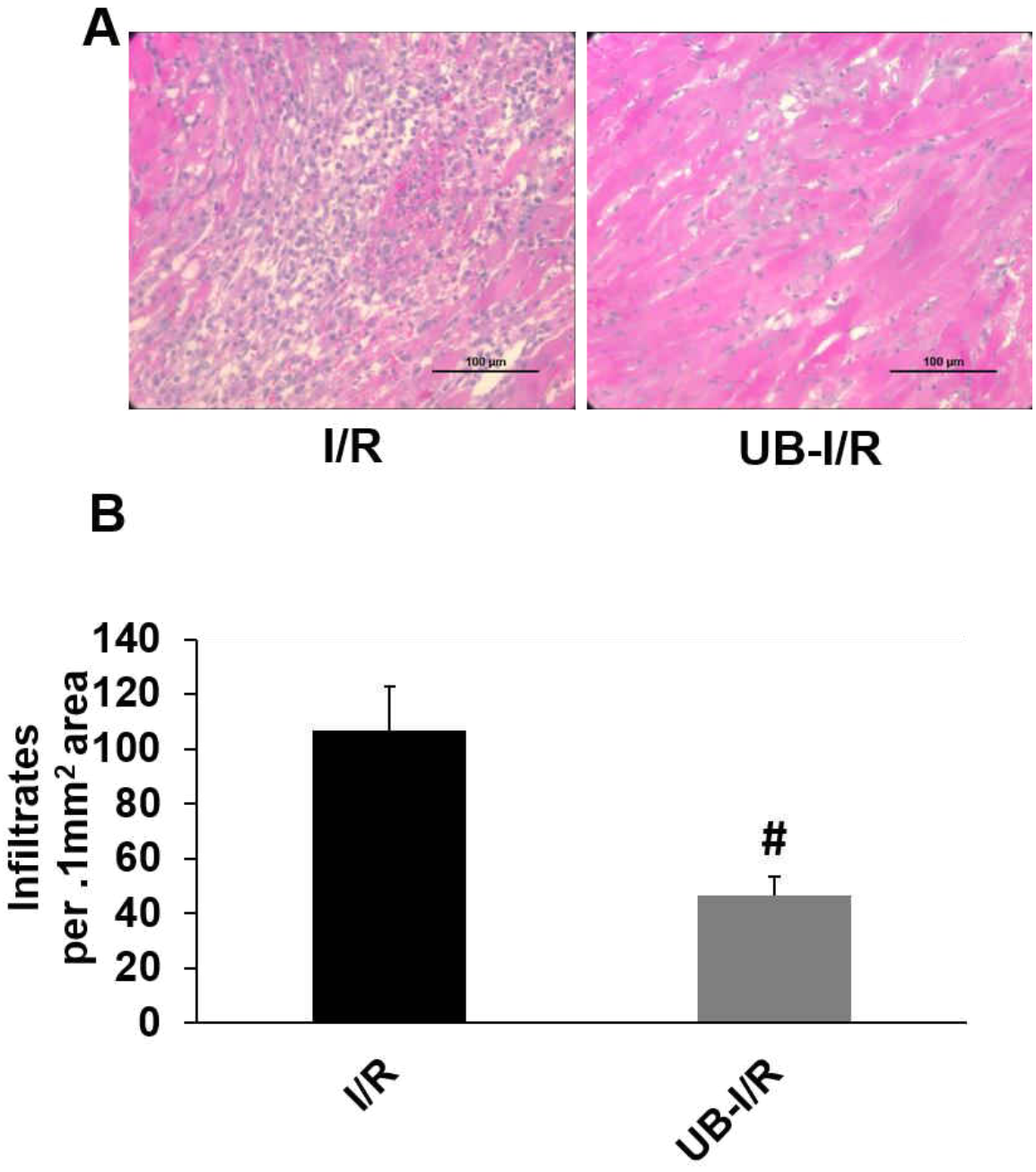

Figure 3.3. UB Infusion Decreases Inflammatory Infiltrates. Heart sections were stained with hematoxylin and eosin (H&E). The number of inflammatory infiltrates was quantified using NIS elements software. Upper panel exhibits H&E stained images of the LV regions from I/R and UB-I/R groups. Blue staining represents nuclei, while pink staining represents cytoplasm. Lower

panel exhibits quantitative analysis of inflammatory infiltrates 3 days post-I/R; *P<0.05 vs I/R; n=3.

Neutrophil number and activity

Sham and UB alone groups showed the presence of only a few neutrophils in the LV region with no significant difference between the two groups. I/R increased the number of neutrophils in the infarct regions of both I/R groups. However, the number of neutrophils was significantly lower in UB-I/R vs I/R group (Neutrophil per 0.1mm^2, Sham, 0.46 ± 0.34, UB, 0.58 ± 0.32; I/R, 87.81 ± 6.83*; UB-I/R, 20.27 ± 7.55$^{\#}$; *P<0.05 vs sham and UB; #P<0.05 vs I/R; n=3-5; Fig 3.4A&B).

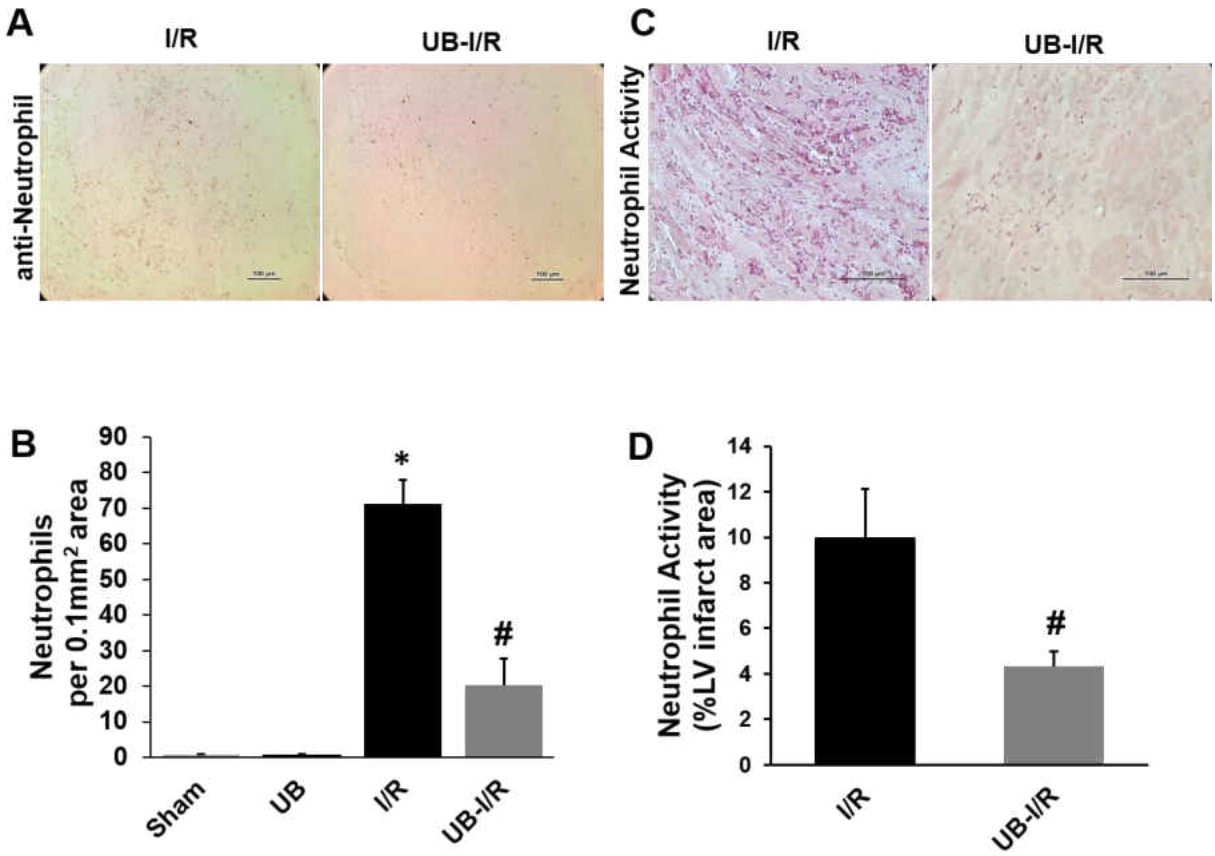

Figure 3.4 UB Decreases Neutrophil Number and Activity 3 Days Post-I/R. A. Image panel depicts stained images of infarct LV from I/R and UB-I/R groups. Brown represents positive immunostaining using anti-neutrophil primary antibodies. B. The number of immune-positive cells per 0.1mm^2 of infarcted LV area was quantified using NIS elements software. C. Image panel depicts neutrophil activity in LV infarct regions of I/R and UB-I/R groups. Red staining indicates neutrophil activity. D. The percentage stained positive for neutrophil activity within the

infarct LV was quantified using NIS elements software; *P<0.05 vs sham or UB, #P<0.05 vs I/R; n=3-5.

Measurement of neutrophil activity using Napthol AS-D Choloracetate esterase kit showed that the neutrophils present in the infarct region were in fact active. Neutrophil activity was significantly lower in UB-I/R vs I/R group (Neutrophil activity, % of Infarct Area; I/R, 9.95 ± 2.18; UB-I/R, 4.33 ± 2.18#; #P<0.05 vs I/R; n=3; Fig 3.4C&D).

Macrophage number

Sham and UB alone groups showed presence of few macrophages in the infarct LV region with no significant difference between the sham and UB alone groups. I/R significantly increased the number of macrophages in both I/R groups. However, the number of macrophages was significantly lower in UB-I/R vs I/R group (Macrophage per $0.1mm^2$, sham, 0.84 ± 0.54, UB, 0.63 ± 0.30; I/R, 91.33 ± 26.32*; UB-I/R, 28.84 ± 5.22#; *P<0.05 vs sham and UB; #P<0.05 vs I/R; n=3-5; Fig 3.5).

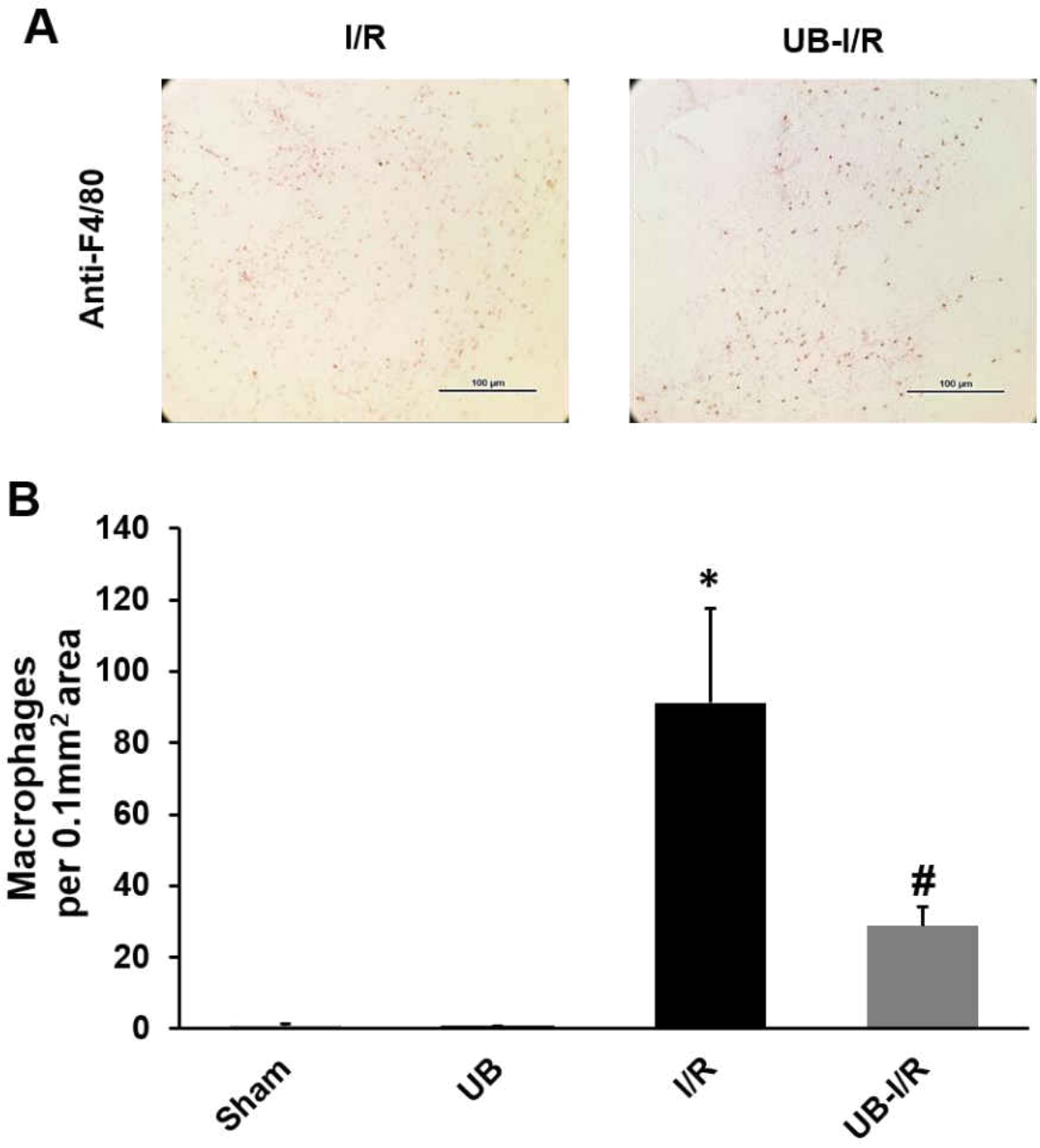

Figure 3.5. UB Decreases Macrophage Number 3 Days Post-I/R. A. Stained images of infarct LV from I/R and UB-I/R groups. Brown represents positive immunostaining using anti-F4/80 primary antibodies. B. The number of macrophages per 0.1mm2 of infarcted LV area was quantified using NIS elements software; $^{\#}P<0.05$ vs I/R; n=5.

Expression and activity of MMPs

MMPs (MMP-2 and MMP-9) are key players in myocardial fibrosis and remodeling processes[29]. Western blot analysis of LV lysates revealed increased levels of MMP-2 (72 kDa) in I/R and UB-I/R groups. The expression of MMP-2 was significantly higher in the UB-I/R vs I/R group (Fold change vs sham, sham, 1.00 ± 0.15; UB, 1.03 ± 0.10; I/R, 1.41 ± 0.05*; UB-I/R, 1.67 ± 0.02*#; *P<0.05 vs sham or UB, #P<0.05 vs I/R,; n=3; Fig 3.6). UB alone had no effect on the expression of MMP-2 in the heart.

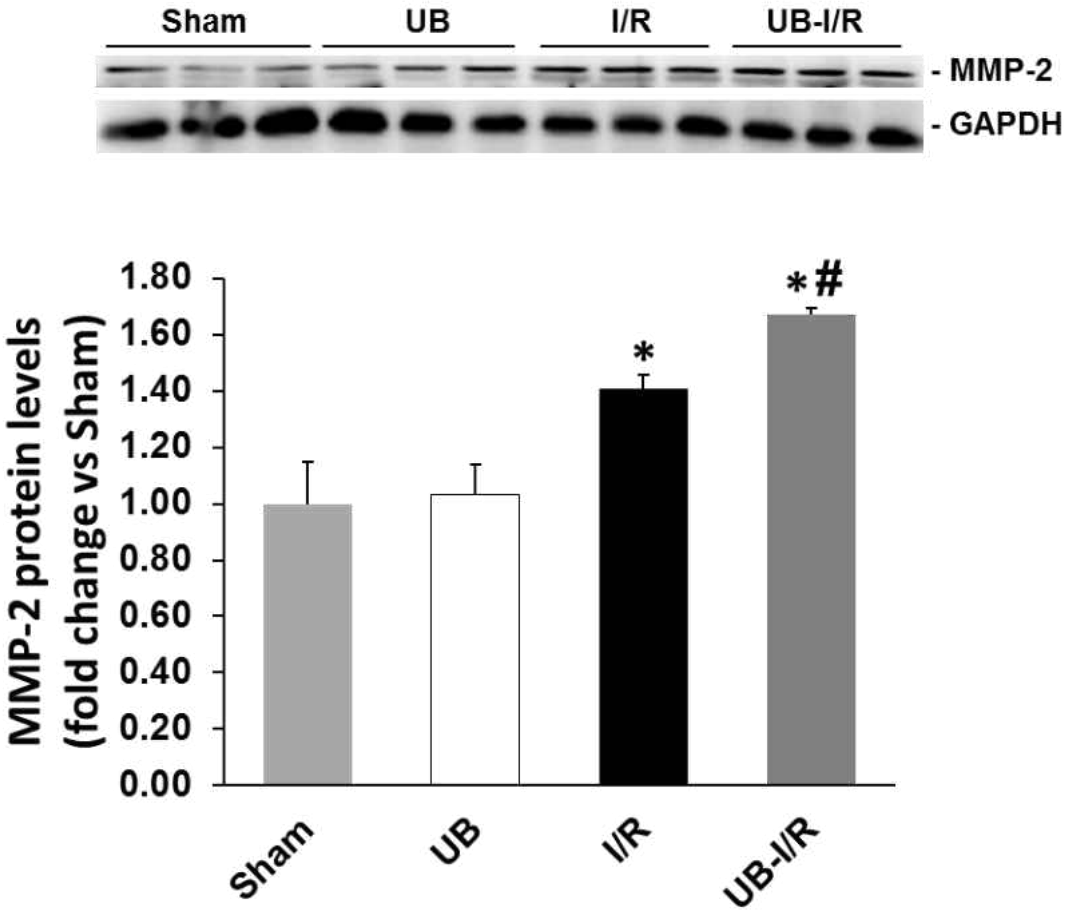

Figure 3.6. UB Increases Protein Levels of MMP-2. Total LV lysates (50µg) were analyzed by western blot using anti-MMP-2 antibodies. The upper panel depicts MMP-2 or GAPDH immunostaining. The lower panel exhibits quantitative analysis of MMP-2 normalized to GAPDH; *P<0.05 vs sham or UB; #P<0.05 vs I/R; n=3.

In gel zymography showed increased activity of MMP-9 in both I/R groups vs shams. However, the increase in MMP-9 activity was significantly higher in UB-I/R group vs I/R group (Fold change vs shams; shams, 1.00 ± 0.23; I/R, 9.61 ± 1.02*; UB-I/R, 14.42 ± 1.58*#; *P<0.05 vs sham or UB, #P<0.05 vs I/R; n=3-4; Fig 3.7).

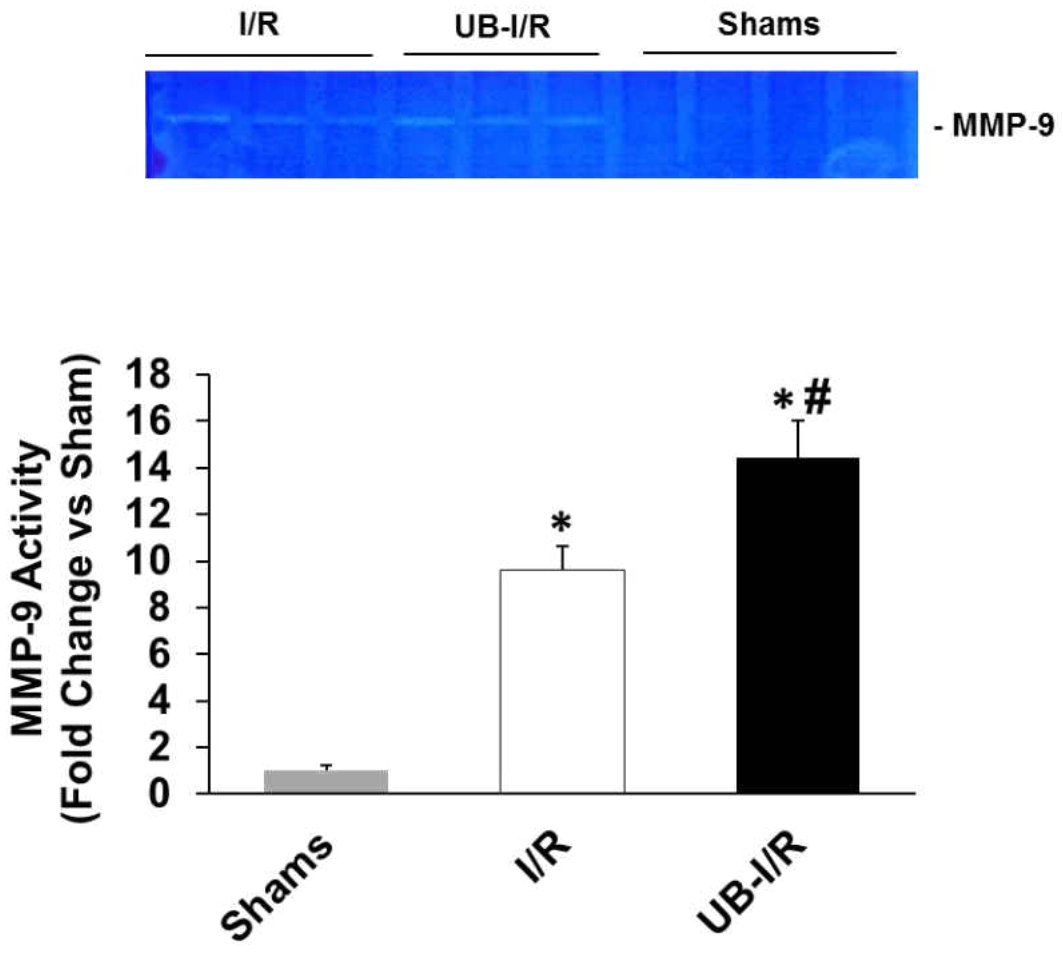

Figure 3.7. UB Increases MMP-9 Activity. Total LV lysates (50µg) were analyzed by gelatin zymography for MMP-9 activity (~90 kDa); *P<0.05 vs Shams; #P<0.05 vs I/R; n=3-4.

Expression of TGF-β

TGF-β1 plays an important role in myocardial remodeling via its involvement in differentiation of fibroblasts into myofibroblasts and ECM deposition. TGF-β1 is expressed as a 44 kDa

protein. Western blot analysis showed expression of TGF-β1 in sham and UB groups with no difference between the two groups. TGF-β1 expression remained unchanged in I/R group. However, expression of TGF-β1 was significantly higher in UB-I/R vs I/R group (Fold change vs. sham; sham, 1 ± 0.03; UB, 0.97 ± 0.15; I/R, 0.92 ± 0.16, UB-I/R, 1.45 ± 0.07*#; *P<0.05 vs sham, #P<0.05 vs I/R; n= 3-4; Fig 3.8).

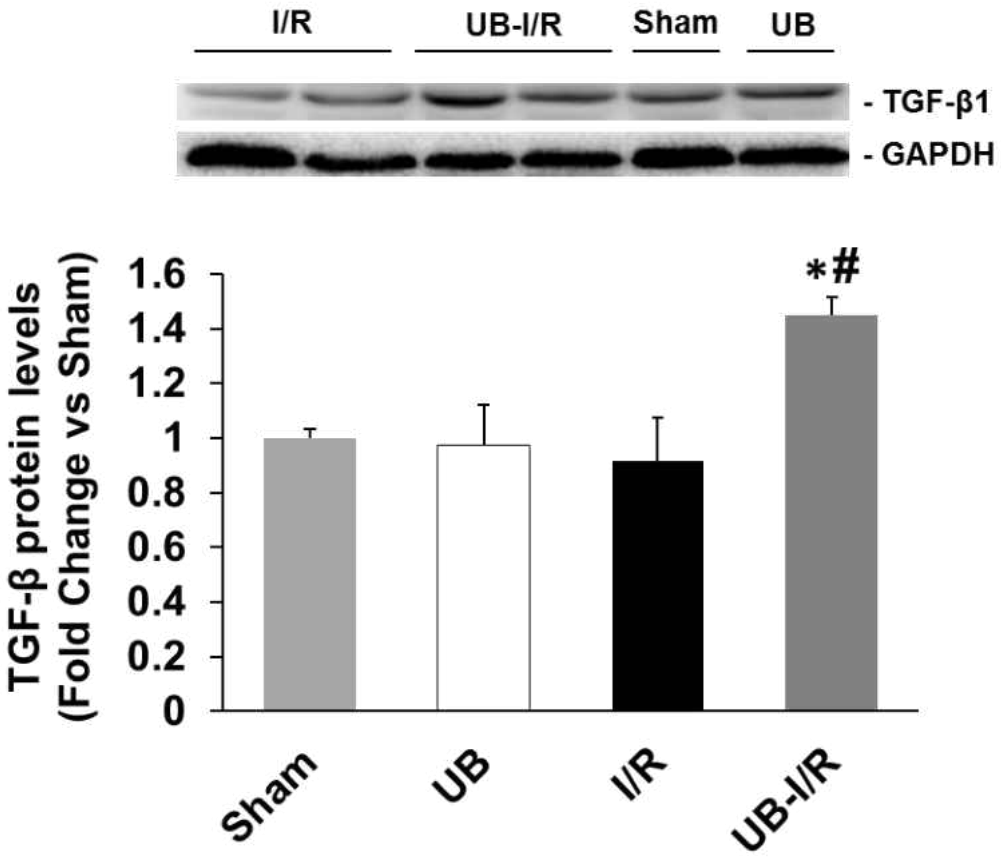

Figure 3.8. UB Increases Protein Levels of TGF-β. Total LV lysates (50µg) were analyzed by western blot using anti-TGF-β1 antibodies. The upper panel depicts TGF-β1 or GAPDH immunostaining. The lower panel exhibits quantitative analysis of TGF-β1 normalized to GAPDH; *P<0.05 vs sham or UB; #P<0.05 vs I/R; n=3-4.

Discussion

Previously, our lab has provided evidence that sympathetic stimulation (β-AR) increases extracellular levels of UB, and treatment with UB plays an anti-apoptotic role against β-AR-stimulated apoptosis *in vitro* in isolated adult rat cardiac myocytes[14] and *in vivo* in mouse hearts[15]. This is the first study investigating the role of exogenous UB in the heart in response to myocardial I/R injury. The main findings of the study are – 1) UB infusion decreases % infarct size 3 days post-I/R; 2) UB infusion improves heart function as evidenced by improved %FS and EF; 3) UB infusion decreases inflammatory response as evidenced by decreased number of infiltrates, number and activity of neutrophils and number of macrophages; 4) UB infusion increases expression of MMP-2 and activity of MMP-9; and 5) UB infusion increases expression of TGF-β1.

The heart experiences an increase in sympathetic nerve activity post-I/R[21]. Chronic β-AR stimulation induces cardiac myocyte death, creates infarct-like lesions and increases myocardial fibrosis in rodent models[22, 23]. Prolonged β-adrenergic stimulation also leads to the development of heart failure and increased mortality in animals and human patients[24, 25]. Previously using β-AR-stimulation as a model, our lab provided evidence that UB infusion in mice decreases myocardial fibrosis[15]. This study provides evidence that UB treatment significantly decreased infarct size 3 days post-I/R injury. Cardiac dysfunction post-I/R injury is related to infarct size[26]. The observed improvement in heart function in UB-infused hearts 3 days post-I/R injury in this study is likely due to decreased infarct size. These data suggest that UB signaling has the potential to decrease the severity of cardiac injury during the acute phase post I/R.

Systolic dysfunction is characterized by decreased contractility and therefore decreased pumping function of the heart[27]. In general, I/R injury, and the associated myocardial death,

results in LV dilation and systolic dysfunction[28]. Consistent with these findings, we observed reduced systolic function 3 days post-I/R as observed by decreased %FS and EF. Interestingly, UB-infused hearts suffered a lesser degree of impairment in systolic function post-I/R injury. In fact, cardiac function in UB-I/R group was not significantly different versus the UB group. Previously, we have shown that UB-infusion returns systolic function to normal levels during chronic β-AR stimulation[15]. UB treatment is shown to promote intracellular Ca^{2+} flux and reduce cAMP levels via interaction with G protein-coupled receptor, CXCR-4, in a THP-1 leukemia cell line[29, 30]. Sustained systolic function in the UB-I/R group may be due in part to UB's interaction with CXCR-4 potentially leading to modulation of intracellular Ca^{2+} flux and cAMP levels.

I/R injury is associated with a large inflammatory response. Post ischemic tissue is plagued by oxidative stress, cell damage and production of proinflammatory cytokines that act to activate and recruit neutrophils to the area of injury[31]. Neutrophils begin to infiltrate into the infarcted myocardium within hours of the ischemic event peaking 24 hours post-I/R injury[32]. The inflammatory mediators of neutrophil infiltration also contribute to further recruitment of leukocytes including the recruitment and activation of spleen-derived monocytes that macrophage populations are then derived from[33]. These neutrophils and macrophages clear the infarcted myocardium from cellular and matrix debris.

Consistent with these reports, we observed an increased number of neutrophils and macrophages in the infarct LV region 3 days post-I/R. Interestingly, the inflammatory cell count was significantly lower in UB-infused hearts post-I/R. These data suggest an anti-inflammatory role for UB post-I/R. It should be noted that a great deal of evidence exists to support a theory that activated neutrophils release cytotoxic oxidants and enzymes to exacerbate myocardial injury at the time of reperfusion[34]. In a canine myocardial ischemic injury model, depleting the

amount of neutrophils in circulation by ~77% resulted in ~43% decrease in infarct size[35]. Therefore, the observed decrease in infarct size in UB-infused hearts 3 days post-I/R could be due to the decreased neutrophil count and/or activity. Neutrophil recruitment to the site of injury is carried out by chemotactic signals released by necrotic cells during ischemic injury[36]. To determine the exact effect UB infusion exerts regarding the involvement of molecular signals in the post-I/R inflammatory response, further investigations are needed.

UB is proposed to have a role in the modulation of immune response in a number of pathological conditions. Extracellular UB is found to decrease the levels of pro-inflammatory cytokine, tumor necrosis factor-alpha (TNF-α), in animal models of trauma and endotoxic shock[11, 12, 37]. In a I/R model in rat lung, UB was found to improve function, reduce edema and increase the expression of Th2 cytokines which can be associated with anti-inflammatory processes[38]. In this study, the observed decrease in total inflammatory infiltrates, neutrophil and macrophage count, and neutrophil activity suggests that UB may be playing an anti-inflammatory role in the I/R injured myocardium.

The extracellular matrix (ECM) of the heart provides a complex lattice of proteins wherein the contractile myocytes, fibroblasts and other cell types rest. The ECM provides structural integrity for the heart, a functional arrangement of the cells so that they can communicate electrical and paracrine signals and it also provides the perfect mechanical environment for the cells to thrive and work together. The makeup of the myocardial extracellular matrix plays a critical role in cardiac homeostasis and wound healing. Matrix metalloproteinases (MMPs) are a family of endopeptidases that proteolytically degrade extracellular matrix proteins[39]. We observed that there is a significant increase in protein levels of MMP-2 (Fig 3.6). Our findings that MMP-2 protein levels are increased in I/R hearts is consistent with findings from multiple

reports that hypoxic and reperfusion conditions result in transcriptional upregulation of the MMP-2 protein and mRNA transcripts[40-43]. We also observed increased MMP-9 activity in both I/R and UB-I/R groups vs shams. UB infusion significantly enhanced MMP-9 activity vs I/R group (Fig 3.7). In a pig model of myocardial infarction, MMP-9 was increased as quickly as 2 hours post injury[44]. The increase in MMP-2 expression and MMP-9 activity could indicate that enhanced degradation of ECM may also contribute to the observed decrease in infarct size.

TGF-β1 is well known for its role in initiating differentiation of cardiac fibroblasts into their activated wound-healing phenotype, myofibroblasts, which act to deposit collagen-based fibrosis into the injured area[45]. Although some level of fibrosis after I/R injury is needed to maintain structural integrity of the heart, excessive deposition of collagen-based matrix may interfere with the rhythmic contraction and relaxation of the heart. In this study we found that UB infusion increases TGF-β1 expression 3 days post-I/R (Fig 3.8). Therapies targeted against the TGF gene showed that TGF-inhibition during the inflammatory phase resulted in enhanced neutrophil infiltration and a worse degree of left ventricular dysfunction[17]. Therefore, our finding raises the possibility that increased TGF-β expression may be increasing fibroblast activation while also contributing to the reduction of the inflammatory response post I/R injury.

Conclusion and study limitations

All the mice were male, C57Bl/6 background, ~25 g and 8-12 weeks old. Patient populations with respect to heart diseases vary in terms of age, sex and are often plagued by multiple comorbidities. Additionally there are many organismal differences between mice and humans. Another important point is that all the observations were made 3 days post-I/R injury. Infarct healing process involves 3 overlapping phases: inflammation, proliferation and maturation and remodeling can last up to 28 days post-I/R. Going forward, this study should be

expanded to encompass female animals as well as other time points to understand the anti-inflammatory and cardioprotective potential of exogenous UB in the heart after I/R injury.

The data presented are novel and important because sympathetic stimulation increases after myocardial I/R injury. Sympathetic stimulation increases extracellular levels of UB in adult cardiac myocytes *in vitro*[14]. The present study provides evidence for a cardioprotective role of exogenous UB after I/R injury *in vivo*. It is interesting that extracellular UB reduced the extent of the inflammatory response, changed the composition of proteins related to ECM deposition and reduced the extent of adverse cardiac remodeling. Cardiac remodeling is known to be maleficial to cardiac function so reducing remodeling will prove advantageous in terms of recovery and outcomes post myocardial I/R injury. It should be emphasized that the study investigated the role of exogenous UB 3 days post-I/R and UB-infusion was started 12 h prior to myocardial infarction. This study should be continued to investigate different time points during the remodeling process in the following ways; 1) extend the time point to study fully remodeled heart and the mature scar, 2) decrease the time point to study early inflammation and 3) use UB as a treatment at the time of reperfusion instead of as a 12 h pretreatment to determine if UB has potential to treat acute cardiac events.

Funding

This work was supported by Merit Review awards (BX002332 and BX000640) from the Biomedical Laboratory Research and Development Service of the Veterans Affairs Office of Research and Development, National Institutes of Health (R15HL129140), and funds from Institutional Research and Improvement account. The project is supported in part by the National Institutes of Health grant C06RR0306551.

Acknowledgement

Technical help received from Barbara A. Connelly is appreciated.

Conflicts of interest

None.

References

1. Griebenow M, Casalis P, Woiciechowsky C, Majetschak M, Thomale UW. Ubiquitin reduces contusion volume after controlled cortical impact injury in rats. *J Neurotrauma*. 2007;24:1529-1535
2. Strous GJ, van Kerkhof P. The ubiquitin-proteasome pathway and the regulation of growth hormone receptor availability. *Mol Cell Endocrinol*. 2002;197:143-151
3. Asseman C, Pancre V, Delanoye A, Capron A, Auriault C. A radioimmunoassay for the quantification of human ubiquitin in biological fluids: Application to parasitic and allergic diseases. *Journal of Immunological Methods*. 1994;173:8
4. Takagi M, Yamauchi M, Toda G, Takada K, Hirakawa T, Ohkawa K. Serum ubiquitin levels in patients with alcoholic liver disease. *Alcohol Clin Exp Res*. 1999;23 Suppl s4:76S-80S
5. Akarsu E, Pirim I, Capoğlu I, Deniz O, Akçay G, Unüvar N. Relationship between electroneurographic changes and serum ubiquitin levels in patients with type 2 diabetes. *Diabetes Care*. 2001;24:100-103
6. Okada M, Miyazaki S, Hirasawa Y. Increase in plasma concentration of ubiquitin in dialysis patients: Possible involvement in beta 2-microglobulin amyloidosis. *Clin Chim Acta*. 1993;220:135-144
7. Akarsu E, Pirim I, Selçuk NY, Tombul HZ, Cetinkaya R. Relation between serum ubiquitin levels and kt/v in chronic hemodialysis patients. *Nephron*. 2001;88:280-282
8. Majetschak M, King DR, Krehmeier U, Busby LT, Thome C, Vajkoczy S, Proctor KG. Ubiquitin immunoreactivity in cerebrospinal fluid after traumatic brain injury: Clinical and experimental findings. *Crit Care Med*. 2005;33:1589-1594
9. Sharma HS, Maulik N, Gho BC, Das DK, Verdouw PD. Coordinated expression of heme oxygenase-1 and ubiquitin in the porcine heart subjected to ischemia and reperfusion. *Mol Cell Biochem*. 1996;157:111-116
10. Pancré V, Pierce RJ, Fournier F, Mehtali M, Delanoye A, Capron A, Auriault C. Effect of ubiquitin on platelet functions: Possible identity with platelet activity suppressive lymphokine (pasl). *Eur J Immunol*. 1991;21:2735-2741
11. Majetschak M, Krehmeier U, Bardenheuer M, Denz C, Quintel M, Voggenreiter G, Obertacke U. Extracellular ubiquitin inhibits the tnf-alpha response to endotoxin in peripheral blood mononuclear cells and regulates endotoxin hyporesponsiveness in critical illness. *Blood*. 2003;101:1882-1890
12. Majetschak M, Cohn SM, Nelson JA, Burton EH, Obertacke U, Proctor KG. Effects of exogenous ubiquitin in lethal endotoxemia. *Surgery*. 2004;135:536-543
13. Daino H, Matsumura I, Takada K, Odajima J, Tanaka H, Ueda S, Shibayama H, Ikeda H, Hibi M, Machii T, Hirano T, Kanakura Y. Induction of apoptosis by extracellular ubiquitin in human hematopoietic cells: Possible involvement of stat3 degradation by proteasome pathway in interleukin 6-dependent hematopoietic cells. *Blood*. 2000;95:2577-2585
14. Singh M, Roginskaya M, Dalal S, Menon B, Kaverina E, Boluyt MO, Singh K. Extracellular ubiquitin inhibits beta-ar-stimulated apoptosis in cardiac myocytes: Role of gsk-3beta and mitochondrial pathways. *Cardiovasc Res*. 2010;86:20-28
15. Daniels CR, Foster CR, Yakoob S, Dalal S, Joyner WL, Singh M, Singh K. Exogenous ubiquitin modulates chronic β-adrenergic receptor-stimulated myocardial remodeling:

Role in akt activity and matrix metalloproteinase expression. *Am J Physiol Heart Circ Physiol*. 2012;303:H1459-1468
16. Frangogiannis NG, Smith CW, Entman ML. The inflammatory response in myocardial infarction. *Cardiovasc Res*. 2002;53:31-47
17. Bujak M, Frangogiannis NG. The role of tgf-beta signaling in myocardial infarction and cardiac remodeling. *Cardiovasc Res*. 2007;74:184-195
18. Fan D, Takawale A, Lee J, Kassiri Z. Cardiac fibroblasts, fibrosis and extracellular matrix remodeling in heart disease. *Fibrogenesis Tissue Repair*. 2012;5:15
19. Scofield SL, Singh K. Confirmation of myocardial ischemia and reperfusion injury in mice using surface pad electrocardiography. *J Vis Exp*. 2016
20. Xie Z, Singh M, Singh K. Differential regulation of matrix metalloproteinase-2 and -9 expression and activity in adult rat cardiac fibroblasts in response to interleukin-1beta. *J Biol Chem*. 2004;279:39513-39519
21. Jardine DL, Charles CJ, Ashton RK, Bennett SI, Whitehead M, Frampton CM, Nicholls MG. Increased cardiac sympathetic nerve activity following acute myocardial infarction in a sheep model. *J Physiol*. 2005;565:325-333
22. Rona G, Chappel CI, Balazs T, Gaudry R. An infarct-like myocardial lesion and other toxic manifestations produced by isoproterenol in the rat. *AMA Arch Pathol*. 1959;67:443-455
23. Brooks WW, Conrad CH. Isoproterenol-induced myocardial injury and diastolic dysfunction in mice: Structural and functional correlates. *Comp Med*. 2009;59:339-343
24. Communal C, Singh K, Pimentel DR, Colucci WS. Norepinephrine stimulates apoptosis in adult rat ventricular myocytes by activation of the beta-adrenergic pathway. *Circulation*. 1998;98:1329-1334
25. Fan GC, Yuan Q, Song G, Wang Y, Chen G, Qian J, Zhou X, Lee YJ, Ashraf M, Kranias EG. Small heat-shock protein hsp20 attenuates beta-agonist-mediated cardiac remodeling through apoptosis signal-regulating kinase 1. *Circ Res*. 2006;99:1233-1242
26. Simonis G, Strasser RH, Ebner B. Reperfusion injury in acute myocardial infarction. *Crit Care*. 2012;16
27. Foster CR, Daniel LL, Daniels CR, Dalal S, Singh M, Singh K. Deficiency of ataxia telangiectasia mutated kinase modulates cardiac remodeling following myocardial infarction: Involvement in fibrosis and apoptosis. *PLoS One*. 2013;8:e83513
28. Sutton MG, Sharpe N. Left ventricular remodeling after myocardial infarction: Pathophysiology and therapy. *Circulation*. 2000;101:2981-2988
29. Tripathi A, Davis JD, Staren DM, Volkman BF, Majetschak M. Cxc chemokine receptor 4 signaling upon co-activation with stromal cell-derived factor-1α and ubiquitin. *Cytokine*. 2014;65:121-125
30. Tripathi A, Saini V, Marchese A, Volkman BF, Tang WJ, Majetschak M. Modulation of the cxc chemokine receptor 4 agonist activity of ubiquitin through c-terminal protein modification. *Biochemistry*. 2013;52:4184-4192
31. Marchant DJ, Boyd JH, Lin DC, Granville DJ, Garmaroudi FS, McManus BM. Inflammation in myocardial diseases. *Circ Res*. 2012;110:126-144
32. Carbone F, Nencioni A, Mach F, Vuilleumier N, Montecucco F. Pathophysiological role of neutrophils in acute myocardial infarction. *Thromb Haemost*. 2013;110:501-514
33. Frodermann V, Nahrendorf M. Neutrophil-macrophage cross-talk in acute myocardial infarction. *Eur Heart J*. 2017;38:198-200

34. Lefer DJ. Do neutrophils contribute to myocardial reperfusion injury? *Basic Res Cardiol*. 2002;97:263-267
35. Romson JL, Hook BG, Kunkel SL, Abrams GD, Schork MA, Lucchesi BR. Reduction of the extent of ischemic myocardial injury by neutrophil depletion in the dog. *Circulation*. 1983;67:1016-1023
36. Jordan JE, Zhao ZQ, Vinten-Johansen J. The role of neutrophils in myocardial ischemia-reperfusion injury. *Cardiovasc Res*. 1999;43:860-878
37. Majetschak M, Cohn SM, Obertacke U, Proctor KG. Therapeutic potential of exogenous ubiquitin during resuscitation from severe trauma. *J Trauma*. 2004;56:991-999; discussion 999-1000
38. Garcia-Covarrubias L, Manning EW, Sorell LT, Pham SM, Majetschak M. Ubiquitin enhances the th2 cytokine response and attenuates ischemia-reperfusion injury in the lung. *Crit Care Med*. 2008;36:979-982
39. DeCoux A, Lindsey ML, Villarreal F, Garcia RA, Schulz R. Myocardial matrix metalloproteinase-2: Inside out and upside down. *J Mol Cell Cardiol*. 2014;77:64-72
40. Jacob-Ferreira AL, Schulz R. Activation of intracellular matrix metalloproteinase-2 by reactive oxygen-nitrogen species: Consequences and therapeutic strategies in the heart. *Arch Biochem Biophys*. 2013;540:82-93
41. Bergman MR, Cheng S, Honbo N, Piacentini L, Karliner JS, Lovett DH. A functional activating protein 1 (ap-1) site regulates matrix metalloproteinase 2 (mmp-2) transcription by cardiac cells through interactions with junb-fra1 and junb-fosb heterodimers. *Biochem J*. 2003;369:485-496
42. Alfonso-Jaume MA, Bergman MR, Mahimkar R, Cheng S, Jin ZQ, Karliner JS, Lovett DH. Cardiac ischemia-reperfusion injury induces matrix metalloproteinase-2 expression through the ap-1 components fosb and junb. *Am J Physiol Heart Circ Physiol*. 2006;291:H1838-1846
43. Ben-Yosef Y, Lahat N, Shapiro S, Bitterman H, Miller A. Regulation of endothelial matrix metalloproteinase-2 by hypoxia/reoxygenation. *Circ Res*. 2002;90:784-791
44. Etoh T, Joffs C, Deschamps AM, Davis J, Dowdy K, Hendrick J, Baicu S, Mukherjee R, Manhaini M, Spinale FG. Myocardial and interstitial matrix metalloproteinase activity after acute myocardial infarction in pigs. *Am J Physiol Heart Circ Physiol*. 2001;281:H987-994
45. Brønnum H, Eskildsen T, Andersen DC, Schneider M, Sheikh SP. Il-1β suppresses tgf-β-mediated myofibroblast differentiation in cardiac fibroblasts. *Growth Factors*. 2013;31:81-89

CHAPTER 4

EXTRACELLULAR UBIQUITIN AFFECTS CARDIAC FIBROBLAST FUNCTION AND PROLIFERATION

Stephanie L.C. Scofield[1], Suman Dalal[1], Mahipal Singh[1], Krishna Singh[1,2,3]

[1]Department of Biomedical Sciences, James H Quillen College of Medicine
[2]James H Quillen Veterans Affairs Medical Center
[3]Center of Excellence for Inflammation, Infectious Disease and Immunity
East Tennessee State University
Johnson City, TN 37614

Running Title: Extracellular ubiquitin and cardiac fibroblasts

Key words: Ubiquitin, Fibroblast, CXCR-4, Heart

#Correspondence: Krishna Singh, Ph.D., FAHA, FAPS
Dept of Biomedical Sciences
James H Quillen College of Medicine
East Tennessee State University
PO Box 70582, Johnson City, TN 37614
Ph: 423-439-2049
Fax: 423-439-2052
E-mail: singhk@etsu.edu

Abstract

Aims: Chronic β-adrenergic receptor (β-AR) stimulation increases levels of exogenous ubiquitin (UB). Exogenous UB plays a protective role against β-AR-stimulated cardiac remodeling including reducing the extent of myocardial fibrosis. Cardiac fibroblasts are non-polar cells of mesenchymal origin that are vital to extracellular matrix (ECM) turnover and homeostasis of the heart. Cardiac fibroblasts are also key players in the deposition of fibrosis that contributes to structural remodeling of the heart in response to myocardial injury or chronic stress. This study tested the hypothesis that exogenous UB interacts with chemokine receptor CXCR-4 to affect cardiac fibroblast function. Methods and Results: Primary cultures of cardiac fibroblasts were isolated from adult rat hearts. Using FITC-labeled UB we offer evidence that FITC-UB interacts with cardiac fibroblasts and is internalized into the cells at 1 h. UB/CXCR-4 interaction was determined using biotinylated-UB (b-UB) and streptavidin magnetic beads. UB inhibited fetal bovine serum (FBS) mediated increases in fibroblast proliferation at 24 h. Lastly, UB increased the contractility of cardiac fibroblasts in a collagen gel contraction assay. Conclusion: Exogenous UB interacts with CXCR-4 and associates with inhibition of fibroblast proliferation and increased fibroblast contractility.

Introduction

Heart disease is the leading cause of death, accounting for 630,000 or 25% of American deaths per year. The most common type of heart disease is coronary artery disease. (Statistics provided by the Centers for Disease Control). Each year 785,000 Americans will have their first heart attack and 470,000 will have another heart attack. (Statistics provided by the American Heart Association). This statistic is both positive and negative because it sheds light on the fact that many Americans are surviving heart attacks but also, that many Americans are living with some degree of heart damage from these heart attacks. After an injury such as a heart attack, the dead portion of the heart muscle is often replaced by collagen rich scar material called fibrosis(20).

Myocardial fibrosis refers to the accumulation of extracellular matrix (ECM) within the myocardium. Myocardial fibrosis consists mainly of fibrillar collagens(11). The over-deposition of collagen may contribute to structural changes in the heart, which impair function(12). The phenomenon of cardiac structure changing in response to stress or injury is called myocardial remodeling and is usually undesirable. Deposition of too much collagen increases the rigidity of the heart muscle which then begins to interfere with the rhythmic contraction and relaxation function of the heart(5). Once the collagen deposits begin to impair the heart's beating efficiency, the downward progression towards heart failure begins.

Cardiac fibroblasts are mesenchymal cells and are the main mediators of ECM production and collagen deposition. Under injury conditions, fibroblasts transdifferentiate into myofibroblasts which adopt characteristics of smooth muscle cells by enhancing stress fibers and thereby contractility(20). Myofibroblasts have enhanced contractility and secretory capabilities that function to repair wounds post myocardial infarction(19). Fibroblast to myofibroblast

transdifferentiation is typically initiated by transforming growth factor β1 (TGF-β1) which is proposed to induce activation of proteins related to increased fibroblast proliferation(18, 20, 21, 36). An understanding of fibroblast's role in myocardial remodeling and how to manipulate the phenotype and function of fibroblasts is vital to effectively preventing and/or treating heart failure.

Previously, our lab demonstrated that sympathetic β-adrenergic receptor (β-AR) stimulation increases extracellular concentrations of ubiquitin (UB) in adult rat cardiac myocytes(37). UB is a small molecular weight protein (~8.5 kDa) best known for its intracellular role in flagging damaged or misfolded proteins for proteasomal degradation(17). Low levels of UB are normal in plasma. Elevated levels of UB are described in the serum or plasma of patients with various pathologies including parasitic and allergic diseases(4), alcoholic liver disease(39), type-2 diabetes(1), β2-microglobulin amyloidosis(27) and chronic hemodialysis(2). Patients with traumatic brain injury are shown to have increased UB levels in the cerebrospinal fluid(24). Extracellular UB is proposed to have pleiotropic functions including regulation of immune response, anti-inflammatory and neuroprotective activities(23, 25, 28), as well as regulation of growth and apoptosis in hematopoietic cells(8). Our lab has also shown that treatment of adult rat ventricular myocytes with UB inhibits β-AR-stimulated apoptosis(37).

Our lab also provided evidence that UB treatment reduces β-AR-stimulated increases in myocardial fibrosis(10). Evidence suggests that extracellular UB, which is structurally identical to intracellular UB(41), can function as a signaling protein. UB's ability to bind C-X-C chemokine receptor type 4 (CXCR-4) has been demonstrated in THP-1 human monocytic cell line cells(31). UB-CXCR-4 interaction follows a two-site binding mechanism in which the

hydrophobic surface patch surrounding Phe-4 and Val-70 are important for receptor binding, while the flexible C-terminus facilitates receptor activation(32).

The objective of this study was to investigate the role of UB on cardiac fibroblast phenotype and function, and to define the role of CXCR-4 in the modulation of fibroblast phenotype and function in response to UB. We hypothesized that extracellular UB influences fibroblast phenotype and function by interacting with CXCR-4. The data presented here suggest that UB interacts with CXCR-4, and increases collagen gel contractile activity of fibroblasts, while inhibiting FBS-stimulated cell proliferation.

Materials and Methods

Vertebrate Animals

All experiments and procedures were reviewed and approved by the East Tennessee State University Institutional Committee on Animal Care and conform to the Guide for the Care and Use of Laboratory Animals published by the US National Institutes of Health (NIH Publication No. 85-23, revised 1996). Primary cultures of cardiac fibroblast were isolated from male Sprague-Dawley rats (average wt: 200-225g; Harlan, Indianapolis, IN). For cardiac excision, rats were anesthetized using a mixture of isoflurane (2.5%) and oxygen (0.5 l/min). The heart was then removed from the chest cavity following a bilateral diaphragm incision. Rat euthanasia was achieved by exsanguination.

Fibroblast isolation and treatment

Cardiac fibroblasts were isolated as previously described[42]. Cardiac fibroblasts were grown to ~90% confluence and serum-starved for 48 h to achieve cell cycle arrest before use. Experiments were performed using cells from passage 1-3. Depending on the treatment group, cells were

pretreated with AMD-3100 (AMD; 10 µM; Sigma) for 30 min followed by treatment with UB (10 µg/ml; Sigma).

Fluorescence/Confocal Microscopy

Fibroblasts, plated on glass bottom dishes, were allowed to grow with serum for 24 hours. FITC conjugated UB (FITC-UB; 1µg/mL; Cal Biochem) or anti-rabbit FITC secondary (negative control) were introduced to the culture and allowed to incubate at 37° for 1 hour before washing and fixation with 4% paraformaldehyde. Cells were co-stained with Hoechst 33258 for nuclear localization. Images were taken on a confocal microscope (Olympus, Leica). Multiple cells per dish were imaged at differing magnifications in z-stack and orthogonal views.

UB/CXCR4 interaction

Confluent cultures of fibroblasts (two p100 dishes) were lysed using RIPA buffer (10 mM Tris·HCl (pH 7.2), 158 mM NaCl, 1 mM EGTA, 0.1% SDS, 1% sodium deoxycholate, 1% Triton X-100, 1 mM sodium orthovanadate, and 0.2 mM phenylmethylsulfonyl fluoride) and divided into two equal parts. Total lysates were centrifuged at 20,000 g for 15 min to separate soluble and membrane-bound proteins. Membrane fractions were resuspended in RIPA buffer and agitated. In a separate tube, biotinylated-UB (b-UB; 10µg/mg of Dynabeads) and pre-washed Dynabeads (M280, Invitrogen) were incubated at room temperature for 1 h to allow a bond to form between the Dynabeads and the b-UB herein referred to as Dyna-b-UB. After 1 h, the magnetic beads were washed 3x with PBS containing 1% BSA. Fibroblast lysates were incubated with Dyna-b-UB or Dynabeads alone overnight at 4° on a rocker. Dynabeads were then washed 3x with PBS containing 1% BSA. The dynabeads were then suspended in RIPA buffer and boiled for 15 m at 95°. After cooling, the dynabeads were separated from proteins using a magnet. The protein samples were then resolved by SDS-PAGE and transferred onto a

PVDF membrane. The membranes were then probed with anti-CXCR-4 antibodies (abcam). Band intensities were visualized using x-ray film.

Proliferation assay

An equal number of fibroblasts were seeded onto glass coverslips and incubated in DMEM supplemented with 10% serum for 2 hours at 37°C. The cells were then serum starved for 48 h. The cells were then treated with FBS (1%) with or without UB (10µg/ml) for 24 h. The cells were fixed using methanol for 10 min followed by washing with PBS. The cells were then incubated in blocking solution (5% BSA in PBS) for 1 h followed by incubation with anti-Ki-67 antibodies (abcam) at 1:100 dilution overnight at 4°C. After washing, the cells were incubated with FITC-labeled secondary antibodies for 1 h at room temperature in the dark. After washing, the cells were incubated in hochest 33342 (10µM; nuclear stain). The cells were then washed, mounted and visualized using a fluorescent microscope (EVOS).

Images were acquired using Life Technologies EVOS FL Auto microscope. A cell was determined to be actively proliferating if FITC-Ki-67 positive staining co0localized with nuclear staining. The percentage of Ki-67-positive cells relative to the total number of nuclei was determined by counting five randomly chosen fields per coverslip. Percentages were normalized to 0 h and expressed as fold-change vs control.

Collagen contraction assay

Serum starved fibroblasts were mixed with collagen solution (1 mg/ml) to achieve the final cell count of 3 x 105 cells/ml. 500µl of this suspension was aliquoted into a 24 well culture pate and allowed to polymerize at 37°C for 30 min. The gels were released from wells, transferred to p60 culture dishes, floated in DMEM and incubated at 37°C for 24 h. Fibroblast containing gels were treated with UB (10µg/ml) or AMD3100 (AMD; 10µM; CXCR-4 antagonist) for 24 h. For

AMD+UB, AMD was added 30 min prior to UB treatment. TGF-β1 (10nM) treatment was used as a positive control. Images were acquired at 0 h and 24 h to assess the degree of gel contraction. The area of each collagen gel pad was measured using NIS elements software (Nikon).

Statistical analysis

Data are expressed as the mean ± SEM. Data were analyzed using Student's t-test or a two-way analysis of variance (ANOVA) followed by Student-Newman-Keuls test. Probability (p) values of <0.05 were considered to be significant.

Results

Interaction of extracellular UB

Stacked and orthogonal views using confocal microscopy revealed clear colocalization of FITC-UB with cardiac fibroblasts (Fig 4.1A&B). Orthogonal images revealed colocalization of FTIC-UB within the cell as well as the nucleus (Fig 4.1C).

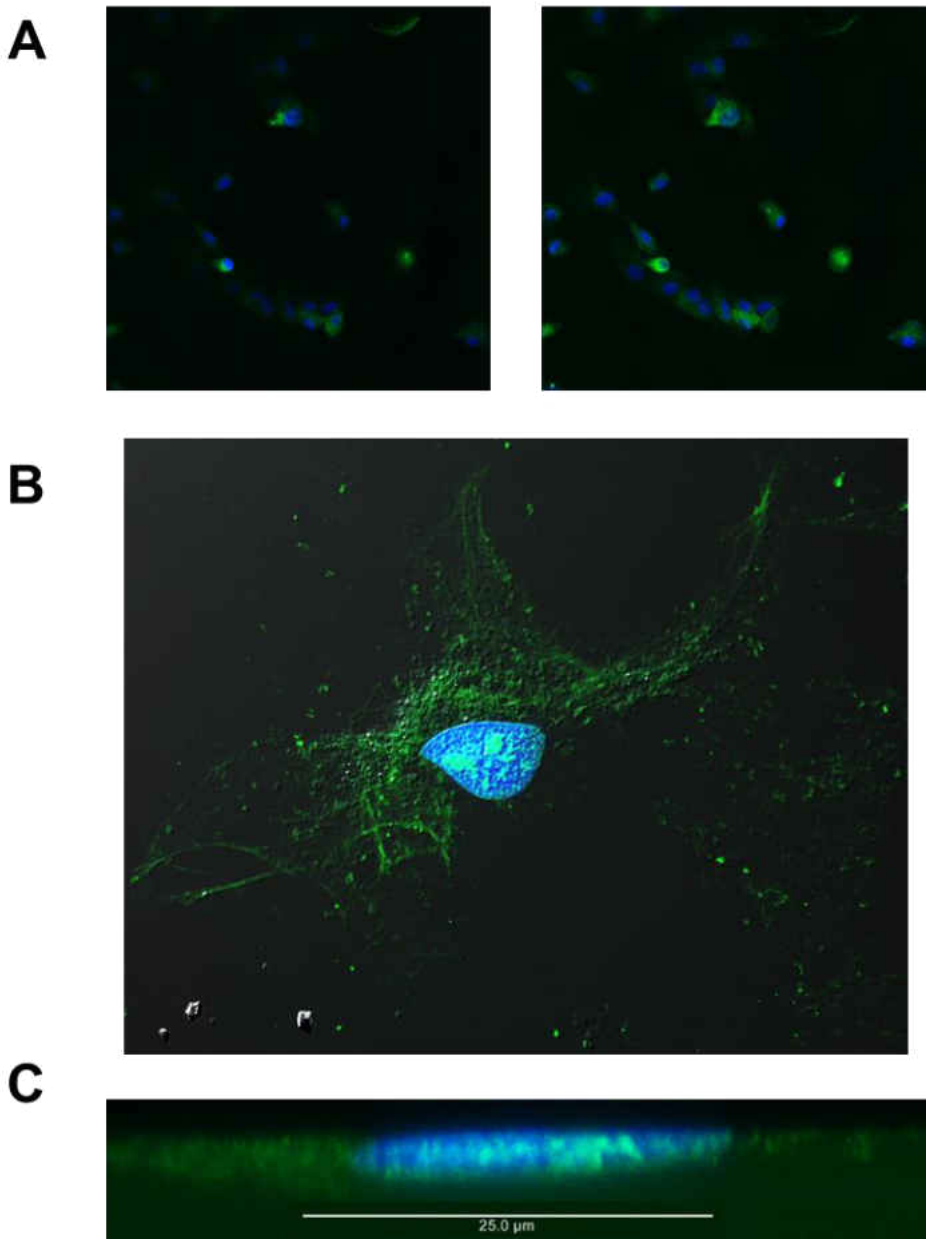

Figure 4.1. Interaction and Internalization of Extracellular UB: Fibroblasts were incubated with FITC-UB (1 µg/ml) for 1 hr. Live cells were visualized using confocal microscopy and photographed. Green staining indicates FITC-labeled UB, while blue staining indicates nuclear staining using Hoechst 33258 (n=3). A. Two images from a Z-stack of the same area of fibroblasts. B. A single fibroblast Z-stack composite image incorporating DIC. C. Orthogonal view of a single fibroblast at the epicenter of the nucleus.

Interaction of UB with CXCR-4

Analyses of cytosolic and membrane fractions using biotinylated UB and dynabead incubation assay revealed clear interaction of UB with VXCR-4 in the membrane fraction. There was no detectable signal for CXCR-4 in the cytosolic fraction (Fig 4.2).

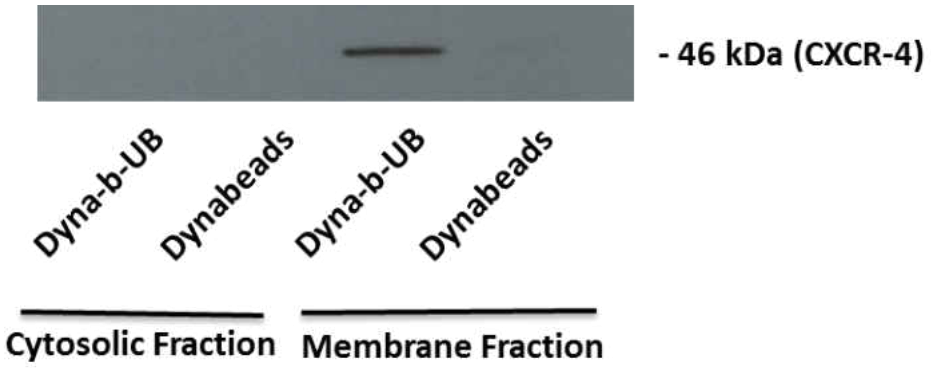

Figure 4.2. Interaction of Extracellular UB with CXCR-4: Fibroblast lysates (cytosolic and membrane fractions) were incubated with Dynabeads (negative control) or Dyna-b-UB complexes overnight at 4°C. Dynabeads or Dyna-b-UB complexes were separated using SDS-PAGE and transferred to PVDF membranes. The membranes were probed with anti-CXCR-4 antibodies. Band intensities were detected using autoradiography. The visible band shows interaction between UB and CXCR-4 (a transmembrane receptor) in the membrane fraction (n=3).

Extracellular UB inhibits proliferation of fibroblasts

Ki-67 is found in the nucleus of proliferative cells. It is undetectable during G0 phase and reaches peak levels during G2/mitosis(14). Ki-67 is commonly used as an index of proliferation(22). 24 h UB treatment alone had no effect on fibroblast proliferation. The number of Ki-67-positive cells was not significantly different between control and UB-treated samples. FBS significantly increased fibroblast proliferation vs control. UB in the presence of FBS significantly reduced the FBS-stimulated increase in fibroblast proliferation. (CTL, 1.63±0.13; FBS, 3.76±0.85*; FBS+UB, 1.56±0.16$; UB, 1.31±0.25; *$p<0.05$ vs CTL; $p<0.05$ vs FBS; n = 3-4; Fig 4.3).

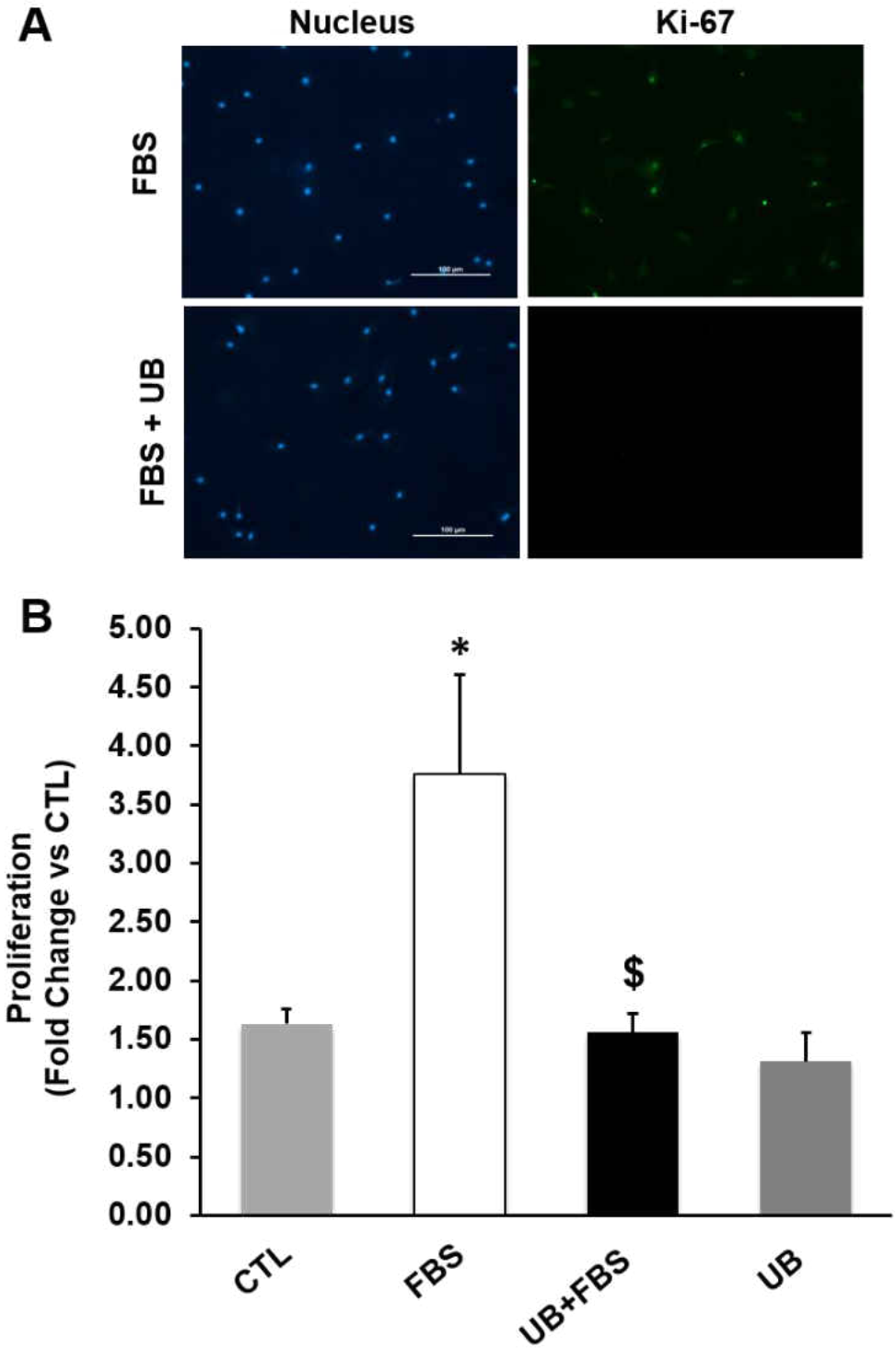

Figure 4.3. Extracellular UB inhibits FBS-Mediated Increase in Fibroblast Proliferation: Fibroblasts were grown on glass coverslips and serum starved for 48 h. The cells were treated with FBS (1%) in the presence or absence of UB (10 μg/mL) for 24 h. The cells were immunostained using anti-Ki-67 antibodies. A. The first panel depicts images from FBS and UB+FBS treated cells. Green fluorescence indicates Ki-67-positive staining, while blue staining

indicates the nucleus, stained using Hoechst 33258. B. The second panel depicts a graphic representation of proliferation as fold change vs CTL. *P<0.05 vs CTL, $P<0.05 vs FBS, n=3-4.

Extracellular UB increases contraction of fibroblast-populated collagen gel pads

Fibroblast-seeded collagen gel pad contraction assay revealed that UB significantly increases fibroblast-mediated collagen gel pad contraction versus control. AMD alone had no effect on collagen gel contraction. However, pretreatment with AMD significantly inhibited UB-mediated increase in collagen gel pad contraction. TGF-β1, positive control, also enhanced collagen gel contraction. The extent of contraction of fibroblast-populated collagen gels using TGF-β1 is similar to that of UB (Fold Change; CTL, 1.00±0; UB, 1.08±0.02*; AMD, 0.86±0.07; AMD+UB, 0.89±0.05$; TGF-β1, 1.21±0.04*; *p<0.05 vs CTL; $p<0.05 vs UB; n=3-6; Fig 4.4).

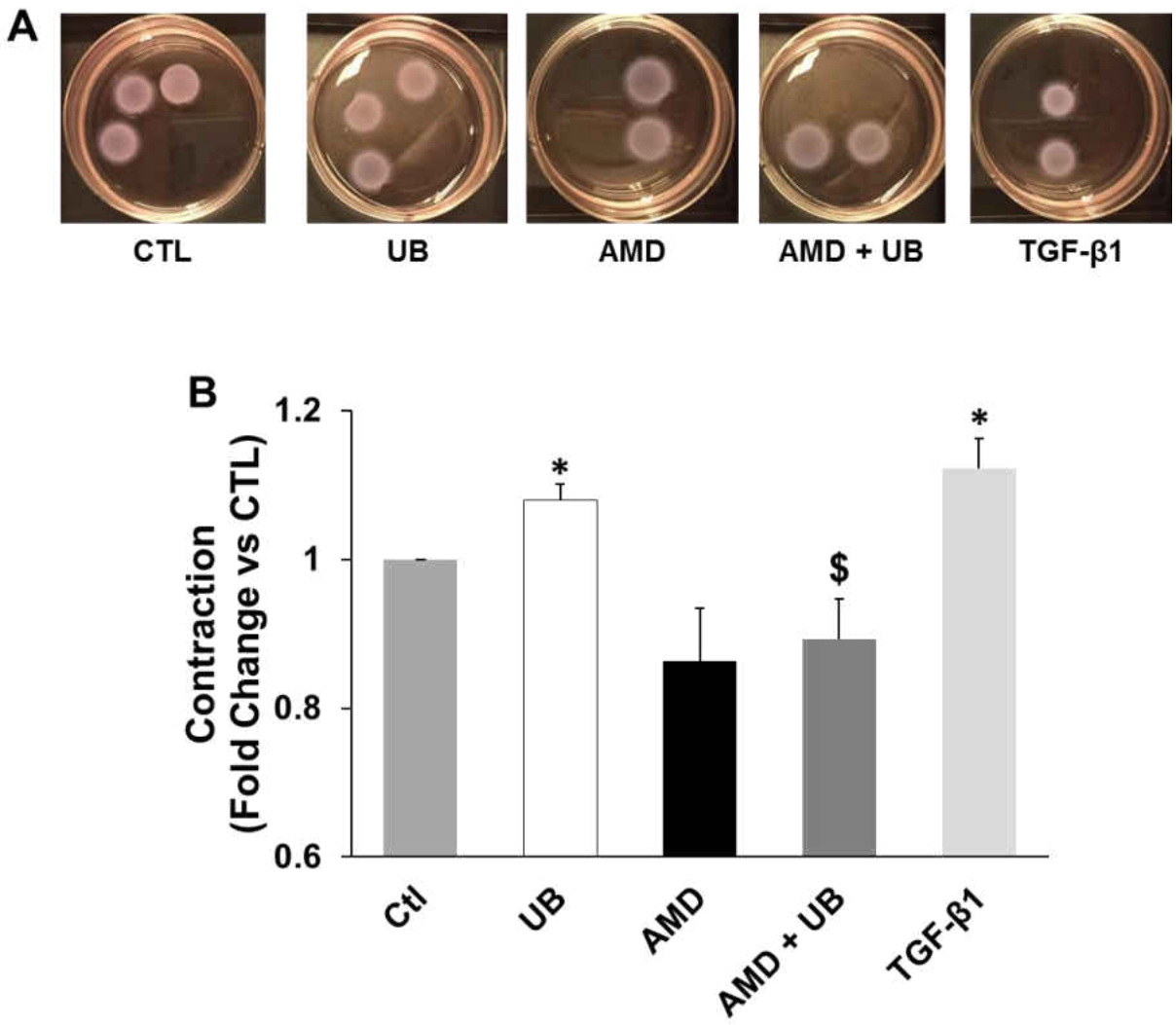

Figure 4.4. Extracellular UB Increases Collagen Gel Contraction: Fibroblasts were seeded in collagen gels. Collagen pads were pretreated with AMD3100 for 30 min followed by treatment with UB for 24 h. TGF-β1 treatment served as a positive control. A. Panel A depicts collagen gel pads 24 h following treatments. B. Panel B shows quantitative analyses of fibroblast-populated collagen gel pads; *P<0.05 vs CTL; n = 4-6.

Discussion

Cardiac fibroblasts play a key role in pathological fibrosis, wound healing and cardiac homeostasis through ECM production and maintenance. This study investigated the role of exogenous UB on cardiac fibroblast phenotype and function. Here, we provide evidence that

extracellular UB interacts with CXCR-4 and influences fibroblast phenotype and function. Our findings demonstrate that 1) UB interacts with CXCR-4 in cardiac fibroblasts; 2) UB treatment inhibits FBS-stimulated cell proliferation; and 3) UB treatment enhances contraction of fibroblast populated collagen gel pads. These data taken together provide evidence that extracellular UB, most likely acting via CXCR-4, influences fibroblast phenotype and function.

UB is a normal component of plasma. Plasma levels of UB are found to be increased under a variety of pathological conditions(35). Biological functions of extracellular UB are not yet completely understood. Based on few reports, extracellular UB is proposed to have multiple functions including neuroprotection after traumatic brain injury, anti-inflammatory properties in response to lipopolysaccharide infusion, regulation of the immune response in terms of the Th2 cytokine response, and growth and apoptosis of hematopoetic cell types(8, 9, 13, 15, 25). Previously our lab demonstrated that β adrenergic receptor (β-AR) stimulation significantly increased interaction of UB with adult rat ventricular myocytes(37). The use of N-terminal biotin-labeled UB demonstrated that adult rat ventricular myocytes can interact with and uptake extracellular UB(37). The use of N-terminal fluorescein-labeled UB demonstrated interaction and uptake of extracellular UB in monocytic leukemia cells as well as human peripheral blood mononuclear cells(26). Here we demonstrate uptake of FITC-labeled UB in cardiac fibroblasts.

CXCR-4, a G-protein coupled receptor, is known for its role in HIV-entry and cancer metastasis(6). Stromal derived factor-1 alpha (SDF-1α) is a cognate ligand for CXCR-4. SDF-1α interaction with CXCR-4 plays an important role in regulating the homing of bone marrow derived stem cells and their mobilization into peripheral blood(29). Saini *et al.* identified CXCR-4 as the cell surface receptor for extracellular UB in THP-1 human monocytic cell line(31). Using CXCR-4 antagonist, AMD3100, our lab previously provided evidence that UB/CXCR-4

interaction plays a role in stimulating angiogenesis in cardiac microvascular endothelial cells(38). Here using b-UB, we provide evidence that extracellular UB is interacting with CXCR-4. It is interesting to note that confocal microscopy (Fig 4.1) demonstrates cytosolic and nuclear presence of FITC-UB in fibroblasts. However, using dynabeads, our b-UB assay shows no interaction of b-UB with CXCR-4 in cytosolic fractions. The reason for lack of detection of interaction between b-UB and CXCR-4 may be due to negligible presence of CXCR-4 in the cytosol, since it is a transmembrane receptor. SDF-1α binding induces internalization of CXCR-4 in leukocytes(3). Extracellular UB is proposed to be internalized into human monocytic leukemia cells (THP-1) via CXCR-4(31). In this study, UB interaction with CXCR-4 was investigated using membrane and cytosolic fractions as opposed to live cells. Future experiments are needed to investigate potential UB/CXCR-4 internalization in cardiac fibroblasts.

Myofibroblasts have the ability to contract to close wounds effectively because of their α-SMA reinforced actin structure(7). Once the myofibroblasts adhere to multiple points in the wounded or stressed area, the α-SMA reinforced fibers pull the adherence points closer together generating wound contracture. This effect is mirrored in the collagen gel contraction assays *in vitro*(33). In hepatic stellate cells, stimulation of CXCR-4 with SDF-1α is shown to promote the contraction of collagen gels, which is inhibited by pretreatment with AMD3100(30). Here we show that UB treatment stimulates collagen gel contraction, and that CXCR-4 antagonist, AMD3100, negates UB-mediated increases in collagen gel contraction. These data suggest a role for the UB/CXCR-4 axis in modulation of fibroblast function.

Compromising the ECM composition after large injuries such as myocardial infarction (MI) destabilizes the heart and predisposes it to cardiac rupture(34, 40). Since fibroblasts play an integral role in composition of the ECM and collagen-based scar formation, it is likely that

inhibition of fibroblast proliferation would predispose the heart to cardiac rupture post-MI. Conversely, rapid proliferation of fibroblasts and subsequent deposition of extracellular matrix post-MI also associates with adverse effects on cardiac structure and function(16). Therefore, a well-controlled balance between fibroblast proliferation and ECM deposition is integral in the maintenance of ECM homeostasis. Here, we observed that UB significantly inhibits FBS-mediated increases in proliferation of cardiac fibroblasts. UB alone had no effect on fibroblast proliferation. In T cell line KT-3 and myeloid cell line HL-60, UB is shown to inhibit cell growth via selective degradation of the STAT3 transcription factor(8). Previously, our lab has provided evidence that UB inhibits β-AR stimulated increases in cardiac fibrosis(10). UB treatment also enhanced expression of matrix metalloproteinases (MMP-2 and MMP-9). Together, these data suggest that UB has the potential to decrease myocardial fibrosis by modulating expression of MMPs and/or fibroblast proliferation.

The data presented are important because cardiac fibroblasts play a major role in wound healing post myocardial injury. This present study provides evidence that extracellular UB influences fibroblast function and proliferation, most likely by interacting with CXCR-4. The finding that UB decreases FBS-stimulated increases in fibroblast proliferation may imply that UB-mediated decrease in fibroblast proliferation may help modulate scar formation in the heart, specifically post-MI. However, further investigations are needed to investigate the role of UB in wound healing processes of the heart post-MI.

Perspectives

Investigation of signaling mechanisms leading to UB-mediated regulation of cardiac fibroblast function and proliferation may help uncover strategies to improve cardiac remodeling and function.

Funding

This work was supported by Merit Review awards (BX002332 and BX000640) from the Biomedical Laboratory Research and Development Service of the Veterans Affairs Office of Research and Development, National Institutes of Health (R15HL129140), and funds from Institutional Research and Improvement account. The project is supported in part by the National Institutes of Health grant C06RR0306551.

Acknowledgement

We appreciate the technical support of Bobbie Connelly.

Conflicts of Interest

None.

References

1. Akarsu E, Pirim I, Capoğlu I, Deniz O, Akçay G, and Unüvar N. Relationship between electroneurographic changes and serum ubiquitin levels in patients with type 2 diabetes. *Diabetes Care* 24: 100-103, 2001.
2. Akarsu E, Pirim I, Selçuk NY, Tombul HZ, and Cetinkaya R. Relation between serum ubiquitin levels and KT/V in chronic hemodialysis patients. *Nephron* 88: 280-282, 2001.
3. Amara A, Gall SL, Schwartz O, Salamero J, Montes M, Loetscher P, Baggiolini M, Virelizier JL, and Arenzana-Seisdedos F. HIV coreceptor downregulation as antiviral principle: SDF-1alpha-dependent internalization of the chemokine receptor CXCR4 contributes to inhibition of HIV replication. *J Exp Med* 186: 139-146, 1997.
4. Asseman C, Pancré V, Delanoye A, Capron A, and Auriault C. A radioimmunoassay for the quantification of human ubiquitin in biological fluids: application to parasitic and allergic diseases. *J Immunol Methods* 173: 93-101, 1994.
5. Berk BC, Fujiwara K, and Lehoux S. ECM remodeling in hypertensive heart disease. *J Clin Invest* 117: 568-575, 2007.
6. Busillo JM and Benovic JL. Regulation of CXCR4 signaling. *Biochim Biophys Acta* 1768: 952-963, 2007.
7. Chen W and Frangogiannis NG. Fibroblasts in post-infarction inflammation and cardiac repair. *Biochim Biophys Acta* 1833: 945-953, 2013.
8. Daino H, Matsumura I, Takada K, Odajima J, Tanaka H, Ueda S, Shibayama H, Ikeda H, Hibi M, Machii T, Hirano T, and Kanakura Y. Induction of apoptosis by extracellular ubiquitin in human hematopoietic cells: possible involvement of STAT3 degradation by proteasome pathway in interleukin 6-dependent hematopoietic cells. *Blood* 95: 2577-2585, 2000.
9. Daino H, Shibayama H, Machii T, and Kitani T. Extracellular ubiquitin regulates the growth of human hematopoietic cells. *Biochem Biophys Res Commun* 223: 226-228, 1996.
10. Daniels CR, Foster CR, Yakoob S, Dalal S, Joyner WL, Singh M, and Singh K. Exogenous ubiquitin modulates chronic β-adrenergic receptor-stimulated myocardial remodeling: role in Akt activity and matrix metalloproteinase expression. *Am J Physiol Heart Circ Physiol* 303: H1459-1468, 2012.
11. Díez J, González A, and Ravassa S. Understanding the Role of CCN Matricellular Proteins in Myocardial Fibrosis. *J Am Coll Cardiol* 67: 1569-1571, 2016.
12. Engebretsen KV, Skårdal K, Bjørnstad S, Marstein HS, Skrbic B, Sjaastad I, Christensen G, Bjørnstad JL, and Tønnessen T. Attenuated development of cardiac fibrosis in left ventricular pressure overload by SM16, an orally active inhibitor of ALK5. *J Mol Cell Cardiol* 76: 148-157, 2014.
13. Garcia-Covarrubias L, Manning EW, Sorell LT, Pham SM, and Majetschak M. Ubiquitin enhances the Th2 cytokine response and attenuates ischemia-reperfusion injury in the lung. *Crit Care Med* 36: 979-982, 2008.
14. Gerdes J, Lemke H, Baisch H, Wacker HH, Schwab U, and Stein H. Cell cycle analysis of a cell proliferation-associated human nuclear antigen defined by the monoclonal antibody Ki-67. *J Immunol* 133: 1710-1715, 1984.
15. Griebenow M, Casalis P, Woiciechowsky C, Majetschak M, and Thomale UW. Ubiquitin reduces contusion volume after controlled cortical impact injury in rats. *J Neurotrauma* 24: 1529-1535, 2007.

16. Gurtner GC, Werner S, Barrandon Y, and Longaker MT. Wound repair and regeneration. *Nature* 453: 314-321, 2008.
17. Hershko A, Ciechanover A, Heller H, Haas AL, and Rose IA. Proposed role of ATP in protein breakdown: conjugation of protein with multiple chains of the polypeptide of ATP-dependent proteolysis. *Proc Natl Acad Sci U S A* 77: 1783-1786, 1980.
18. Hinz B. Formation and function of the myofibroblast during tissue repair. *J Invest Dermatol* 127: 526-537, 2007.
19. Hinz B, Phan SH, Thannickal VJ, Galli A, Bochaton-Piallat ML, and Gabbiani G. The myofibroblast: one function, multiple origins. *Am J Pathol* 170: 1807-1816, 2007.
20. Kong P, Christia P, and Frangogiannis NG. The pathogenesis of cardiac fibrosis. *Cell Mol Life Sci* 71: 549-574, 2014.
21. Leask A, Holmes A, and Abraham DJ. Connective tissue growth factor: a new and important player in the pathogenesis of fibrosis. *Curr Rheumatol Rep* 4: 136-142, 2002.
22. Liu J, Hu F, Tang J, Tang S, Xia K, Wu S, Yin C, Wang S, He Q, Xie H, and Zhou J. Homemade-device-induced negative pressure promotes wound healing more efficiently than VSD-induced positive pressure by regulating inflammation, proliferation and remodeling. *Int J Mol Med* 39: 879-888, 2017.
23. Majetschak M, Cohn SM, Nelson JA, Burton EH, Obertacke U, and Proctor KG. Effects of exogenous ubiquitin in lethal endotoxemia. *Surgery* 135: 536-543, 2004.
24. Majetschak M, King DR, Krehmeier U, Busby LT, Thome C, Vajkoczy S, and Proctor KG. Ubiquitin immunoreactivity in cerebrospinal fluid after traumatic brain injury: clinical and experimental findings. *Crit Care Med* 33: 1589-1594, 2005.
25. Majetschak M, Krehmeier U, Bardenheuer M, Denz C, Quintel M, Voggenreiter G, and Obertacke U. Extracellular ubiquitin inhibits the TNF-alpha response to endotoxin in peripheral blood mononuclear cells and regulates endotoxin hyporesponsiveness in critical illness. *Blood* 101: 1882-1890, 2003.
26. Majetschak M, Ponelies N, and Hirsch T. Targeting the monocytic ubiquitin system with extracellular ubiquitin. *Immunol Cell Biol* 84: 59-65, 2006.
27. Okada M, Miyazaki S, and Hirasawa Y. Increase in plasma concentration of ubiquitin in dialysis patients: possible involvement in beta 2-microglobulin amyloidosis. *Clin Chim Acta* 220: 135-144, 1993.
28. Pancré V, Pierce RJ, Fournier F, Mehtali M, Delanoye A, Capron A, and Auriault C. Effect of ubiquitin on platelet functions: possible identity with platelet activity suppressive lymphokine (PASL). *Eur J Immunol* 21: 2735-2741, 1991.
29. Ratajczak MZ, Kim CH, Abdel-Latif A, Schneider G, Kucia M, Morris AJ, Laughlin MJ, and Ratajczak J. A novel perspective on stem cell homing and mobilization: review on bioactive lipids as potent chemoattractants and cationic peptides as underappreciated modulators of responsiveness to SDF-1 gradients. *Leukemia* 26: 63-72, 2012.
30. Saiman Y, Agarwal R, Hickman DA, Fausther M, El-Shamy A, Dranoff JA, Friedman SL, and Bansal MB. CXCL12 induces hepatic stellate cell contraction through a calcium-independent pathway. *Am J Physiol Gastrointest Liver Physiol* 305: G375-382, 2013.
31. Saini V, Marchese A, and Majetschak M. CXC chemokine receptor 4 is a cell surface receptor for extracellular ubiquitin. *J Biol Chem* 285: 15566-15576, 2010.
32. Saini V, Marchese A, Tang WJ, and Majetschak M. Structural determinants of ubiquitin-CXC chemokine receptor 4 interaction. *J Biol Chem* 286: 44145-44152, 2011.

33. Saxena A, Dobaczewski M, Rai V, Haque Z, Chen W, Li N, and Frangogiannis NG. Regulatory T cells are recruited in the infarcted mouse myocardium and may modulate fibroblast phenotype and function. *Am J Physiol Heart Circ Physiol* 307: H1233-1242, 2014.
34. Schellings MW, Vanhoutte D, Swinnen M, Cleutjens JP, Debets J, van Leeuwen RE, d'Hooge J, Van de Werf F, Carmeliet P, Pinto YM, Sage EH, and Heymans S. Absence of SPARC results in increased cardiac rupture and dysfunction after acute myocardial infarction. *J Exp Med* 206: 113-123, 2009.
35. Scofield SL, Amin P, Singh M, and Singh K. Extracellular Ubiquitin: Role in Myocyte Apoptosis and Myocardial Remodeling. *Compr Physiol* 6: 527-560, 2015.
36. Shinde AV and Frangogiannis NG. Fibroblasts in myocardial infarction: a role in inflammation and repair. *J Mol Cell Cardiol* 70: 74-82, 2014.
37. Singh M, Roginskaya M, Dalal S, Menon B, Kaverina E, Boluyt MO, and Singh K. Extracellular ubiquitin inhibits beta-AR-stimulated apoptosis in cardiac myocytes: role of GSK-3beta and mitochondrial pathways. *Cardiovasc Res* 86: 20-28, 2010.
38. Steagall RJ, Daniels CR, Dalal S, Joyner WL, Singh M, and Singh K. Extracellular ubiquitin increases expression of angiogenic molecules and stimulates angiogenesis in cardiac microvascular endothelial cells. *Microcirculation* 21: 324-332, 2014.
39. Takagi M, Yamauchi M, Toda G, Takada K, Hirakawa T, and Ohkawa K. Serum ubiquitin levels in patients with alcoholic liver disease. *Alcohol Clin Exp Res* 23: 76S-80S, 1999.
40. Tao ZY, Cavasin MA, Yang F, Liu YH, and Yang XP. Temporal changes in matrix metalloproteinase expression and inflammatory response associated with cardiac rupture after myocardial infarction in mice. *Life Sci* 74: 1561-1572, 2004.
41. Vijay-Kumar S, Bugg CE, and Cook WJ. Structure of ubiquitin refined at 1.8 A resolution. *J Mol Biol* 194: 531-544, 1987.
42. Xie Z, Singh M, and Singh K. Differential regulation of matrix metalloproteinase-2 and -9 expression and activity in adult rat cardiac fibroblasts in response to interleukin-1beta. *J Biol Chem* 279: 39513-39519, 2004.

CHAPTER 5

CONCLUSIONS

The development of therapies to combat the enormous prevalence of cardiovascular disease in the United States is of key interest to healthcare providers and scientists alike. Currently, multiple different therapies and pharmaceutic targets are being investigated as potential avenues for the treatment of myocardial infarction, I/R injury and heart failure. In order to advance the science and practice of medicine, a more complete understanding of the processes associated with myocardial remodeling and cardiac dysfunction must be elucidated[67].

Heart disease is the leading cause of death and disease in the United States[68]. Heart disease often displays as coronary artery disease, which can lead to myocardial infarction (MI), pathological remodeling and an ultimate decrease in cardiac function. In a healthy heart, many cell types work synergistically to ensure the proper function of the heart. Cardiac myocytes make up the contractile force behind the rhythmic pumping of the heart. Myocytes have limited regenerative capacity[69]. Cardiac fibroblasts are responsible for creating an environment of extracellular matrix (ECM) to maintain the structural and functional integrity of the heart[27]. Cardiac fibroblasts are also responsible for wound healing and fibrosis in the injured heart. Thus, if there is a large loss of myocytes, the wounded area is replaced with fibrosis. Although fibrosis maintains the structural integrity of the heart, it increases cardiac rigidity and leads to a decrease in function[6; 70]. Investigating myocardial remodeling in terms of fibrotic processes and characterization of ECM components may eventually lead to the discovery of novel therapeutics and new investigative targets.

Following I/R injury there is an increase in sympathetic nerve activity in the heart[71]. This increase in sympathetic activity occurs acutely in order to sustain cardiac function post-injury but eventually leads to deleterious effects on cardiac function as well as myocardial structure[72].

Myocardial remodeling associated with sustained β-AR stimulation is characterized by left ventricle (LV) chamber dilation, myocyte apoptosis and decreased contractile function[73].Chronic activation of β-adrenergic receptors (β-AR) increases cardiac myocyte death and worsens the development of heart failure[65; 66; 74]. Our lab has previously shown that chronic β-AR stimulation with the agonist Isoproterenol (ISO) increases myocardial apoptosis and fibrosis *in vivo*[66].

UB is a protein that is expressed intracellularly in all eukaryotic cells[75]. However, UB is also found to be present extracellularly in various bodily fluids including in circulation[33]. Extracellular levels of UB are described as elevated in various biological fluids in patients and animal models across many different pathologies. These pathologic conditions include traumatic brain injury, burn with inhalation injury, and alcoholic liver disease, among many others[40; 43; 50]. Previously, our lab has demonstrated that UB decreases β-AR-stimulated increases in myocyte apoptosis and myocardial fibrosis[66]. Extracellular UB is proposed to have anti-inflammatory roles that are demonstrated by an increase in Th2 cytokines *in vivo* in a swine model of lung ischemia/reperfusion injury and by a decrease in the tumor necrosis factor-α (TNF-α) response from peripheral blood monocular cells treated with endotoxin *ex vivo*[52; 55]. The roles of extracellular UB in myocardial remodeling post-myocardial I/R injury have not yet been determined.

The data presented in this study suggest that extracellular UB has a role in cardiac fibroblast function and proliferation as well as a cardioprotective role in remodeling processes post-myocardial I/R injury. First, we validated a method of consistently measuring ischemia and reperfusion in real time using electrocardiography. Second, we found that extracellular UB interacts with CXCR-4 receptor in cardiac fibroblast lysates, associates with decreases in serum-stimulated fibroblast proliferation, and associates with increases in contraction of fibroblast

seeded collagen gels. Third, we discovered that UB plays a cardioprotective role in remodeling after myocardial I/R injury with effects on infarct size, cardiac function, inflammatory response, and ECM protein levels.

Validating a method of consistently measuring ischemia and reperfusion in real time using electrocardiography was important to the success of the second aim of investigating UB's role in I/R remodeling processes. In order to obtain consistent and accurate experimental results in the study, there must be confirmation of successful ischemia and successful reperfusion. The extent of ischemia and or reperfusion can be difficult to determine based on myocardial color changes alone. Real time ECG allowed us to begin recording the time of ischemia at the time when the SJT segment elevated. After 45-minutes of SJT elevation, reperfusion was then confirmed by the immediate changes to the SJT segment. Furthermore, the development of deep Q-waves indicated myocardial tissue damage due to the ischemia and subsequent reperfusion. Therefore, real time use of the ECG platform ensured that the animals in the study received adequate periods of ischemia and confirmed that they experienced full reperfusion and myocardial damage.

The schematic diagram of the proposed effects of exogenous UB on myocardial remodeling post-I/R injury is shown in Figure 5.1. We found that extracellular UB decreases the inflammatory response as evidenced by decreased infiltration of inflammatory infiltrates including macrophages and neutrophils as well as decreased neutrophil activity. The decreased extent of inflammation in UB-infused hearts could contribute to the observed decrease in infarct size. We also noted that extracellular UB influences the expression of MMP-2 and TGF-β, two proteins involved in ECM remodeling, as well as the activity of MMP-9. UB associated increases in these ECM protein levels and activity may be responsible for the observed reduction in

collagen-based scar. Lastly, the data revealed that extracellular UB resulted in improved cardiac function 3 days post-I/R. Observed increases in cardiac function may result from the culmination of multiple factors associated with UB administration such as reduced inflammatory infiltration and activity, reduced infarct size and an increase in the protein levels and activity of key ECM proteins.

The finding that UB-infusion induced proteomic changes in the myocardium and the extracellular matrix is very interesting. UB is reported to bind CXCR-4 in THP-1 cells, among others[45]. CXCR-4 is a G protein-coupled receptor that contains 7 transmembrane helices and is proposed to induce multiple signaling events upon stimulation with its cognate ligand, SDF-1α, via interaction with heterotrimeric G_i-proteins[76]. The signaling pathways activated via CXCR-4 include increases in activation of focal adhesion molecules, ERK1/2, PI3-k and the JAK/STAT pathway[76]. Additionally, SDF-1α is recognized to mediate CXCR-4 receptor internalization via G protein-coupled kinases and β-arrestin[76]. There are conflicting reports regarding the specific effects of receptor activation versus receptor internalization. However, using mutated forms of CXCR-4, it was discovered that receptor internalization is not required for downstream phosphorylation of signaling targets[76].

This raises multiple questions regarding the role of signaling initiated by UB binding CXCR-4. Previously, our lab found UB to increase phosphorylation of AKT in ISO treated cardiac fibroblasts and decrease phosphorylation of JNK in the LV of ISO treated mouse hearts[66]. Interestingly, UB had no significant effect on phosphorylation of ERK1/2 in the LV lysates of mouse myocardium[66]. These findings suggest that SDF-1α and UB illicit different signaling pathways despite a shared receptor. Regulation of ERK1/2 phosphorylation was correlated with increased MMP-2 and MMP-9 expression in an atherosclerosis study[77]. It is

possible that the observed increases in MMP-2 protein levels and MMP-9 activity are due to CXCR-4 mediated activation of ERK1/2 signaling. However, without ERK1/2 data specific to our model, it is difficult to speculate. To investigate this in the future, phosphorylation of ERK1/2 should be studied and receptor endocytosis should be inhibited to determine if the events associated with UB-infusion are mediated via receptor internalization or internalization-independent signaling events.

Cardiac fibroblasts are the main mediators of ECM homeostasis and ECM remodeling under wound healing conditions[27]. In this study, extracellular UB associated with changes in fibroblast function and proliferation. UB is shown to interact with cardiac fibroblasts and CXCR-4 in the membrane fraction of fibroblast lysates. Our finding is supported by reports of UB-CXCR-4 interaction in THP-1 cells among others[45]. We also present evidence that UB associates with functional changes in cardiac fibroblasts. UB reduced serum-stimulated increases in fibroblast proliferation. Interestingly, this is not the first time UB has been implicated in cell-specific growth inhibition. Extracellularly administered UB caused the growth arrest of *Schizosaccharomyces pombe* cells[78]. In that study, it was determined that inhibiting the proteasomal degradation pathway reversed the growth-inhibition that was initiated by administration of extracellular UB[78]. A proteasomal inhibitor should be used in future investigations to determine the role of the UB-proteosome pathway in exogenous-UB-mediated proliferative changes. The implications of the observed reduction in the serum-stimulated proliferation of fibroblasts may include fewer fibroblasts in the injured area, which in turn, may contribute to our observation of reduced fibrotic infarct size in UB-I/R hearts.

UB also increased the contraction of fibroblast seeded collagen gels. Increased contraction of fibroblast seeded collagen gels could indicate that UB treated fibroblasts may have

enhanced wound contracture capabilities. CXCR-4, the proposed receptor for UB, associates with increased activation of focal adhesion proteins[76]. This represents a possible mechanism for increased contraction of fibroblast-seeded gel pads. However, our findings regarding fibroblast function are *in vitro*. Myocardial remodeling remains a complex and multifactorial process. While these findings may shed light on possible explanations for our *in vivo* I/R observations, UB's influence on fibroblast function ultimately must be investigated *in vivo*.

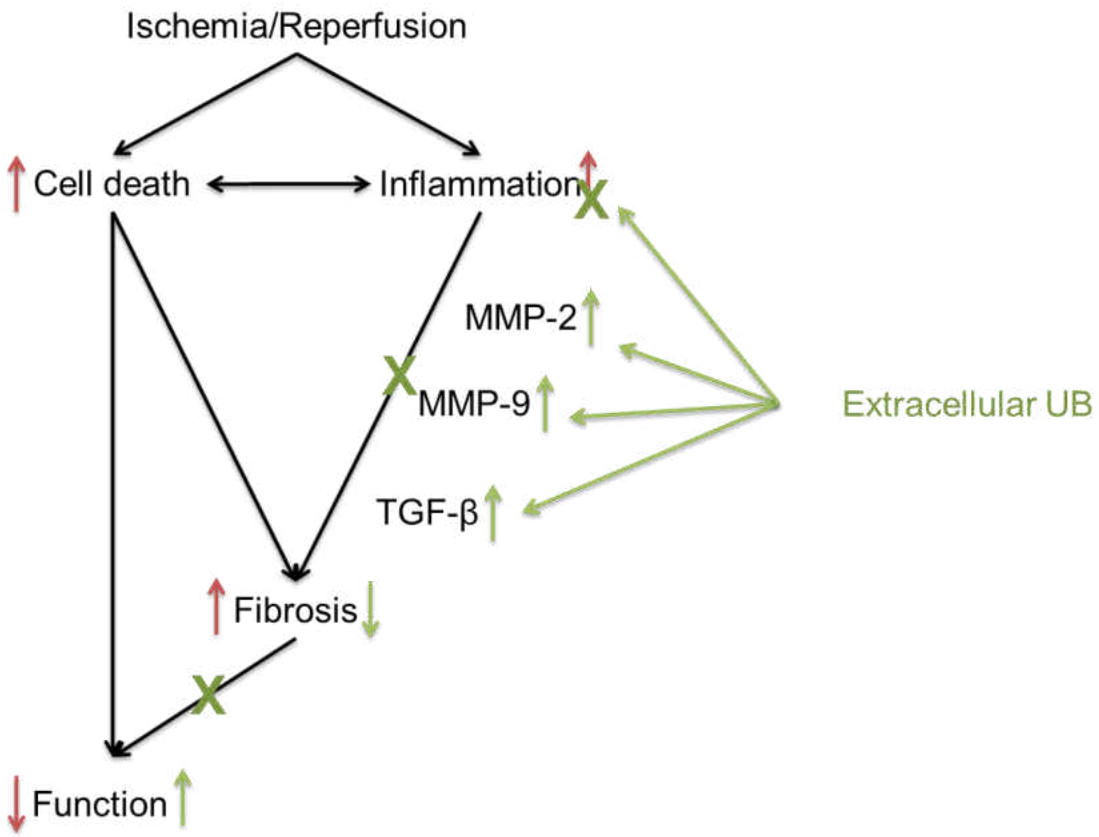

Figure 5.1. Schematic diagram representing the results of extracellular UB infusion post-ischemia/reperfusion injury with regards to our hypothesis. MMP-2, matrix metalloproteinase 2; MMP-9, matrix metalloproteinase 9; TGF-β, transforming growth factor β1. Green coloring indicates the observed effects when UB infusion was administered. Red coloring indicates the effects of ischemia/reperfusion injury.

There are additional avenues to further investigate this topic in the future. The current study investigated the role of extracellular UB *in vitro* in cardiac fibroblasts and also *in vivo* 3 days after myocardial I/R injury. The I/R study should be extended to 7 day and 28 day time points to determine if cardioprotective effects of UB are sustained long term. The I/R study should also be reduced to a 1 day or 4 hour study to determine early signaling events and their role in cardiac remodeling outcomes. Injured hearts are often able to sustain function for a short time by compensating loss of efficiency with increased work. However, compensative changes to the heart are unsustainable and the heart will eventually decompensate and begin to fail. A 28-day time point would give insight into whether UB-mediated functional sustainment is permanent or compensative. Future studies should investigate the contents of the infarcted area and the scar such as collagen composition as well as other ECM proteins. It would be interesting to develop a timeline of cytokine expression using serum to determine differences in inflammatory signaling in UB-I/R vs I/R groups. This current study was conducted using UB infusion as a pretreatment. Administering UB at the time of reperfusion would strengthen this study, as that would truly investigate the clinical potential for UB as a therapeutic agent in a clinical setting.

REFERENCES

1. The 10 leading causes of death in the world. 2012. [accessed 2016 March 22]. http://www.who.int/mediacentre/factsheets/fs310/en/.
2. Million hearts. [accessed 2016]. http://millionhearts.hhs.gov/learn-prevent/cost-consequences.html.
3. Cassar A, Holmes DR, Rihal CS, Gersh BJ. 2009. Chronic coronary artery disease: Diagnosis and management. Mayo Clin Proc. 84(12):1130-1146.
4. Chilton RJ. 2004. Pathophysiology of coronary heart disease: A brief review. J Am Osteopath Assoc. 104(9 Suppl 7):S5-8.
5. Bentzon JF, Otsuka F, Virmani R, Falk E. 2014. Mechanisms of plaque formation and rupture. Circ Res. 114(12):1852-1866.
6. Shinde AV, Frangogiannis NG. 2014. Fibroblasts in myocardial infarction: A role in inflammation and repair. J Mol Cell Cardiol. 70:74-82.
7. O'Gara PT, Kushner FG, Ascheim DD, Casey DE, Chung MK, de Lemos JA, Ettinger SM, Fang JC, Fesmire FM, Franklin BA et al. 2013. 2013 accf/aha guideline for the management of st-elevation myocardial infarction: Executive summary: A report of the american college of cardiology foundation/american heart association task force on practice guidelines: Developed in collaboration with the american college of emergency physicians and society for cardiovascular angiography and interventions. Catheter Cardiovasc Interv. 82(1):E1-27.
8. Peter AK, Bjerke MA, Leinwand LA. 2016. Biology of the cardiac myocyte in heart disease. Mol Biol Cell. 27(14):2149-2160.
9. Laflamme MA, Murry CE. 2011. Heart regeneration. Nature. 473(7347):326-335.
10. Quijada P, Sussman MA. 2015. Circulating around the tissue: Hematopoietic cell-based fusion versus transdifferentiation. Circ Res. 116(4):563-565.
11. Kalogeris T, Baines CP, Krenz M, Korthuis RJ. 2012. Cell biology of ischemia/reperfusion injury. Int Rev Cell Mol Biol. 298:229-317.
12. Vinten-Johansen J, Jiang R, Reeves JG, Mykytenko J, Deneve J, Jobe LJ. 2007. Inflammation, proinflammatory mediators and myocardial ischemia-reperfusion injury. Hematol Oncol Clin North Am. 21(1):123-145.
13. Yellon DM, Hausenloy DJ. 2007. Myocardial reperfusion injury. N Engl J Med. 357(11):1121-1135.
14. Marchant DJ, Boyd JH, Lin DC, Granville DJ, Garmaroudi FS, McManus BM. 2012. Inflammation in myocardial diseases. Circ Res. 110(1):126-144.
15. Liu J, Wang H, Li J. 2016. Inflammation and inflammatory cells in myocardial infarction and reperfusion injury: A double-edged sword. Clin Med Insights Cardiol. 10:79-84.
16. Litt MR, Jeremy RW, Weisman HF, Winkelstein JA, Becker LC. 1989. Neutrophil depletion limited to reperfusion reduces myocardial infarct size after 90 minutes of ischemia. Evidence for neutrophil-mediated reperfusion injury. Circulation. 80(6):1816-1827.
17. Hayward R, Campbell B, Shin YK, Scalia R, Lefer AM. 1999. Recombinant soluble p-selectin glycoprotein ligand-1 protects against myocardial ischemic reperfusion injury in cats. Cardiovasc Res. 41(1):65-76.

18. Ma XL, Tsao PS, Lefer AM. 1991. Antibody to cd-18 exerts endothelial and cardiac protective effects in myocardial ischemia and reperfusion. J Clin Invest. 88(4):1237-1243.
19. Zhao ZQ, Lefer DJ, Sato H, Hart KK, Jefforda PR, Vinten-Johansen J. 1997. Monoclonal antibody to icam-1 preserves postischemic blood flow and reduces infarct size after ischemia-reperfusion in rabbit. J Leukoc Biol. 62(3):292-300.
20. Jessup M, Brozena S. 2003. Heart failure. N Engl J Med. 348(20):2007-2018.
21. Stroumpoulis KI, Pantazopoulos IN, Xanthos TT. 2010. Hypertrophic cardiomyopathy and sudden cardiac death. World J Cardiol. 2(9):289-298.
22. Garza MA, Wason EA, Zhang JQ. 2015. Cardiac remodeling and physical training post myocardial infarction. World J Cardiol. 7(2):52-64.
23. Frangogiannis NG, Smith CW, Entman ML. 2002. The inflammatory response in myocardial infarction. Cardiovasc Res. 53(1):31-47.
24. Hayashidani S, Tsutsui H, Shiomi T, Ikeuchi M, Matsusaka H, Suematsu N, Wen J, Egashira K, Takeshita A. 2003. Anti-monocyte chemoattractant protein-1 gene therapy attenuates left ventricular remodeling and failure after experimental myocardial infarction. Circulation. 108(17):2134-2140.
25. Koh TJ, DiPietro LA. 2011. Inflammation and wound healing: The role of the macrophage. Expert Rev Mol Med. 13:e23.
26. van Putten S, Shafieyan Y, Hinz B. 2016. Mechanical control of cardiac myofibroblasts. J Mol Cell Cardiol. 93:133-142.
27. Chen W, Frangogiannis NG. 2013. Fibroblasts in post-infarction inflammation and cardiac repair. Biochim Biophys Acta. 1833(4):945-953.
28. Schneider L, Cammer M, Lehman J, Nielsen SK, Guerra CF, Veland IR, Stock C, Hoffmann EK, Yoder BK, Schwab A et al. 2010. Directional cell migration and chemotaxis in wound healing response to pdgf-aa are coordinated by the primary cilium in fibroblasts. Cell Physiol Biochem. 25(2-3):279-292.
29. Barallobre-Barreiro J, Didangelos A, Schoendube FA, Drozdov I, Yin X, Fernández-Caggiano M, Willeit P, Puntmann VO, Aldama-López G, Shah AM et al. 2012. Proteomics analysis of cardiac extracellular matrix remodeling in a porcine model of ischemia/reperfusion injury. Circulation. 125(6):789-802.
30. Spinale FG. 2002. Matrix metalloproteinases: Regulation and dysregulation in the failing heart. Circ Res. 90(5):520-530.
31. Galis ZS, Sukhova GK, Lark MW, Libby P. 1994. Increased expression of matrix metalloproteinases and matrix degrading activity in vulnerable regions of human atherosclerotic plaques. J Clin Invest. 94(6):2493-2503.
32. Goldstein G, Scheid M, Hammerling U, Schlesinger DH, Niall HD, Boyse EA. 1975. Isolation of a polypeptide that has lymphocyte-differentiating properties and is probably represented universally in living cells. Proc Natl Acad Sci U S A. 72(1):11-15.
33. Scofield SL, Amin P, Singh M, Singh K. 2015. Extracellular ubiquitin: Role in myocyte apoptosis and myocardial remodeling. Compr Physiol. 6(1):527-560.
34. Vijay-Kumar S, Bugg CE, Cook WJ. 1987. Structure of ubiquitin refined at 1.8 a resolution. J Mol Biol. 194(3):531-544.
35. Goldberg AL. 2003. Protein degradation and protection against misfolded or damaged proteins. Nature. 426(6968):895-899.

36. Dammer EB, Na CH, Xu P, Seyfried NT, Duong DM, Cheng D, Gearing M, Rees H, Lah JJ, Levey AI et al. 2011. Polyubiquitin linkage profiles in three models of proteolytic stress suggest the etiology of alzheimer disease. J Biol Chem. 286(12):10457-10465.
37. Chaugule VK, Walden H. 2016. Specificity and disease in the ubiquitin system. Biochem Soc Trans. 44(1):212-227.
38. Thompson SJ, Loftus LT, Ashley MD, Meller R. 2008. Ubiquitin-proteasome system as a modulator of cell fate. Curr Opin Pharmacol. 8(1):90-95.
39. Asseman C, Pancre V, Delanoye A, Capron A, Auriault C. 1994. A radioimmunoassay for the quantification of human ubiquitin in biological fluids: Application to parasitic and allergic diseases. Journal of Immunological Methods. 173(1):8.
40. Takagi M, Yamauchi M, Toda G, Takada K, Hirakawa T, Ohkawa K. 1999. Serum ubiquitin levels in patients with alcoholic liver disease. Alcohol Clin Exp Res. 23(4 Suppl):76S-80S.
41. Okada M, Miyazaki S, Hirasawa Y. 1993. Increase in plasma concentration of ubiquitin in dialysis patients: Possible involvement in beta 2-microglobulin amyloidosis. Clin Chim Acta. 220(2):135-144.
42. Asseman C, Pancré V, Delanoye A, Capron A, Auriault C. 1994. A radioimmunoassay for the quantification of human ubiquitin in biological fluids: Application to parasitic and allergic diseases. J Immunol Methods. 173(1):93-101.
43. Majetschak M, King DR, Krehmeier U, Busby LT, Thome C, Vajkoczy S, Proctor KG. 2005. Ubiquitin immunoreactivity in cerebrospinal fluid after traumatic brain injury: Clinical and experimental findings. Crit Care Med. 33(7):1589-1594.
44. Earle SA, Proctor KG, Patel MB, Majetschak M. 2005. Ubiquitin reduces fluid shifts after traumatic brain injury. Surgery. 138(3):431-438.
45. Saini V, Marchese A, Majetschak M. 2010. Cxc chemokine receptor 4 is a cell surface receptor for extracellular ubiquitin. J Biol Chem. 285(20):15566-15576.
46. Wu B, Chien EYT, Mol CD, Fenalti G, Liu W, Katritch V, Abagyan R, Brooun A, Wells P, Bi FC et al. 2010. Structures of the cxcr4 chemokine receptor in complex with small molecule and cyclic peptide antagonists. Science. 330(6007):5.
47. Tripathi A, Davis JD, Staren DM, Volkman BF, Majetschak M. 2014. Cxc chemokine receptor 4 signaling upon co-activation with stromal cell-derived factor-1α and ubiquitin. Cytokine. 65(2):121-125.
48. Freitas C, Desnoyer A, Meuris F, Bachelerie F, Balabanian K, Machelon V. 2014. The relevance of the chemokine receptor ackr3/cxcr7 on cxcl12-mediated effects in cancers with a focus on virus-related cancers. Cytokine Growth Factor Rev. 25(3):307-316.
49. Saini V, Marchese A, Tang WJ, Majetschak M. 2011. Structural determinants of ubiquitin-cxc chemokine receptor 4 interaction. J Biol Chem. 286(51):44145-44152.
50. Majetschak M, Zedler S, Hostmann A, Sorell LT, Patel MB, Novar LT, Kraft R, Habib F, de Moya MA, Ertel W et al. 2008. Systemic ubiquitin release after blunt trauma and burns: Association with injury severity, posttraumatic complications, and survival. J Trauma. 64(3):586-596; discussion 596-588.
51. Majetschak M, Cohn SM, Nelson JA, Burton EH, Obertacke U, Proctor KG. 2004. Effects of exogenous ubiquitin in lethal endotoxemia. Surgery. 135(5):536-543.
52. Majetschak M, Krehmeier U, Bardenheuer M, Denz C, Quintel M, Voggenreiter G, Obertacke U. 2003. Extracellular ubiquitin inhibits the tnf-alpha response to endotoxin in

peripheral blood mononuclear cells and regulates endotoxin hyporesponsiveness in critical illness. Blood. 101(5):1882-1890.
53. Schedi MP, Goldstein G, Boyce EA. 1975. Differentiation of t cells in nude mice. Science. 190(4220):1211-1213.
54. Majetschak M, Cohn SM, Obertacke U, Proctor KG. 2004. Therapeutic potential of exogenous ubiquitin during resuscitation from severe trauma. J Trauma. 56(5):991-999; discussion 999-1000.
55. Garcia-Covarrubias L, Manning EW, Sorell LT, Pham SM, Majetschak M. 2008. Ubiquitin enhances the th2 cytokine response and attenuates ischemia-reperfusion injury in the lung. Crit Care Med. 36(3):979-982.
56. Daino H, Matsumura I, Takada K, Odajima J, Tanaka H, Ueda S, Shibayama H, Ikeda H, Hibi M, Machii T et al. 2000. Induction of apoptosis by extracellular ubiquitin in human hematopoietic cells: Possible involvement of stat3 degradation by proteasome pathway in interleukin 6-dependent hematopoietic cells. Blood. 95(8):2577-2585.
57. Griebenow M, Casalis P, Woiciechowsky C, Majetschak M, Thomale UW. 2007. Ubiquitin reduces contusion volume after controlled cortical impact injury in rats. J Neurotrauma. 24(9):1529-1535.
58. Brooks WW, Conrad CH. 2009. Isoproterenol-induced myocardial injury and diastolic dysfunction in mice: Structural and functional correlates. Comp Med. 59(4):339-343.
59. Willerson JT, Buja LM. 1988. Beta-adrenergic mechanisms during severe myocardial ischemia and evolving infarction. Postgrad Med. Spec No:27-32.
60. Schömig A, Dart AM, Dietz R, Mayer E, Kübler W. 1984. Release of endogenous catecholamines in the ischemic myocardium of the rat. Part a: Locally mediated release. Circ Res. 55(5):689-701.
61. Seyfarth M, Feng Y, Hagl S, Sebening F, Richardt G, Schömig A. 1993. Effect of myocardial ischemia on stimulation-evoked noradrenaline release. Modulated neurotransmission in rat, guinea pig, and human cardiac tissue. Circ Res. 73(3):496-502.
62. Seyfarth M, Richardt G, Mizsnyak A, Kurz T, Schömig A. 1996. Transient ischemia reduces norepinephrine release during sustained ischemia. Neural preconditioning in isolated rat heart. Circ Res. 78(4):573-580.
63. Rona G. 1985. Catecholamine cardiotoxicity. J Mol Cell Cardiol. 17(4):291-306.
64. Remondino A, Kwon SH, Communal C, Pimentel DR, Sawyer DB, Singh K, Colucci WS. 2003. Beta-adrenergic receptor-stimulated apoptosis in cardiac myocytes is mediated by reactive oxygen species/c-jun nh2-terminal kinase-dependent activation of the mitochondrial pathway. Circ Res. 92(2):136-138.
65. Singh M, Roginskaya M, Dalal S, Menon B, Kaverina E, Boluyt MO, Singh K. 2010. Extracellular ubiquitin inhibits beta-ar-stimulated apoptosis in cardiac myocytes: Role of gsk-3beta and mitochondrial pathways. Cardiovasc Res. 86(1):20-28.
66. Daniels CR, Foster CR, Yakoob S, Dalal S, Joyner WL, Singh M, Singh K. 2012. Exogenous ubiquitin modulates chronic β-adrenergic receptor-stimulated myocardial remodeling: Role in akt activity and matrix metalloproteinase expression. Am J Physiol Heart Circ Physiol. 303(12):H1459-1468.
67. Bloom MW, Greenberg B, Jaarsma T, Januzzi JL, Lam CSP, Maggioni AP, Trochu JN, Butler J. 2017. Heart failure with reduced ejection fraction. Nat Rev Dis Primers. 3:17058.

68. Heron M. 2016. Deaths: Leading causes for 2014. Centers for Disease Control and Prevention.
69. Nadal-Ginard B, Kajstura J, Leri A, Anversa P. 2003. Myocyte death, growth, and regeneration in cardiac hypertrophy and failure. Circ Res. 92(2):139-150.
70. Kong P, Christia P, Frangogiannis NG. 2014. The pathogenesis of cardiac fibrosis. Cell Mol Life Sci. 71(4):549-574.
71. Jardine DL, Charles CJ, Ashton RK, Bennett SI, Whitehead M, Frampton CM, Nicholls MG. 2005. Increased cardiac sympathetic nerve activity following acute myocardial infarction in a sheep model. J Physiol. 565(Pt 1):325-333.
72. Colucci WS. 1998. The effects of norepinephrine on myocardial biology: Implications for the therapy of heart failure. Clin Cardiol. 21(12 Suppl 1):I20-24.
73. Colucci WS, Sawyer DB, Singh K, Communal C. 2000. Adrenergic overload and apoptosis in heart failure: Implications for therapy. J Card Fail. 6(2 Suppl 1):1-7.
74. Fowler MB, Laser JA, Hopkins GL, Minobe W, Bristow MR. 1986. Assessment of the beta-adrenergic receptor pathway in the intact failing human heart: Progressive receptor down-regulation and subsensitivity to agonist response. Circulation. 74(6):1290-1302.
75. Schlesinger DH, Goldstein G, Niall HD. 1975. The complete amino acid sequence of ubiquitin, an adenylate cyclase stimulating polypeptide probably universal in living cells. Biochemistry. 14(10):2214-2218.
76. Roland J, Murphy BJ, Ahr B, Robert-Hebmann V, Delauzun V, Nye KE, Devaux C, Biard-Piechaczyk M. 2003. Role of the intracellular domains of cxcr4 in sdf-1-mediated signaling. Blood. 101(2):399-406.
77. Shih MF, Pan KH, Cherng JY. 2015. Possible mechanisms of di(2-ethylhexyl) phthalate-induced mmp-2 and mmp-9 expression in a7r5 rat vascular smooth muscle cells. Int J Mol Sci. 16(12):28800-28811.
78. Kutty BC, Pasupathy K, Mishra KP. 2005. Effects of exogenous ubiquitin on cell division cycle mutants of schizosaccharomyces pombe. FEMS Microbiol Lett. 244(1):187-191.

VITA
STEPHANIE L.C. SCOFIELD

Education:	State University of New York College at Oswego, Oswego, New York B.A. Political Science, 2011
	James H. Quillen College of Medicine, East Tennessee State University, Johnson City, Tennessee Ph.D., Biomedical Sciences, 2017
Professional Experience:	Graduate Assistant, James H. Quillen College of Medicine East Tennessee State University, Department of Biomedical Sciences, August 2013-December 2017
Publications:	**Scofield, S.L.C.**, Amin, P., Singh, M., Singh, K. Extracellular ubiquitin: role in myocyte apoptosis and myocardial remodeling. *Comprehensive Physiology*. 2015; 6(1): 527-560.
	Daniel, L.L., **Scofield, S.L.C.**, Thrasher, P., Dalal, S., Daniels, C.R., Foster, C.R., Singh, M., Singh, K. Ataxia Telangiectasia Mutated Kinase Deficiency Exacerbates Left Ventricular Dysfunction and Remodeling Late After Myocardial Infarction. *American Journal of Physiology-Heart and Circulatory Physiology*. 2016; 311(2): H445-52.
	Scofield, S.L.C., Singh, K. Confirmation of myocardial ischemia and reperfusion in mice using surface pad electrocardiography. *Journal of Visualized Experiments*. 2016; (117).
	Beaumont, E., Campbell, R.P., Andresen, M., **Scofield, S.L.C.**, Singh, K. Libbus, I., KenKnight, B.H., Snyder, L., Cantrell, N. Clinically-styled vagus nerve stimulation augments spontaneous discharge in second and higher order sensory neurons in rat nucleus of the solitary tract. *American Journal of Physiology-Heart and Circulatory Physiology*. 2017; doi: 10.1152/ajpheart.00070.2017.
Honors:	1st place in poster presentation, Appalachian Student Research Forum, April 2016